REGULATION OF AUDITORY SYSTEM PLASTICITY

by

Benjamin Schwartz

A Dissertation Submitted to the Faculty of the

GRADUATE INTERDISCIPLINARY PROGRAM IN NEUROSCIENCE

In Partial Fulfillment of the Requirements

For the Degree of

DOCTOR OF PHILOSOPHY

In the Graduate College

THE UNIVERSITY OF ARIZONA

2021

THE UNIVERSITY OF ARIZONA
GRADUATE COLLEGE

As members of the Dissertation Committee, we certify that we have read the dissertation prepared by: ***Benjamin Schwartz***, titled: ***Regulation of Auditory System Plasticity*** and recommend that it be accepted as fulfilling the dissertation requirement for the Degree of Doctor of Philosophy in Neuroscience.

_____ Date: Nov 18, 2021
[Dissertation Chair Konrad Zinsmaier]

_____ Date: Nov 18, 2021
[Dissertation Research Advisor Shaowen Bao]

_____ Date: Nov 18, 2021
[Committee Member Anita Koshy]

_____ Date: Nov 18, 2021
[Committee Member Martha Bhattacharya]

Final approval and acceptance of this dissertation is contingent upon the candidate's submission of the final copies of the dissertation to the Graduate College.

I hereby certify that I have read this dissertation prepared under my direction and recommend that it be accepted as fulfilling the dissertation requirement.

_____ Date: Nov 18, 2021
Konrad Zinsmaier
Dissertation Committee Chair
Graduate Interdisciplinary Program in Neuroscience

I hereby certify that I have read this dissertation prepared under my direction and recommend that it be accepted as fulfilling the dissertation requirement.

_____ Date: Nov 18, 2021
Shaowen Bao
Dissertation Research Advisor
Graduate Interdisciplinary Program in Neuroscience

This dissertation is dedicated to my wife and my parents for their enduring support through my PhD process. I would not be where I am today without them.

Table of Contents

List of Figures

REGULATION OF AUDITORY SYSTEM PLASTICITY

By
Ben Schwartz

Doctor of Philosophy in Neuroscience
University of Arizona
Shaowen Bao
November 2021

Abstract

Plasticity is defined as the brain's ability to change in response to intrinsic and extrinsic stimuli by reorganizing its structure function and connections. Plasticity is a feature of brain function that underlies complex mechanisms such as learning and memory, neural development and disease pathogenesis. Plasticity levels throughout the brain are highest during a discrete time early in development known as the critical period. During this time, the high levels of plasticity facilitate experience-dependent wiring of our sensory cortices to ensure proper adaptation to the external environment. Following the critical period, plasticity levels in the brain drop precipitously, leading to different requirements for the induction of plasticity. During the critical period, plasticity can be induced via passive exposure to sensory stimuli, while in adulthood, plasticity induction requires sustained attention towards the sensory stimuli. In the auditory system, this takes form as frequency map plasticity. Exposing animals to a pure tone of a specific frequency increases the area dedicated to that frequency within primary auditory cortex (Figure 1.1). This passive exposure-based plasticity does not occur in adulthood. The significant difference in requirements for plasticity induction underscores the importance of understanding the factors that promote plasticity during the critical period and the factors that restrict plasticity

in adulthood. A deeper understanding of these factors is vital for understanding how plasticity is regulated within the cortex.

The introduction of this dissertation will explore our current understanding of the mechanisms that progress the critical period. The critical period itself is a dynamic epoch in development that is controlled both by environmental and genetic factors. A detailed mechanistic understanding of the cellular, molecular and physiological processes that progressively shifts the brain from a plastic, to a non-plastic state will provide the context for the experiments discussed in later chapters.

In the second chapter, I clarify the relationship between DNA methylation (DNA-ME) dynamics and the progression of the critical period. I show that as animals progress from the critical period into adulthood, their auditory cortices accumulate DNA-ME. Furthermore, removing DNA-ME from adult mice, via pharmacological injections of a DNA methylation inhibitor, re-established the capacity for frequency map plasticity in the auditory cortex of adult mice. These results correlate with results showing that reduction of DNA methylation in adulthood reversed characteristics of gene expression and synaptic transmission back to levels seen during the critical period. Together, these results implicate accumulation DNA-ME as a crucial mechanism for progression of the critical period. In the conclusion, I will discuss how these results influence our understanding of certain developmental disorders such as Rett Syndrome.

In the third chapter, I show that homeostatic plasticity, a form of plasticity that regulates synaptic strength off a certain baseline, plays an important role in closing the critical period. Animals

deficient in Tumor-necrosis factor-alpha (TNF-α), an important mediator of homeostatic plasticity in the central nervous system, retain frequency map plasticity into adulthood. Furthermore, TNF-α deficient animals display reduced Parvalbumin positive (PV) neuron density, increased excitatory synaptic transmission, and signatures of elevated cortical excitation levels. Together these results show that without the contributions of TNF-α the brain fails to progress out of the critical period, thus implicating homeostatic plasticity in the regulation of critical period plasticity.

In the fourth chapter, I explore the relationship between central nervous system damage and cortical plasticity. I show that under normal conditions, the contralateral auditory pathway transmits signal faster, contains larger bandwidth receptive fields, and elicits stronger auditory evoked responses than the ipsilateral auditory pathway. Following unilateral hearing lesion, latencies along the ipsilateral pathway decrease, while receptive field bandwidth increases. Furthermore, unilateral hearing lesion re-stablishes frequency map plasticity along the ipsilateral auditory pathway. Together, these results indicate that in the presence of noise-induced neural damage, the brain engages plasticity mechanisms to re-map damaged areas of cortex and shift hearing bias from the contralateral to the ipsilateral auditory pathway.

1

Introduction: The Progression of the Critical Period

Spontaneous activity pre-wires sensory cortices prior to the beginning of the critical period.

The first account of spontaneous activity playing a role in development of the critical period comes from Hubel and Wiesel's seminal experiments describing the effects of monocular deprivation on kittens (Wiesel and Hubel, 1963). In their study, they report on the presence of spontaneous activity within the kitten striate cortex; "The 5 remaining cells could not be driven from either eye, and would have gone unnoticed had it not been for their spontaneous activity. The presence in most of these penetrations of a small number of unresponsive cells is worth stressing, since in normal adult cats it has been possible to drive all cells with appropriate visual stimuli." This was the first report to establish the relationship that as development progresses, spontaneous activity decreases.

More recent studies have extended this finding and have begun to establish the role spontaneous activity plays in shaping sensory cortex. Before the onset of hearing and the auditory critical period, spontaneous activity along the auditory pathway is generated via release of ATP from inner supporting cells onto inner hair cells, leading to their depolarization and the generation of burst action potentials in spiral ganglion neurons (Tritsch and Bergles, 2010). This activity propagates from the cochlea, through the brain stem (Sonntag et al., 2009), to what will become primary auditory cortex (Babola et al., 2018). Recent *in vivo* imaging studies have revealed that co-activation of neurons within specific spatial and temporal bands in the inferior colliculus corresponded with the future tonotopic organization of the inferior colliculus. Furthermore, those

pathways that eventually carried tonotopic information were preserved from the inferior colliculus through to the auditory cortex (Babola et al., 2018). These results indicate that spontaneous activity serves as a guide for the creation of tonotopic maps that will eventually drive auditory perception. This phenomena of correlated spontaneous activity during development has also been reported in the retina, spinal cord, hippocampus and cerebellum (Blankenship and Feller, 2010). These results serve to highlight the importance of neuronal activity in shaping our sensory and motor circuits in the absence of environmental stimuli.

Experience provides the cue for proper cortical wiring

Once the cortex has been pre-wired, sensory perception turns on, and the critical period opens. Rather than spontaneous activity, environmental experience is now driving and directing the proper wiring of the cortex. In the auditory system, experience shapes the confounds of the tonotopic map within primary auditory cortex, and fine tunes features of auditory processing. These features include receptive field bandwidth, latency, threshold, evoked amplitude, and frequency modulation selectivity (Zhang et al., 2001; Chang et al., 2005; Villers-Sidani, 2007; Insanally et al., 2009). The window through which tonotopic map plasticity can be induced has been determined to be approximately between post-natal (PN) day 9 and PN day 13. Following PN 13, the ability to induce experience-dependent map changes drops precipitously (Figure 1.2). However, features such as response latency, bandwidth, and threshold are continuously fine-tuned up to PN day 60 (Villers-Sidani, 2007).

Different types of auditory experiences will exert varying effects on the structure and function of the auditory cortex. As mentioned previously, pulsed pure-tone exposure during the critical

period will yield an expansion of cortical area within the exposure frequency band (Zhang et al., 2001; Villers-Sidani, 2007). Exposure to pulsed white noise leads to degraded processing features such as enlarged receptive field bandwidth, multi-peak receptive fields, and lack of tonotopicity within A1 (Zhang et al., 2002). Exposure to continuous moderate-level tones also enlarged receptive field bandwidths, but flattened receptive field peaks, and shifted the tonotopicity of primary auditory cortex to skew away from low frequency receptive fields and towards high frequency receptive fields (Zhou et al., 2008). These results indicate that when the critical period window is open, the structure and function of the auditory cortex is sensitive to the substance of the auditory experience.

Experience regulates progression through the critical period.

Experience not only provides the cue for proper cortical wiring, but also regulates the timing of critical period progression. This notion is supported by experiments examining the effects of environmental noise on tonotopic map development in the primary auditory cortex of rats. In general, the tonotopic maps of developing rats are characterized by a wide area of auditory responsive regions, mainly dominated by high frequency sensitive areas. The tonotopic maps of adult rats are considerably smaller in auditory responsive area, and are far more ordered in regard to tonotopy. Results show that rearing rats in an environment where they are exposed to continuous white noise, holds the tonotopic map in an immature state (Figure 1.3). Furthermore, after exposing the animals to continuous white noise, removing them from that environment and then exposing them to pure-tones, led to frequency map expansion in the exposed frequency (Chang and Merzenich, 2003). This expansion occurred at PN day 50, which is long after the natural critical period closure day in rats, PN day 13 (Villers-Sidani, 2007). This indicates that

continuous white noise exposure held the auditory cortex in an immature state, regardless of the age of the animal.

The effect of experience on critical period progression is so sensitive, that exposing animals to continuous noise in specific frequency bands can hold the specific region of the auditory cortex sensitive to those frequency of sounds in an immature state. Using exposure paradigms referred to as “notched noise” and “band-limited noise”, these experimenters showed that frequency bands exposed to noise, retained immature characteristics such as reduced PV interneuron density, and enlarged receptive field bandwidth, while neighboring isofrequency bands properly matured (de Villers-Sidani et al., 2008). Together, with results showing that temporally modulated noise can accelerate the closure of the critical period (Zhang et al., 2002; Zhou et al., 2008), these results indicate that the critical period window itself is plastic, and tightly regulated by the experiences of the organism.

Experience-dependent release of transcription factor, OTX2, leads to progression through the critical period.

As mentioned in the previous chapter, the rate of progression through the critical period is sensitive to the quality of sensory experience. This finding naturally leads to the question, how does experience regulate progression through the critical period? Local release of homeoproteins has been shown to play an important role in neural development (Spatazza et al., 2013a; Nord et al., 2015). Researchers were led to transcription factor OTX2, due to its controlled expression along the visual pathway before the critical period begins (Nothias et al., 1998). A study exploring the experience-dependent nature of OTX2 release showed that enucleation of the eye

led to a significant decrease in the expression of OTX2 within the visual cortex (Sugiyama et al., 2008). Furthermore, increasing OTX2 expression prematurely, via direct infusions to the visual cortex, leads to a shift in the visual critical period window, such that the critical period starts and ends earlier. This study established that the transcription factor OTX2 links experience, to progression through the critical period.

Studies have extended the role of OTX2 and the progression of the critical period. First, it was shown that OTX2 regulates the formation of perineuronal nets (PNNs). PNNs are extracellular matrix structures that condense around neurons at the end of the critical period. They consist of chondroitin sulfate proteoglycans that form an inhibitory barrier to the creation of new neuronal processes and subsequently the formation of new synapses (Sorg et al., 2016). Heterozygous OTX2 knock out led to a considerable decrease in the density of PNNs within visual cortex (Sugiyama et al., 2008). More recent studies have shown that OTX2 actually binds to specific glucosaminoglycan sequences within PNNs, which leads to internalization of OTX2 by the cells encaged by PNNs. Disrupting the binding of OTX2 to PNNs in adulthood, disrupted the formation of PNNs and was sufficient to re-establish visual plasticity in adulthood (Beurdeley et al., 2012). This study was extended by showing that knocking down OTX2 expression in the neural location where OTX2 is produced (the choroid plexus) is also sufficient to re-open critical period plasticity in adulthood (Spatazza et al., 2013b). Similar results were found in the auditory system, in that disruption of OTX2 binding to perineuronal nets delayed the maturation of primary auditory cortex (Lee et al., 2017). Together, these results establish a complex role for OTX2 within critical period progression. OTX2 transfer to the cortex progresses the critical

period in an experience-dependent fashion, and through its actions on PNNs, holds the brain in a state of reduced plasticity, following the critical period.

OTX2 engages epigenetic mechanisms, which have been shown to change dynamically over the course of the critical period.

OTX2 produces significant genetic and structural changes in the region of sensory cortex to which it is transferred. Recent studies have illuminated an interaction between OTX2 internalization and modulation of DNA-ME. DNA-ME is an epigenetic mechanism in which a methyl-group is covalently attached to the 5-prime end of a cytosine. The carbon-carbon bond formed is chemically stable, thus requiring significant energy to demethylate (Jones, 2012). While DNA-ME is canonically associated with transcriptional repression (Jones et al., 1998; Martinowich et al., 2003), recent evidence suggests that DNA-ME can act to enhance transcription as well (Chahrour et al., 2008; Bahar Halpern et al., 2014; Torres et al., 2017), pointing to the possibility of DNA-ME as a broad regulator of gene transcription. The OTX2 protein was shown to have a DNA binding domain that recognizes a sequence within the promotor of the Gadd45b/g gene; a gene that codes for a DNA demethylase (Apulei et al., 2018). Injection of recombinant OTX2 protein directly into the visual cortex, significantly increased the expression of Gadd45b/g. However, OTX2 differentially effects Gadd45b/g during the CP and in adulthood, with OTX2 stimulating expression of Gadd45b/g early in development, but then having the exact opposite effect, repressing expression, on Gadd45b/g in adulthood. Together, these results indicate OTX2 may be exerting its effects on the cortex through its actions on epigenetic modifications.

In general, epigenetic modifications have been shown to be dynamically regulated over the course of the critical period (Fagiolini et al., 2009; Gallegos et al., 2018; Reh et al., 2020). Histone acetylation, the covalent addition of acetyl groups to histone proteins, is increased in visual cortex of juvenile animals relative to adult animals (Vierci et al., 2016). Furthermore, it was shown that exposing pre-critical period animals to environmental enrichment, accelerated the development of the critical period, and significantly increased the levels of histone acetylation relative to naïve juvenile animals (Baroncelli et al., 2016). Interestingly, the effects of early environmental enrichment could be mimicked by pharmacological injection of histone deacetylase inhibitors, indicating that similarly to OTX2 expression, experience is driving modulation of histone acetylation, which plays a role in regulating the critical period window.

As mentioned previously, OTX2 directly modulates expression of DNA demethylase, Gadd45b/g. Accordingly, DNA-ME patterns, are also shown to dynamically change over the course of the critical period. Bisulfite sequencing (MethylC-Seq) experiments have shown that in early development (between postnatal weeks 2 and 4) frontal cortical and dentate granule neurons rapidly accumulate DNA-ME that persists into adulthood (Lister et al., 2013; Guo et al., 2014). Interestingly, this developmental methylation is usually in the CH context (H referring to any nucleotide that is not guanine) rather than the CG context, and leads to CH methylation being the dominant form of methylation in human neurons. In the visual cortex, induction of ocular dominance plasticity via monocular deprivation during the critical period stimulates the expression of DNA methyltransferase 3A (DMNT), the protein that catalyzes the addition of methyl groups to DNA (Tognini et al., 2015). Pharmacological inhibition of DNA-ME addition via RG108, blocked the ocular dominance shift that usually comes with monocular deprivation

during the critical period, indicating that experience-dependent DNA-ME during the critical period is necessary for the expression of ocular dominance plasticity (Tognini et al., 2015). Furthermore, global knock out of MeCP2 (a methyl-binding protein, and one of the primary effectors of DNA methylation) accelerated the functional maturation of the visual cortex, and accordingly the closure of the visual critical period (Krishnan et al., 2015). Conditional knock out of MeCP2 in parvalbumin-positive neurons (an important inhibitory neuron subtype for critical period dynamics), completely abolished the visual critical period (He et al., 2014). These results indicate that experience-dependent DNA methylation, and the action of its effectors, plays a crucial role in proper post-natal development, but more research is required to better understand its role in regulating critical period plasticity.

Sensory cortex undergoes extensive transcriptional changes during the critical period.

Considering the significant epigenetic modulation that occurs during the critical period, it follows that cortical neurons also experience considerable transcriptional modulation. The transcriptional change is believed to facilitate the functional changes that eventually leads to the closure of the critical period (Gallegos et al., 2018). Early studies investigating transcriptional change in the visual cortex during the critical period showed that at different timepoints throughout the critical period, cortical neurons express distinct sets of gene. Furthermore, they showed that restricting visual experience, via a dark-rearing paradigm, drastically altered the expression of age-dependent gene sets, thus connecting experience to proper transcriptional regulation, and progression through the critical period (Majdan and Shatz, 2006). Many subsequent studies have confirmed the importance of experience-dependent gene regulation in critical period plasticity (Tropea et al., 2006; Lyckman et al., 2008; Sakai and Sugiyama, 2018).

One of the most prominent shifts in expression comes from the calcium buffer protein, Parvalbumin. Parvalbumin has been shown to increase its expression by 30-fold, over the course of the critical period (Okaty et al., 2009). PV interneurons are the most abundant inhibitory interneuron in the brain, and because of this, play a large role in balancing excitatory and inhibitory inputs (Kelsom and Lu, 2013). The development of PV neurons has been shown to be regulated by OTX2 release, which is preferentially internalized by PV neurons (Sugiyama et al., 2008; Beurdeley et al., 2012). This follows with results showing that the maturation of PV neurons is sensitive to the amount and quality of experience the organism has encountered, just as OTX2 release was shown to be similarly dependent (Chattopadhyaya et al., 2004; de Villers-Sidani et al., 2008). The maturation of PV interneurons has been shown to play a significant role in the regulation of critical period plasticity. The acquisition of mature firing and expression profiles within PV neurons, correlates with the end of the critical period, and the drop in plasticity (Hensch, 2005b, a; Reh et al., 2020). Furthermore, inserting newly born inhibitory neurons into an adult visual cortex was sufficient to re-open the visual critical period (Southwell et al., 2010; Tang et al., 2014). Recently, studies show that chemogenetic inactivation of PV interneurons was also sufficient to re-open auditory critical period plasticity in adulthood (Cisneros-Franco and de Villers-Sidani, 2019).

Okaty et al. 2009 performed microarray analysis specifically on fast-spiking PV interneurons to track their transcriptional maturation over the course of the critical period. The studies showed that changes in gene expression correlated strongly with change in electrophysical properties of these neurons. Specifically, PV inhibitory interneurons show a narrowing of the spike wave

form, decrease in the spike frequency adaptation, and accordingly a significant increase in firing frequency, as the critical period progresses (Okaty et al., 2009). These functional characteristics correspond to changes in the expression of many genes coding for ion channels such as an increase in KCNC1 and 2, which contributes to spike repolarization, a decrease in KCNN2, which underlies spike frequency adaptation, and an increase in SCN8a and 4b, which facilitate high frequency firing (Figure 1.4). The significant increase in expression of PV itself (a calcium buffer), also facilitates the high frequency firing behavior of PV interneurons. Together, this data reveals that gene expression profile changes facilitate functional maturation of cortical cell types and this functional maturation is dependent on proper exposure to sensory experience.

Functional changes in neuronal firing properties shifts excitatory/inhibitory balance in the cortex, which influences the critical period window.

As previously mentioned, the genome-wide transcriptional changes in cortical neurons yields a significant shift in their functional properties. For PV neurons, the functional shift leads to a significant increase in firing rate (Okaty et al., 2009). Due to the role PV neurons play in regulating excitatory gain (Isaacson and Scanziani, 2011; Kelsom and Lu, 2013), this increase in their firing rate has a significant effect on network activity within the cortex. This concept underlies a well-established understanding that rising levels of inhibition during the critical period influence the excitatory-inhibitory balance in the brain, which directly regulates the plastic window (Hensch and Fagiolini, 2005).

In the cortex, excitatory synaptic connections develop before inhibitory connections, leading to increased excitation relative to inhibition early in development (Zhang et al., 2011; Reh et al.,

2020). As the critical period progresses, inhibitory connections begin forming leading to steadily increased levels of inhibition, and the ratio between excitation and inhibition approaches one. This concept is supported by data from Okaty et al 2009, which showed that as the critical period progresses, the ratio of mEPSC:mIPSC frequency, within somatosensory cortex, drops by nearly a factor of 4, leading to the frequency of mEPSC's nearly equaling the frequency of mIPSC's. Just as the other factors regulating critical period plasticity (OTX2 release, epigenetic modulation, gene expression changes), the developmental increase in inhibition is sensitive to experience. Depriving animals of light from birth, abolishes the developmental increase in inhibition levels during the critical period (Morales et al., 2002).

Seminal studies from the Hensch lab first established that genetic and pharmacological manipulations of inhibition levels can modulate the opening and closing of the critical period. These studies showed that knock out of GAD65, an enzyme that catalyzes the production of GABA, abolishes the capability for critical period plasticity. This effect can be rescued and critical period plasticity restored by cortical infusions of benzodiazepenes, which boost GABA function, indicating that the critical period window is sensitive to the levels of inhibition in the network (Hensch, 1998). This finding was extended to show that benzodiapenes infused before the critical period both prematurely open and close the visual critical period (Iwai et al., 2003). Furthermore, reduction of inhibition levels in adulthood, is sufficient to re-instate critical period plasticity (Sale et al., 2007). Together, these data suggest a two-threshold mechanism for opening and closing the critical period. One inhibitory threshold opens the critical period, while progressively increasing levels of inhibition during the critical period eventually leads to a

second inhibitory threshold which closes the critical period (Takesian and Hensch, 2013; Ribic and Biederer, 2019).

Homeostatic plasticity establishes new baselines for excitation and inhibition within the cortex. This introduction has primarily focused on associative forms of plasticity when describing activity-dependent changes. For example, the experience-dependent map change that occurs with exposure to sounds is believed to be mainly dictated by spike-time dependent plasticity, and associative LTP and LTD (Buonomano and Merzenich, 1998; Dahmen et al., 2008). A similar mechanism has been proposed for the shaping of whisker columns within the barrel cortex of rodents (Celikel et al., 2004). The visual system differs in that inducing the primary form of visual critical period plasticity, ocular dominance plasticity, engages two different plasticity mechanism. Monocular deprivation initially induces an LTD-dependent reduction in strength of input from the deprived eye. However, a later mechanistic step boosts the strength of input from the non-deprived eye (Kaneko et al., 2008). The theory is that in the absence of input from the deprived eye, the non-deprived eye homeostatically increases the strength of its input, to ensure a baseline of neuronal activity within the visual cortex is met. This form of activity regulation exemplifies what is known as homeostatic plasticity.

Homeostatic plasticity was initially theorized from computational models which suggested that associative forms of plasticity are often destabilizing, and thus there must be a stabilizing form of activity regulation within the brain to counteract the instability brought from LTP and LTD (Miller, 1996). The discovery of what is now referred to as synaptic scaling, has provided experimental evidence for the presence of homeostatic plasticity (Turrigiano, 2012). Inducing

activity blockade in cultured neurons via TTX or CNQX significantly increased mEPSC amplitude, while blockade of GABA mediated inhibition via bicuculine significantly decreased the mEPSC amplitude, indicating neuronal circuits have a way of monitoring their activity levels and regulating it within a set-point (Turrigiano et al., 1998). Researchers have discovered multiple molecular regulators of homeostatic plasticity such as tumor-necrosis factor alpha (TNF-α), retinoic acid, and arc/arg3.1 (Yee et al., 2017). TNF-α has been shown to be especially important to the regulation of homeostatic plasticity (Heir and Stellwagen, 2020). Specifically, TNF-α has been shown to be necessary for the expression of context-dependent synaptic scaling, of both inhibitory and excitatory synapses *in vitro*, and *in vivo* (Ogoshi et al., 2005; Stellwagen and Malenka, 2006; Steinmetz and Turrigiano, 2010; Pribiag and Stellwagen, 2013; Becker et al., 2015; Heir and Stellwagen, 2020).

Homeostatic forms of plasticity have been shown to play an active role during the critical period. In the visual system, other than mediating the second component of ocular dominance plasticity, synaptic scaling was found to stabilize cortical circuitry during peak synaptogenesis. From PN day 12 to PN day 23, there is a significant increase in mEPSC frequency, as well as a concomitant decrease in mEPSC amplitude. This homeostatic change in the synaptic amplitude and frequency of response within visual cortex is prevented by dark rearing (Desai et al., 2002). Interestingly, there may be a critical period window for induction of homeostatic plasticity. For example, induction of homeostatic plasticity during the second PN week of development in the visual system can only occur in layer 4. Synaptic scaling within layer 2/3 cannot be induced until PN 21 (Turrigiano and Nelson, 2004). Together this data implicates homeostatic plasticity as an important factor in critical period plasticity. However, most of the evidence of homeostatic

plasticity's role during the critical period comes from the visual system, which as mentioned previously, engages different plasticity mechanisms than the auditory and somatosensory systems. Therefore, more research is needed to extend our understanding of the role homeostatic plasticity plays within the developing auditory system.

Unanswered questions

The evidence discussed above depicts a logical mechanism for regulation of critical period plasticity. To summarize, spontaneous activity facilitates pre-wiring of sensory pathways prior to the onset of sensory experience. Once the onset of hearing begins, the critical period opens, allowing sensory experience to shape cortical and subcortical sensory maps to the environment the organism exists within. As new connections form, homeostatic mechanisms progressively stabilize cortical networks to accommodate the considerable increase in synaptic transmission. Experience both wires the cortex, and progressively pushes it to a less plastic state through the experience-dependent release of OTX2 from the choroid plexus. The transfer of OTX2 from the choroid plexus leads to internalization of OTX2 by precursor PV neurons. OTX2 engages epigenetic mechanisms to shift the transcriptional profile of PV neurons, which in turn changes PV neuron function. The consequence of this PV neuron functional change is a significant increase in firing frequency from the most common class of inhibitory interneuron in the central nervous system, which in turn shifts the balance of excitation to inhibition in the cortex. The experience-dependent increase in inhibition eventually leads to a specific threshold of inhibition being met, which is hypothesized to close the critical period. This well-established mechanism provides researchers with a strong readout of the plasticity levels within the brain. In addition to directly assessing experience-dependent plasticity, researchers can measure factors such as the

ratio of excitation to inhibition at cortical synapses, or the levels of gene expression for proteins such as parvalbumin or BDNF, to access the plasticity state of the brain. While much of the mechanism of critical period plasticity regulation is established, there are still questions that remain, that if answered, may reveal important information regarding the regulation of plasticity within the central nervous system.

One question that remains is the exact role of DNA methylation during the critical period. There are conflicting reports regarding changes in methylation patterns over the course of the critical period. MethylC-Seq experiments reveal an increase in DNA methylation concentration during the first two post-natal weeks (Lister et al., 2013; Guo et al., 2014), while fluorescent imaging experiments for MeCP2 during the critical period indicate a general shuffling of methylation patterns rather than a gross increase or decrease in concentration (Apulei et al., 2018). Furthermore, there are conflicting results on DNA methylation's relationship to cortical plasticity. One report indicates that inhibition of DNA methylation during the critical period abolishes critical period plasticity, indicating a faciliatory role of DNA methylation to plasticity (Tognini et al., 2015). Another report shows that overexpressing a DNA demethylase re-opens critical period plasticity in adulthood, indicating that methylation may also have an inhibitory role to critical period plasticity (Apulei et al., 2018). The experiments presented in chapter 2 seek to answer these questions.

Another question that remains is the role that homeostatic plasticity plays in the auditory critical period. In the visual system, homeostatic plasticity facilitates the late phase of ocular dominance plasticity by upregulating the strength of input from the non-deprived eye (Kaneko et al., 2008).

In the auditory system, homeostatic plasticity has been shown not to be necessary for the expression of frequency map plasticity (Yang et al., 2014b). TNF-α knock out animals retain the capacity for frequency map plasticity during the critical period. However, the maps of TNF-α knock out animals look immature in that they do not contain the full assortment of frequencies, and the tonotopicity is decreased (Yang et al., 2014b). This opens the possibility that in the auditory system of TNF-α knock out animals, the critical period never closes. This establishes an interesting question regarding the role of homeostatic plasticity in closing the critical period, which is discussed at length in the experiments presented in chapter 3.

The final question this thesis explores is the idea of sensory experiences and stimuli re-opening critical period in adulthood. There have been multiple studies that show this is possible through degradation of PNNs, manipulation of PV neuron function, and even environmental enrichment (Pizzorusso et al., 2002; Sale et al., 2007; Baroncelli et al., 2016; Cisneros-Franco and de Villers-Sidani, 2019). One stimulus that may induce critical period plasticity is traumatic brain injury. Previous reports from our lab indicate that traumatic injury to the auditory system through blast exposure, yields significant changes to the primary auditory cortical frequency map (Masri et al., 2018). However, it is unclear if the changes to the frequency map of blast-exposed animals occurred due to re-wiring caused by increased plasticity, or if these changes are just indicative to the degree of damage that has occurred along the auditory pathway. Furthermore, evidence from our lab suggests that noise-induced hearing lesions shift the balance of excitation and inhibition in the cortex in a TNF-α dependent fashion (Wang et al., 2019), indicating certain markers indicative of increased plasticity are present following noise-induced hearing damage. Chapter

four of this thesis seeks to elucidate the relationship between noise-induced neural damage, and regulation of plasticity within the brain.

1.2: Figures

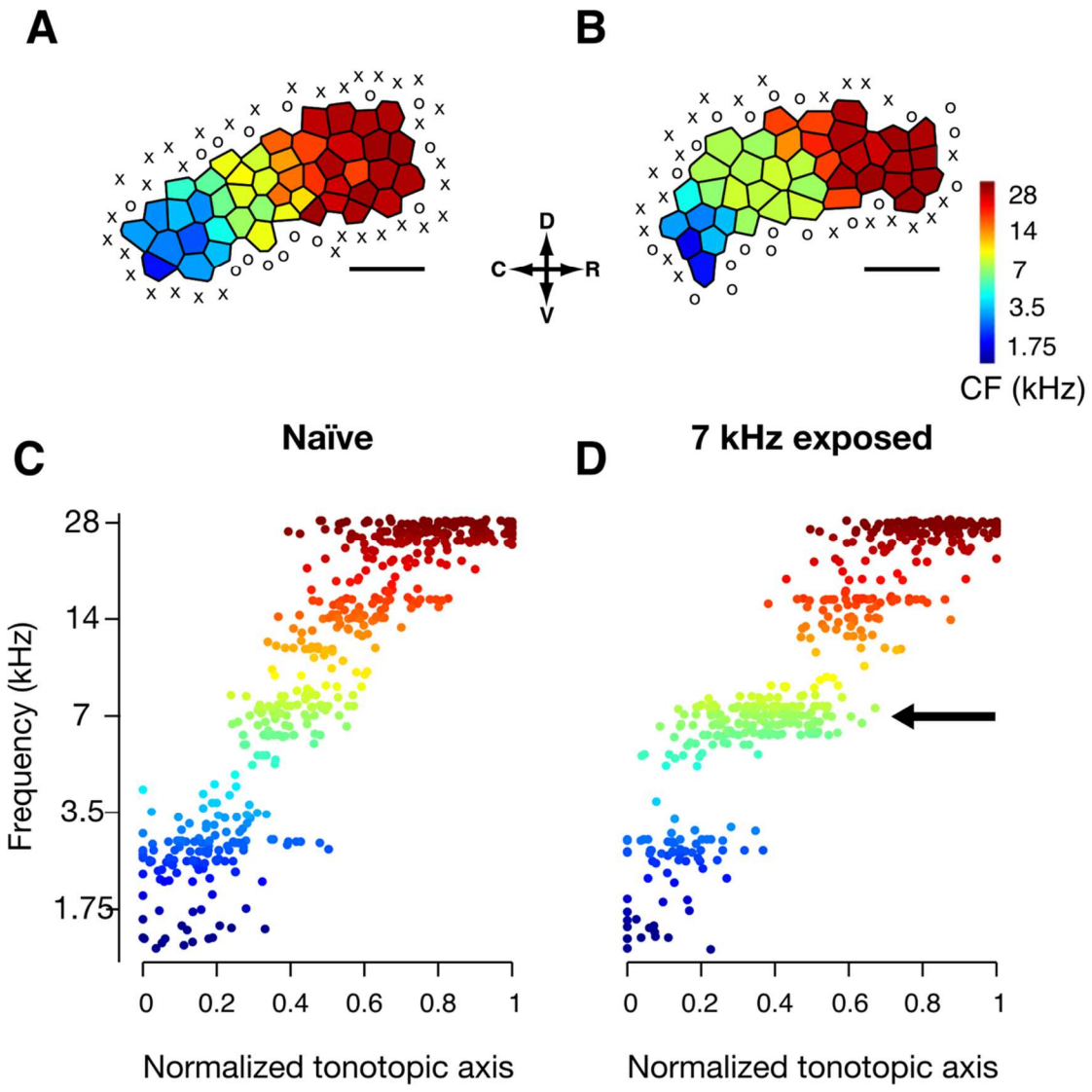

Figure 1.1: Effect of critical period exposure on A1 characteristic-frequency maps. A and **B)** Examples of characteristic-frequency maps for a naïve animal, and one for an animal exposed to 7 kHz pure tones. **C and D)** Plots showing the distribution of characteristic frequencies for naïve and exposed animals. Exposure causes a shift in the distribution of characteristic frequencies towards the exposure frequency (Villers-Sidani, 2007).

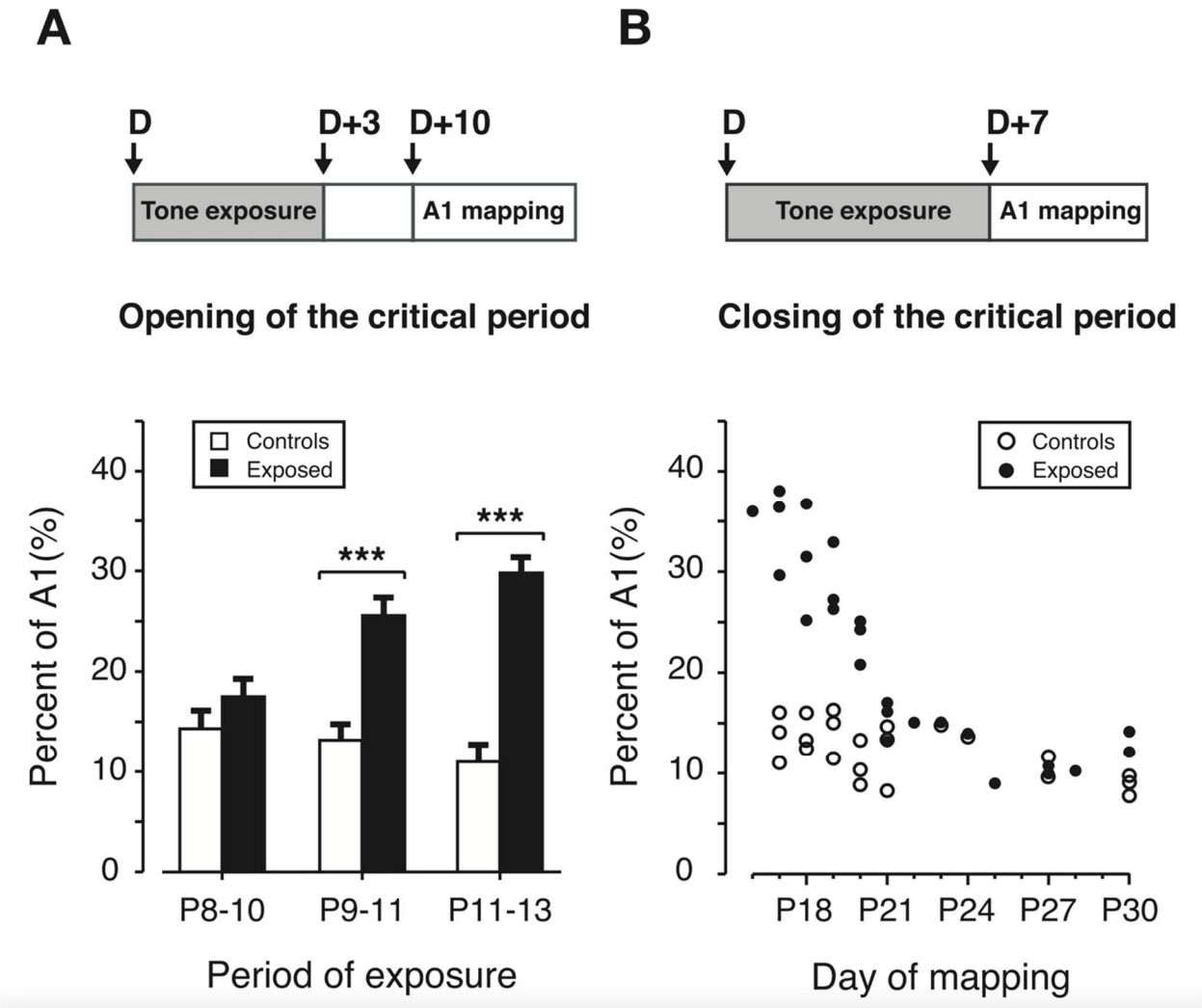

Figure 1.2: Opening and closing of the critical period. A) Schematic of exposure paradigm used to isolate the opening of the critical period. Researchers determined the critical period opens around PN day 9 or PN day 10. **B)** Schematic of exposure paradigm used to isolate the end of the critical period. The ability to induce frequency map changes drops precipitously when exposure begins after PN day 13 or PN day 14. (Villers-Sidani, 2007)

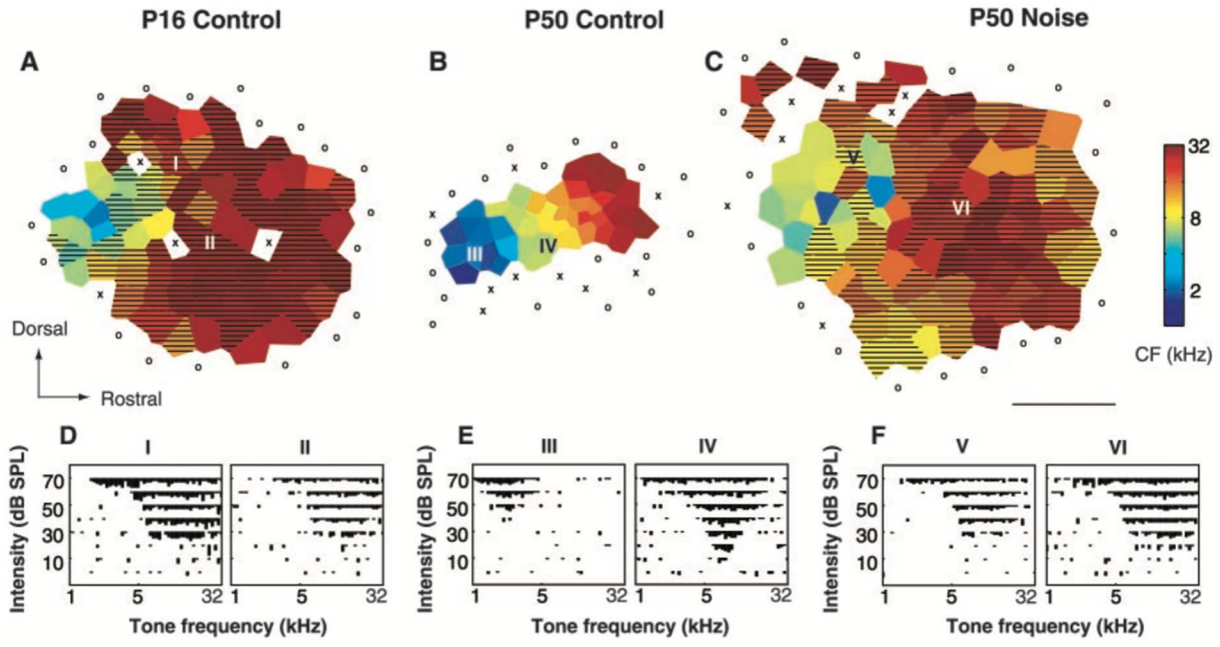

Figure 1.3: Developmental organization of the auditory cortex is prolonged by noise rearing. A) Representative characteristic frequency map for an animal still in the developmental critical period. **B)** Representative characteristic frequency map for an adult naïve animal. **C)** Representative characteristic frequency map for an animal exposed to white noise through PN day 50. Animals exposed to white noise over the duration of the critical period retain an immature frequency map. **D, E and F)** Representative receptive fields from each of the experimental groups. Animals held in white noise retain immature characteristics of receptive fields such as increased bandwidth. Adapted from (Chang and Merzenich, 2003)

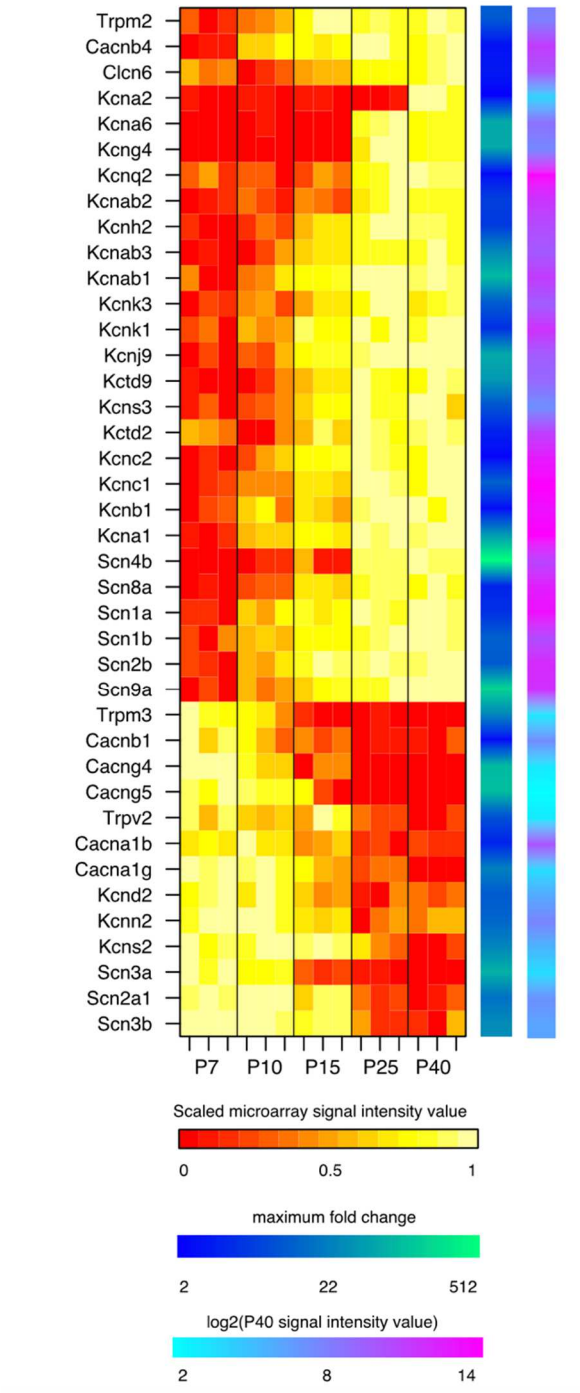

Figure 1.4: Developmentally regulated ion channels. Heat map depicting the significant change in ion channel gene expression that occurs within PV+ neurons over the course of the somatosensory critical period. Adapted from (Okaty et al., 2009)

2

Pharmacological DNA Demethylation Weakens Inhibitory Synapses in the Auditory Cortex and Re-Opens the Critical Period for Frequency Map Plasticity

Adapted with permission from: Schwartz BA, Wang W, Bao S (**2020**) Pharmacological DNA Demethylation Weakens Inhibitory Synapses in the Auditory Cortex and Re-opens the Critical Period for Frequency Map Plasticity. *Neuroscience* 440:239-248

2.1: Abstract

The critical period is a time of maximal plasticity within the cortex. The progression of the critical period is marked by experience-dependent transcriptional alterations in cortical neurons, which in turn shifts the excitatory-inhibitory balance in the brain, and accordingly reduces plasticity. Epigenetic mechanisms, such as DNA methylation, control the transcriptional state of neurons, and have been shown to be dynamically regulated during the critical period. Here we show that adult animals have a significantly higher concentration of DNA methylation than critical period animals. Pharmacological reduction of DNA methylation in adult animals re-establishes critical period auditory map plasticity. Furthermore, the reduction of DNA methylation in adult animals, reverted intrinsic characteristics of inhibitory synapses, and gene expression, to an immature state. Our data suggest that accumulation of DNA methylation during the critical period confers a mature phenotype to cortical neurons, which in turn, facilitates the reduction in plasticity seen after the critical period.

2.2: Introduction

The critical period (CP) is a developmental epoch of heightened cortical plasticity (Hensch, 2005a). Throughout the CP, experience drives the wiring of cortical circuits that refines sensory maps and motor maps (O'Leary, 1994; Katz and Crowley, 2002; Villers-Sidani, 2007). Once the CP is closed, plasticity within the sensory cortex decreases considerably, and requires additional neuromodulatory mechanisms for induction (Keuroghlian and Knudsen, 2007). Elucidating the mechanisms that facilitate plasticity during the CP and the mechanisms that restrict plasticity in adulthood, is vital for understanding how plasticity is regulated in the brain.

The progression of the CP is marked by experience-dependent maturation of inhibitory neurons (Hensch, 1998; Dunning et al., 1999; Huang, 1999; Fagiolini, 2000; Itami et al., 2007) and a shift in the transcriptional profile of these cells (Majdan and Shatz, 2006; Okaty et al., 2009). Recently, studies have begun to probe the contribution of DNA-ME to CP dynamics. Sequencing experiments have shown during early development frontal cortical and dentate granule neurons rapidly accumulate DNA-ME that persists into adulthood (Lister et al., 2013; Guo et al., 2014). Overexpression of GADD45b, a protein involved in activity-dependent DNA demethylation, reopened ocular dominance plasticity in adult mice, suggesting that DNA demethylation enhances plasticity (Apulei et al., 2018). However, inhibition of DNA-ME during the CP via RG108 blocked ocular dominance plasticity, suggesting a facilitating role of DNA-ME on plasticity (Tognini et al., 2015). Conditional knockout of MeCP2 (a methyl-binding protein and one of the primary effectors of DNA-ME) in parvalbumin positive interneurons also blocked ocular dominance plasticity in the critical period (He et al., 2014). These results suggest that

DNA-ME plays a crucial role in postnatal development, but more research is required to understand its role in regulating critical period plasticity. In this study, we measured global levels of DNA-ME in the auditory cortex of adult and CP mice using a quantitative colorimetric ELISA. Adult mice had significantly higher levels of DNA-ME compared to CP mice. Pharmacological DNA demethylation of adult mice, via 5-aza2'-deoxycytidine (5-aza) injections, re-opened CP auditory map plasticity in adult mice, while vehicle injections did not. Global DNA demethylation in adult mice decreased the frequency and increased the decay time constant of miniature inhibitory synaptic currents (mIPSC's) onto pyramidal cells, indicating a shift towards an immature state of inhibitory synapses that is seen during the CP. RT-PCR experiments revealed that BDNF and REST, two genes that are developmentally regulated, and heavily implicated in the maturation of the cortex (Hanover et al., 1999; Huang, 1999; Ballas et al., 2005; Rodenas-Ruano et al., 2012) reverse their transcription levels back to critical period levels. Overall, these results suggest that global levels of DNA-ME influence the maturation of cortex and reducing global levels of DNA-ME can re-open the critical period by reversing characteristics of cortical maturation.

2.3: Methods

Animals: All procedures in this study were approved by the Animal Care and Use committee at the University of Arizona. WT (FVB.129P2-Pde6b^{+}Tyr$^{c\text{-}ch}$/AntJ) mice were originally obtained from The Jackson Laboratory. Both females and males were used in these experiments. A total of 64 mice were used for this experiment.

Sound Exposure: Sound exposure was performed as previously described (Zhang et al., 2001). Litters of 2 to 5 mice were placed in a ventilated, sound-shielded, calibrated test chamber for 7-14 days (depending on the experiment) and exposed to 16 kHz pure tone pips, or tone pips spanning 2kHz-48kHz (acoustic enrichment). A 25-ms tone (5-ms ramps) at 60–70 dB SPL was applied from a speaker placed about 15 cm above the mice, at 6 pulses per second with 1-s intervals to minimize adaptation effects. No noticeable distortion of tonal stimuli was detected from sound spectrum recorded inside the test chamber. There were no significant spectral peaks for the normal environmental noise background. The total sound pressure level in the animal room was 5–10 dB lower than that of exposed tonal stimulus intensity. Inside the sound attenuation chamber with the presence of mice, but in the absence of the tone stimulus, the noise level was about 15–25 dB below that in the animal room at all frequencies within the mouse's hearing spectrum. No significant harmonic signal was found in the chamber when a tonal stimulus was being delivered. Pharmacological inhibition of DNA methyltransferase was achieved using 5-aza2'-deoxycytidine (Chabot et al., 1983; Sales et al., 2011). Adult mice between p60-p120 were injected intraperitoneally with either 2 mg/kg of 5-aza (mixed with DMSO and filtered 1X PBS) or a vehicle injection of just DMSO and filtered 1X PBS. These injections were repeated for 7 days, at approximately the same time every day.

Electrophysiological recording procedure: The primary auditory cortex (AI) of mice was mapped as previously described (Kim et al., 2013), except as follows. Mice were anesthetized with ketamine (100 mg/kg, i.p.) and xylazine (10 mg/kg, i.p.), and kept anesthetized with, a steady flow of 1% isoflurane. The cortex was maintained under a layer of silicone oil, that was reapplied as necessary. Multiunit responses to 25 ms pure tone pips (2–74 or 4 –74 kHz, 0.1 octave increments

at 0–70 dB, 10 dB increments) were recorded using tungsten microelectrodes (FHC) in the thalamorecipient layer of AI (350 – 450 micrometers below the cortical surface). References to neurons in this text refer to multiunit responses recorded extracellularly. Tones were presented to the left ear through an electrostatic speaker (Tucker Davis Technologies) at 3 pips per second and each frequency-intensity combination was repeated three times. Cortical penetration locations were recorded on a high-resolution image, which was later used to construct the map.

AI mapping analysis: Receptive fields and response properties were isolated using custom-made programs in MATLAB as previously described (Insanally et al., 2010), except as follows. The peak of the peristimulus time histogram (PSTH) within a window from 7 to 50 ms after the stimulus onset was defined as the response latency. The response window was defined as a period encompassing the PSTH peak, in which the firing rate was higher than the baseline firing rate. The spikes in the response window were counted to reconstruct the receptive field. The map of AI was generated using the voroni tessellation algorithm, in which the characteristic frequency (CF) of the receptive field is converted to a polygon of a certain area. The area of the polygons dedicated to a CF of 16 kHz (+/- .2 octaves) were summed and then divided by the total area to determine the percent of AI dedicated to 16 kHz. For comparing the ratio of area dedicated to 16kHz, to low frequency, the area of the polygons dedicated to 9.2 kHz and 12.1 kHz (+/- .2 octaves) were summed. We then divided the area dedicated to 16 kHz by the summation of the area dedicated to the two low frequency bins.

AI dissections/DNA extractions/DNA methylation quantification: Mice were anesthetized with ketamine (100 mg/kg, i.p.) and xylazine (10 mg/kg, i.p.). Mice were then perfused with cold 1X

PBS for 10 minutes. Following perfusion, mice were decapitated, and their brains harvested. In a dish filled with cold 1X PBS, the brain was cut just in front of the inferior colliculus, and just behind the region where the two hemispheres connect. The auditory cortex, which is 1 mm above the rhinal fissure, was subsequently dissected from both hemispheres. DNA from these tissue samples were then extracted using the QIAamp Fast DNA Tissue kit. Final DNA concentrations were then measured using a nanodrop. The samples of extracted DNA were then subjected the MethylFlash Methylated DNA 5-mC Quantification kit for quantification DNA-ME. This kit utilizes a colormetric assay with an antibody specific to 5-mc to measure global levels of DNA-ME.

Patch Clamp: Patch clamp electrophysiology was conducted on mice that were injected with 5-aza or treated as different conditions exposure as described below ($n \geq 4$ mice for each group). The brain was extracted and immediately placed in an oxygenated (95% O2/5% CO2) external solution (87 mM NaCl, 2.5 mM KCl, 7 mM MgCl2, 25 mM D-glucose, 25 mM NaHCO3, 1.25 mM NaH2PO4, 0.5 mM CaCl2, and 75 mM Sucrose at pH 7.3). The brain was sectioned along the transverse plane into 300 μm slices with a vibrating microtome (Leica; VT1000S), and brain slices were immersed in oxygenated external solution in a tissue chamber for 30 min at 32.5˚C. Then slices were allowed to acclimate to room temperature for at least 30 min before recording. The recording chamber was continuously perfused with oxygenated artificial cerebrospinal fluid (aCSF) (125 mM NaCl, 2.5 mM KCl, 1 mM MgCl2, 25 mM D-glucose, 25 mM NaHCO3, 1.25 mM NaH2PO4 and 2 mM CaCl2 at pH 7.3) at a rate of 2 mL/min and maintained at 32°C. A fixed stage microscope (Olympus; BX51WI) equipped with differential interference contrast optics and a 40× water-immersion objective was used to visualize individual neurons in the AI.

Patch electrodes had an impedance of 3–5 MΩ when back-filled with the internal solutions for miniature inhibitory postsynaptic currents (mIPSCs) measurement (135 mM CsMs, 10 Mm CsCl, 10 mM Hepes, 0.2 mM EGTA, 4 mM ATP-Mg, 0.4 mM GTP-Na at pH 7.3 and 290 mOsm). The initial access resistance typically ranged from 15 to 23 MΩ and remained stable during the recording session. Series resistance was also continuously monitored with a brief voltage pulse. Recordings were accepted when a cell had a series resistance of 15–25 MΩ (<20% change during the recording session). mIPSCs were recorded in oxygenated aCSF solution containing 1 μM Tetrodotoxin (TTX), 20 μM 6-Cyano-7-nitroquinoxaline-2,3-dione (CNQX), and 100 μM D-2-amino-5-phosphonovalerate (DAP5). Cells were held at 0 mV throughout the experiment. Signals were low pass filtered at 2kHz. Experiments were conducted using Axon Instruments hardware and software (MultiClamp 700B, Digidata 1550A, pClamp 10.5). 0.3% biocytin was added into the internal solution before recording to identify the morphology of pyramidal cells. After recording, data were collected and analyzed with pCLAMP software (Molecular Devices) and MiniAnalysis (Synaptosoft). Slices were prepared from four or more mice for each group, and only one neuron was recorded from each slice. Data analysis shown for both individual neurons as well as the averages per animal in each experimental group.

Quantitative real-time PCR: The harvesting of AI tissue was accomplished in the same way described in the "AI dissections/DNA extractions/DNA methylation quantification" section. The only difference is the tissue samples were stored in an RNA stabilizing reagent, RNA *later* (Qiagen). RNA was extracted from the tissue using the Quick-RNA mini prep kit (Zymo

Research). Immediately following extraction, the total RNA concentration and A260:A280 ratio of each sample were determined via NanoDrop 2000 (Thermo Scientific). The High Capacity cDNA Reverse Transcription kit (Thermo Fischer) was used to generate cDNA in a thermal cycler (ABI9700) for 2 hours at 37°C. Ten nanograms of cDNA were used in each reaction for real-time PCR using the CFX96 Real-Time PCR system (Bio-Rad Laboratories, Hercules, CA). Threshold cycle (Ct) values of the target genes were normalized to the endogenous control gene (GAPDH). The primer sequences are as follows: GAPDH; Forward- ACCTTTGATGCTGGGGCTGGC, Reverse- GGGCTGAGTTGGGATGGGGACT, BDNF; Forward- CAGGAGTACATATCGGCCACCA, Reverse- GTAGGCCAAGTTGCCTTGTCCGT, REST; Forward- CATGGCCTTAACCAACGACAT, Reverse- CGACCAGGTAATCGCAGCAG.

Statistical analysis: Statistical analyses were conducted using SPSS software. When comparing two groups, independent samples t-test was used, unless the distribution wasn't normal, in which case a Mann-Whitney U test was used. Group comparisons of variables were made using a one-way analysis of variance (ANOVA) followed by a *post hoc* least significant difference (LSD) test, unless the data was not homoscedastic, in which case a Kruskal-Wallis H test followed by a *post hoc* Dunn Test with Bonferonni correction for multiple comparisons was performed. Homogeneity of variance was tested using Levene's test (based on median), and normality was t ested using the Kolmogorov-Smirnov test with Lilliefors Significance Correction. A $p < 0.05$ was considered statistically significant.

2.4: Results

Reducing global levels of DNA-ME re-establishes auditory critical period map plasticity

Recent evidence suggests that frontal cortical and dentate granule neurons accumulate DNA-ME over the course of development (Lister et al., 2013; Guo et al., 2014). To confirm that this phenomenon also occurs in sensory cortex, we performed a colorimetric ELISA to measure global levels of DNA-ME in the auditory cortex of adult mice, and mice in the CP. Adult mice between the ages of 2-4 months (n=12), and CP mice (n = 6) at post-natal (PN) day 11 were sacrificed, and their brains harvested for DNA-ME analysis. An independent samples t-test showed that the auditory cortices of adult mice had a significantly higher concentration of DNA-ME than auditory cortices of CP mice ($t_{11.53}$=2.97, degrees of freedom adjusted due to unequal variance, p = 0.012; Figure 2.2 A). These results indicate that along with frontal cortical and subcortical structures, neurons within sensory cortex also accumulate DNA-ME over the course of development.

These results led us to hypothesize that if neurons in the auditory cortex accumulate DNA-ME over the course of development, then reducing the global DNA-ME levels may return adult cortex to a more plastic state as is seen in the critical period. To test this hypothesis, we probed the level of plasticity in the AI frequency map of five different experimental groups (Figure 2.1). The first group were Naïve mice that received no injections nor exposure (Naïve; n = 5). The second group were CP mice exposed to 16 kHz tone pips from PN9 until the day of A1 mapping (PN19-PN23) (CP-expo; n = 5). The third group were adult mice between the ages of 2-4 months that received 7 days of 5-aza injections concurrently with 10-14 days of 16 kHz exposure (Dem-expo; n = 5). The fourth group was a group of adult mice injected with vehicle and concurrently exposed to 16 kHz for 10-14 days (Veh-expo; n = 5). Finally, the fifth group was a group that received 7 days of 5-

aza injections without exposure and were subsequently mapped the day after the final injection (Dem; n = 4). Compared to the Naïve group, both CP-expo and Dem-expo groups showed a significant increase in the average area in AI dedicated to the exposure frequency of 16 kHz, (ANOVA: $F_{4,19}$=20.36, $p < 0.0005$; post hoc LSD: $p < 0.0005$ for both groups, Figure 2.2 B and E). The Veh-expo group, as well as the Dem group, did not show such an increase in the representation of the exposed frequency (post hoc LSD: $p = 0.264$, and $p = 0.922$ respectively). This indicates that neither demethylation, nor sound exposure alone was sufficient to induce a significant expansion in the 16 kHz frequency band of AI in adult mice. We also analyzed the ratio of the area dedicated to 16 kHz to the area dedicated to a low frequency bin (from 8 kHz to 13.91 kHz), in the five experimental groups. The CP-expo and Dem-expo groups showed an increase in the 16 kHz to low frequency area ratio relative to Naïve (Figure 2.2 C; ANOVA: $F_{4,19}$=10.90, $p < 0.0005$; post hoc LSD $p< 0.0005$, and $p=0.002$ respectively). No increase was seen in the 16 kHz to low frequency area ratio for either the Veh-expo nor Dem mice, relative to Naïve mice (post hoc LSD: $p = 0.544$, and $p = 0.729$ respectively). To verify that 5-aza was in fact reducing global methylation levels, we performed another colorimetric ELISA on auditory cortex samples from 5-aza treated mice (n=4) and vehicle treated mice (n=8). Results from the ELISA confirmed that 5-aza treatment facilitated global demethylation. (Figure 2.2 D; Mann-Whitney U test: $U_{8,4}$=2.0, $p = 0.016$). These results indicate that reducing DNA-ME in adult mice can re-establish auditory frequency map plasticity similar to that observed in the critical period.

As previously mentioned, DNA demethylation via overexpression of GADD45b, was sufficient to re-open the critical period for ocular dominance plasticity within primary visual cortex (Apulei et al., 2018). That study also showed that overexpression of GADD45b led to a significant decrease

in overall sensory response strength in both eyes. Therefore, we analyzed the average threshold for receptive fields collected from the five experimental groups, to determine whether pharmacological DNA demethylation also induced a general depression in sensory response. The CP-expo mice had a significantly lower average threshold for auditory evoked signal in AI, relative to the other experimental groups (Figure 2.3 A; ANOVA; $F_{4,19} = 10.52$, $p < 0.0005$; *post hoc* LSD: $p < 0.0005$ [CP-expo compared to Naïve]). Treatment with 5-aza did not significantly alter average threshold relative to the Naïve group for either the dem nor dem-expo group (*post hoc* LSD: $p = 0.139$ and $p = 0.813$, respectively). We also analyzed the average response amplitude between the five groups, and found an overall significant difference between the groups (data not shown: Kruskal-Wallis H Test; $H_4=10.1$, $p < 0.039$). *Post hoc* analysis showed a significant increase in response amplitude for the CP-expo relative to the Naïve group (group means: CP-expo= 10.26 spikes/tone, Naïve = 7.77 spikes/tone; *post hoc* Dunn Test: $p = 0.015$), but there were no significant differences between the Naïve group and the other experimental groups (*post hoc* Dunn Test: $p > 0.05$ for all other groups relative to Naïve). Other receptive field features, such as response latencies, have been shown to change over the course of the critical period. Response latencies decrease most dramatically during the critical period, but continue to decrease through P60 (Villers-Sidani, 2007). We analyzed response latencies in the five experimental groups and found overall significant differences in onset, peak and offset of the auditory response. (onset, Figure 2.3 B: ANOVA; $F_{4,19}=7.79$, $p = 0.001$; peak, Figure 2.3 C: ANOVA; $F_{4,19}=4.86$, $p = 0.007$; offset, Figure 2.3 D: ANOVA; $F_{4,19}= 4.89$, $p =0.007$). More specifically, the CP-expo and the Dem group had significantly longer onset (*post hoc* LSD: $p = 0.001$, and $p =0.011$, respectively), peak (*post hoc* LSD: $p = 0.018$, and $p =0.004$, respectively), and offset (*post hoc* LSD: $p = 0.018$, and p

=0.004, respectively), relative to the Naïve group. This indicates that 5-aza treatment results in longer response latencies as seen during development (Villers-Sidani, 2007).

Reducing global DNA-ME reverts inhibitory synaptic function to an immature state

As maturation of cortical inhibition is shown to parallel the critical period, we hypothesized that global DNA demethylation is affecting inhibitory synaptic transmission in the auditory cortex. To test this hypothesis, we recorded mIPSC's from pyramidal neurons in Layers 2/3 of AI (Figure 2.4 A and B). We used the same experimental groups, with the only difference being that we changed the exposure stimulus from solely 16 kHz tone pips, to tone pips ranging from 2-48 kHz, to assure that all of the frequency sensitive neurons within AI were receiving auditory input during the treatment period. The frequency of mIPSC's (Figure 2.4 C) steadily increased over four days of the CP (PN11-PN14). The overall average frequency of mIPSC's during the CP was less than half the average frequency seen in Naïve adult mice and Veh-expo adult mice. One-way ANOVA revealed a significant main effect (ANOVA on individual neurons: $F_{4,74} = 20.57$, $p < 0.001$; ANOVA on animal average: $F_{4,15} = 7.628$, $p = 0.001$) and *post hoc* analysis showed a significant difference between the CP and Naïve adult groups (*post hoc* LSD: neurons: $p < 0.001$; animals: $p < 0.001$) and between CP and Veh-expo adult groups (*post hoc* LSD: neurons: $p < 0.001$; animals: $p = 0.001$). The mIPSC frequency significantly decreased in the Dem group compared to the Naïve group (*post hoc* LSD: neurons: $p < 0.001$; animals: $p = 0.017$). Dem-exp and Naïve were different only when data from individual neurons were compared (*post hoc* LSD: neurons: $p = 0.035$; animals: $p = 0.361$). When analyzing the amplitude of mIPSC's (Figure 2.4 D), we saw an increase in amplitude over the course of the CP which is expected because this is a time marked by significant synaptogenesis. However, we saw no overall difference across the five experimental

groups in terms of mIPSC amplitude (ANOVA on neurons: $F_{4,74} = 2.41$, $p = 0.068$; ANOVA on aniamls: $F_{4,15} = 2.473$, $p = 0.089$). Finally, we analyzed the mIPSC decay time constant (Figure 2.4 E), which has been shown to decrease as cortical neurons develop (Dunning et al. 1999). Our results confirmed that mIPSC decay time constant decreases from early post-natal life to adulthood. One-way ANOVA revealed a significant main effect (ANOVA on neurons: $F_{4,76}=7.92$, $p = 0.001$; ANOVA on animal mean: $F_{4,15} = 7.92$, $p = 0.004$) and *post hoc* analysis showed significant differences in between the CP group and both the Naïve adult and Veh-expo group adulthood (*post hoc* LSD: comparing neurons: $p = 0.006$ between CP and Naïve, $p < 0.001$ between CP vs. Veh-expo; comparing animals: $p = 0.048$ between CP and Naïve, $p < 0.001$ between CP and Veh-expo; Figure 2E). By contrast, the mIPSC decay time constant was not different between the CP group and the two DNA-demethylated groups (*post hoc* LSD: comparing neurons: $p = 0.059$ between CP and Dem-expo, $p = 0.118$ between CP and Dem,). Global DNA demethylation in exposed and unexposed mice significantly increased the mIPSC decay time constant relative to Veh-expo adult mice (*post hoc* LSD: comparing neurons: $p = 0.025$ between Dem-expo and Veh-expo, $p = 0.005$ between Dem vs. Veh-expo; comparing animals: $p = 0.015$ between Dem-expo and Veh-expo, $p = 0.004$ between Dem and Veh-expo). Overall, these results indicate that reducing global levels of DNA-ME shifts certain aspects of the cortical inhibitory synapse to an immature state similar to that observed in the critical period.

Reducing global DNA-ME reverses expression of developmentally regulated genes to CP levels

The results from the patch clamp experiments revealed that upon treatment with 5-aza, specific characteristics of mature inhibitory synaptic function were reversing to an immature state. These results led us to hypothesize that genes that participate in the maturation of the cortex may also be

reverting back to levels seen during the CP upon treatment with 5-aza. To address this, we investigated the expression levels of two genes that are implicated in cortical maturation during the CP, BDNF exon IV (Hanover et al., 1999; Huang, 1999; Hensch, 2005a), and REST (Ballas et al., 2005; Rodenas-Ruano et al., 2012), via RT-PCR. Our results confirmed that both of these genes are developmentally regulated in that BDNF exon IV expression was significantly lower in CP mice compared to adult Naïve mice (Figure 2.5 A; ANOVA: $F_{4,18} = 4.62$, $p = 0.01$, *post hoc* LSD*:* $p = 0.004$), and REST expression was significantly higher in CP mice compared to adult Naïve mice (Figure 2.5 B; ANOVA: $F_{4,19} = 3.05$, $p = 0.042$, *post hoc* LSD*:* $p = 0.012$). Seven days of 5-aza treatment was sufficient to induce a significant reduction in BDNF exon IV expression (*post hoc* LSD: $p < 0.05$ for both demethylated groups). Mice treated with vehicle for seven days did not see a significant change in BDNF exon IV expression relative to Naïve mice (*post hoc* LSD: $p > 0.05$). In terms of REST expression, neither 5-aza treatment, nor environmental enrichment alone were sufficient to significantly increase REST expression relative to Naïve mice. However, the combination of environmental enrichment and 5-aza treatment significantly increased REST expression levels relative to Naïve mice (*post hoc* LSD: $p < 0.020$). The magnitude of this change was similar to the expression levels seen during the CP. These data suggests that global DNA demethylation facilitates the reversal of expression of genes implicated in cortical maturation and plasticity to levels seen during the CP.

2.5: Discussion

The main finding of this study is that pharmacological DNA demethylation in adult mice enables sound exposure-induced frequency map reorganization, which is typically observed only in the

CP. This elevated cortical plasticity is accompanied by an increase in the response latencies, a reduction in mIPSC frequency and an increase in mIPSC decay time constant to levels that are normally observed during development. Furthermore, DNA demethylation in adult mice also reversed BDNF and REST expression to levels similar to those in critical period. These concerted changes suggest that global demethylation reopens the critical period for frequency map plasticity in the auditory cortex. These results are consistent with the findings that overexpression of GADD45b, a protein involved in DNA demethylation, reopened ocular dominance plasticity in adult visual cortex (Apulei et al., 2018). Considering the differences between inducing auditory map plasticity, and ocular dominance plasticity, as well as the inherent differences between the auditory and visual cortex, we find this confluence of results to be interesting, and suggests that DNA-ME acts as a universal mechanism for regulating plastic states within sensory cortex. Together with reports that histone acetylation modulates ocular dominance plasticity, these results highlight epigenetic modulations as an important contributor to neural plasticity during development and in adulthood (Putignano et al., 2007; Gervain et al., 2013; Baroncelli et al., 2016). However, not all of our findings are consistent with the GADD45b overexpression study. In that study, the authors found a general reduction in visual responses as a result of GADD45b overexpression. Treatment with 5-aza did not lead to a similar reduction in auditory response. The difference in these results could be explained by the different demethylation method. Studies have shown that inhibiting DNA methyltransferases can yield different synaptic effects than over-expressing proteins that catalyze active DNA demethylation (Yu et al., 2015; Sweatt, 2016). More studies are required to better understand how the downstream pathways of inhibiting DNA-ME or strengthening DNA demethylation can yield differing effects on synaptic transmission.

DNA demethylation has been shown to upscale excitatory glutamatergic synapses and enhance intrinsic membrane excitability in cultured cortical neurons (Meadows et al., 2015; Meadows et al., 2016). To our knowledge, our results are the first to show that DNA demethylation also downregulates cortical inhibitory synapses by decreasing mIPSC frequency. This is consistent with the observed reduction of BDNF expression, as BDNF has been shown to upregulate GAD65 expression, increase mIPSC frequency, promote maturation of inhibitory neurons and inhibit ocular dominance shift by monocular deprivation (Hanover et al., 1999; Huang, 1999; Bolton et al., 2000; Galuske et al., 2000; Maffei, 2002; Ohba et al., 2005). As developmental maturation of cortical inhibitory circuit is an important regulator of the critical period (Hensch, 2005a), the observed reversal of inhibitory synaptic properties likely contributed to the reopening of the critical period for frequency map plasticity following DNA demethylation. We also found that DNA demethylation prolongs response latencies to levels seen during the CP. Interestingly, a similar result was found in a transgenic model of MeCP2 duplication syndrome. Transgenic overexpression of MeCP2 led to significantly prolonged response onset and response peak in the AI of the transgenic mice, relative to wild-type control (Zhou et al., 2019). These findings establish a potentially important connection between DNA-ME dynamics and auditory response latencies in the cortex.

The gene expression patterns observed after 5'aza treatment are consistent with reduced inhibitory synaptic transmission observed in this study. For example, 5'aza treatment reduced BDNF expression in our study, which, at first glance, was surprising because increased BDNF expression has been implicated in heightened plasticity levels (West et al., 2001; Lu et al., 2008), and because other studies have shown that DNA-ME negatively regulates BDNF expression (Martinowich et

al., 2003). However, increased BDNF is also heavily implicated in promoting maturation of cortical interneurons during the CP (Hanover et al., 1999; Huang, 1999), correlating with potentiated inhibition levels (Maffei, 2002), and subsequently reduced plasticity. Furthermore, it has been shown that direct BDNF infusions into adult cat visual cortex did not influence orientation selectivity or ocular dominance, suggesting that increased BDNF levels in adult sensory cortex does not re-open critical period plasticity (Galuske et al., 2000). Thus, it follows that the 5-aza induced reduction in BDNF expression may have contributed to the reversal of mature inhibitory synaptic features, and accordingly, the re-instatement of CP plasticity. Another developmentally regulated gene implicated in cortical maturation, REST, was also shown to increase its expression to the critical period level after 5'aza treatment. Studies have shown that developmental downregulation of REST expression is necessary for neurons to acquire mature characteristics (Ballas et al., 2005), and that transient upregulation of REST in adulthood facilitates a shift of neurons towards an immature state (Oh et al., 2018). Together, our results indicate that DNA-ME has a significant effect on the expression of genes that influence cortical maturation.

Although 5-aza treated animals showed a reduction in BDNF expression and increase in REST expression, the possibility remains that these effects are not a direct result from DNA demethylation. One intriguing possibility is that 5-aza treatment may be altering the expression of the multitude of methyl-binding proteins active in neurons. A study in Macaque monkeys showed that neurons in primary cortical areas and associative cortical areas have differing expression levels of methyl-binding proteins. Genes that are expressed in prefrontal cortex were enriched for methyl-binding protein 4 (MBD4) at promotors, while those same gene promotors were enriched for MeCP2 in primary visual cortex (Hata et al., 2013). This indicates that while the methylation status

of certain genes may be the same, their expression may be different due to the effects of different methyl-binding proteins. Finally, it is worth investigating how 5-aza treatment affects the expression of proteins that dictate neuronal fate. For example, during the CP, development of the parvalbumin-positive (PV) interneuron (an important cell-type for CP plasticity), is tightly linked to the expression of homeoprotein, Otx2. Studies have shown that internalization of Otx2 by PV interneurons stimulates their functional maturation, and that the upregulation of Otx2 during the critical period is dependent on proper sensory experience (Sugiyama et al., 2008; Beurdeley et al., 2012; Bernard and Prochiantz, 2016; Sakai and Sugiyama, 2018). Furthermore, blocking PV internalization of Otx2 in adulthood re-establishes ocular dominance plasticity (Beurdeley et al., 2012). Therefore, the changes in gene expression seen in our 5-aza treated animals may be caused by an upstream effect on developmental transcription factors, such as Otx2.

In the present study, DNA-ME in the auditory cortex was significantly lower in CP than in adulthood. This is consistent with developmental upregulation of DNMT3a expression observed from PN Week 1 to Week 4 (Lister et al., 2013; Guo et al., 2014). Interestingly, blocking DNMT, which prevented upregulation of DNA-ME, prevented monocular deprivation-induced ocular dominance shift in visual CP (Tognini et al., 2015). Thus, it appears that while DNA demethylation reopens the critical period in adult cortex, normal critical period plasticity requires DNA-ME (Tognini et al., 2015; Apulei et al., 2018). It is possible that DNA-ME reduces plasticity to solidify experience-dependent circuit changes. Further studies tracking DNA-ME changes on developmentally regulated genes as the CP progresses may elucidate more information on the role of DNA-ME in regulating CP plasticity

2.6: Figures

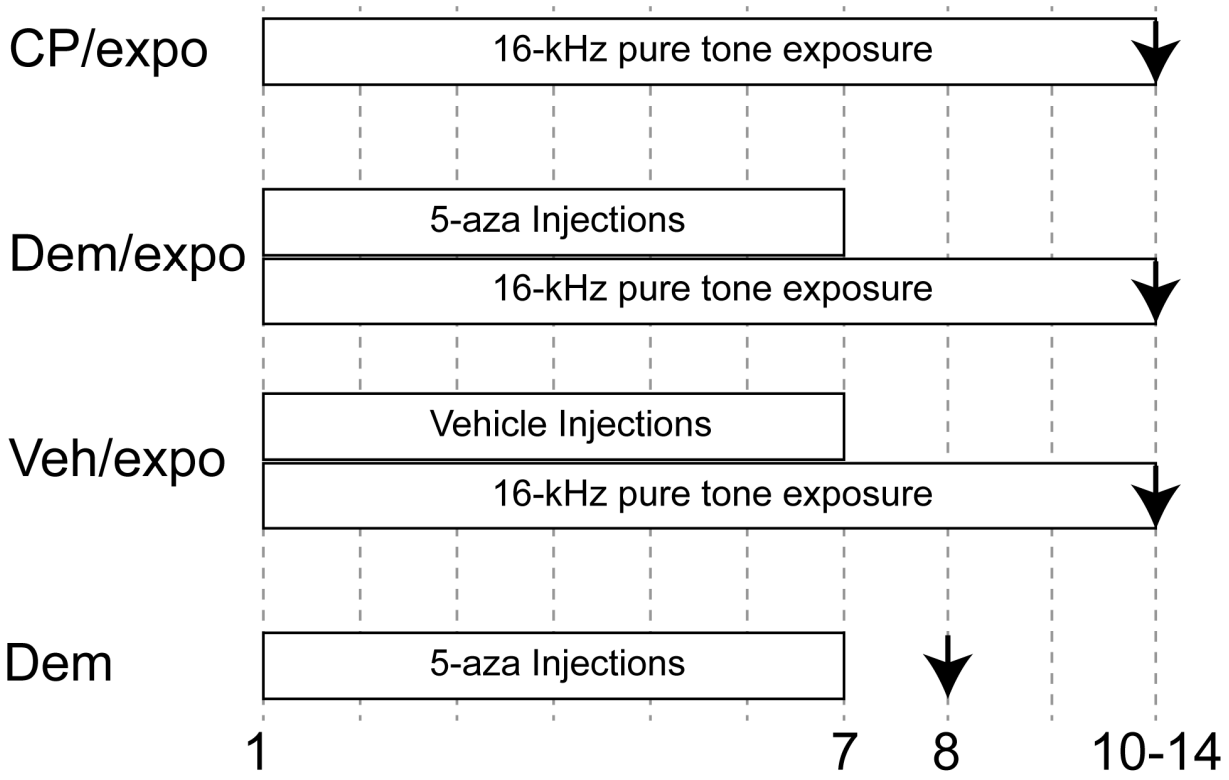

Figure 2.1: Timeline representation of 5-aza injection and sound exposure paradigm. Naïve animals (not shown) were taken directly from the colony with no exposure or injections. CP-expo animals began exposure on PN9, while the other adult groups were between 2 and 4 months of age during the treatment/exposure period.

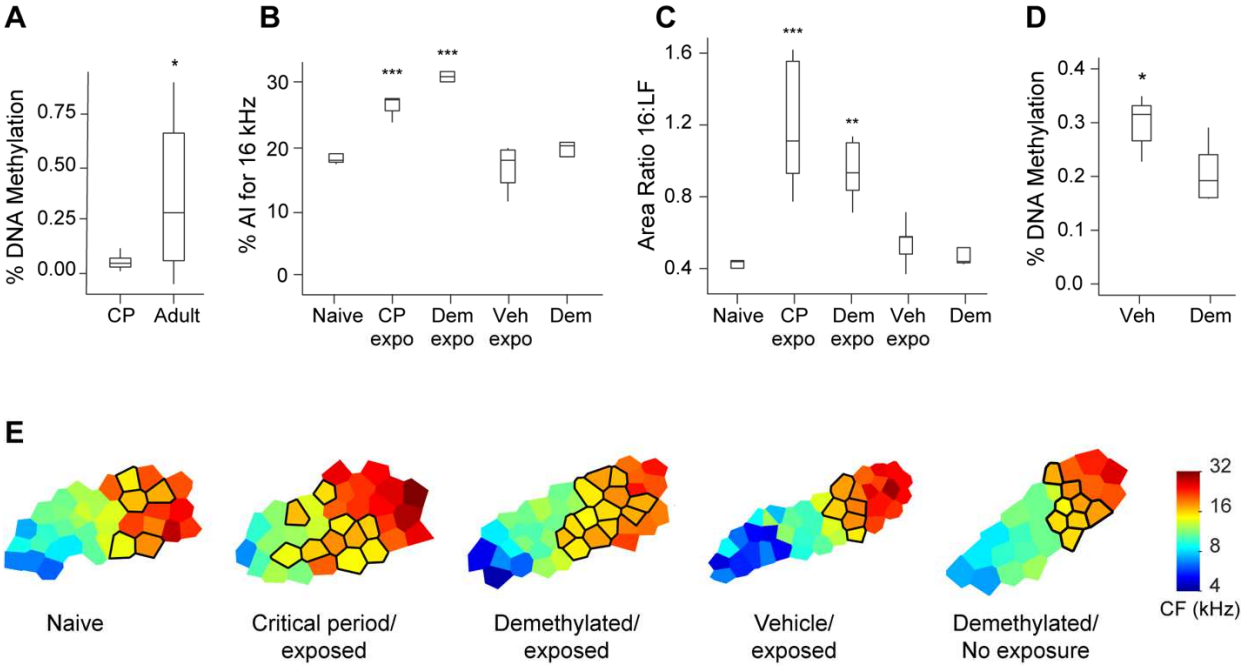

Figure 2.2: Pharmacological DNA demethylation re-establishes auditory critical period map plasticity in adult animals. **A)** Adult animals between 2-4 months of age and CP animals at P11 were sacrificed, and their brains harvested for methylation analysis. Methylation levels from were found to be higher in adult auditory cortices (n = 12) than in the auditory cortices of CP animals (n = 6). **B)** Graph displaying the average area dedicated to sites within the exposure frequency. Both the critical period exposed and the demethylated exposed groups show a significant increase in the representation of 16 kHz (n= 5 for Naïve, CP-expo, Dem-expo and Veh-expo. n=4 for Dem). **C)** Graph displaying the ratio of the area of sites representing 16 kHz to a low frequency in (8kHz-13.9kHz) The ratio was increased in the CP animals and demethylated exposed animals **D)** Graph displaying the difference in global methylation between the auditory cortices of vehicle exposed and demethylated animals. Vehicle treated mice had higher global methylation levels (n = 8) in the auditory cortex than mice treated with 5-aza (n=4). **E)** Example frequency maps of primary auditory cortex in five different groups of mice. Areas outlined in black indicate sites with CFs within the exposure frequency of 16 kHz (+/- 0.2 octaves). *p <0.05, **p<0.005, ***p<0.0005.

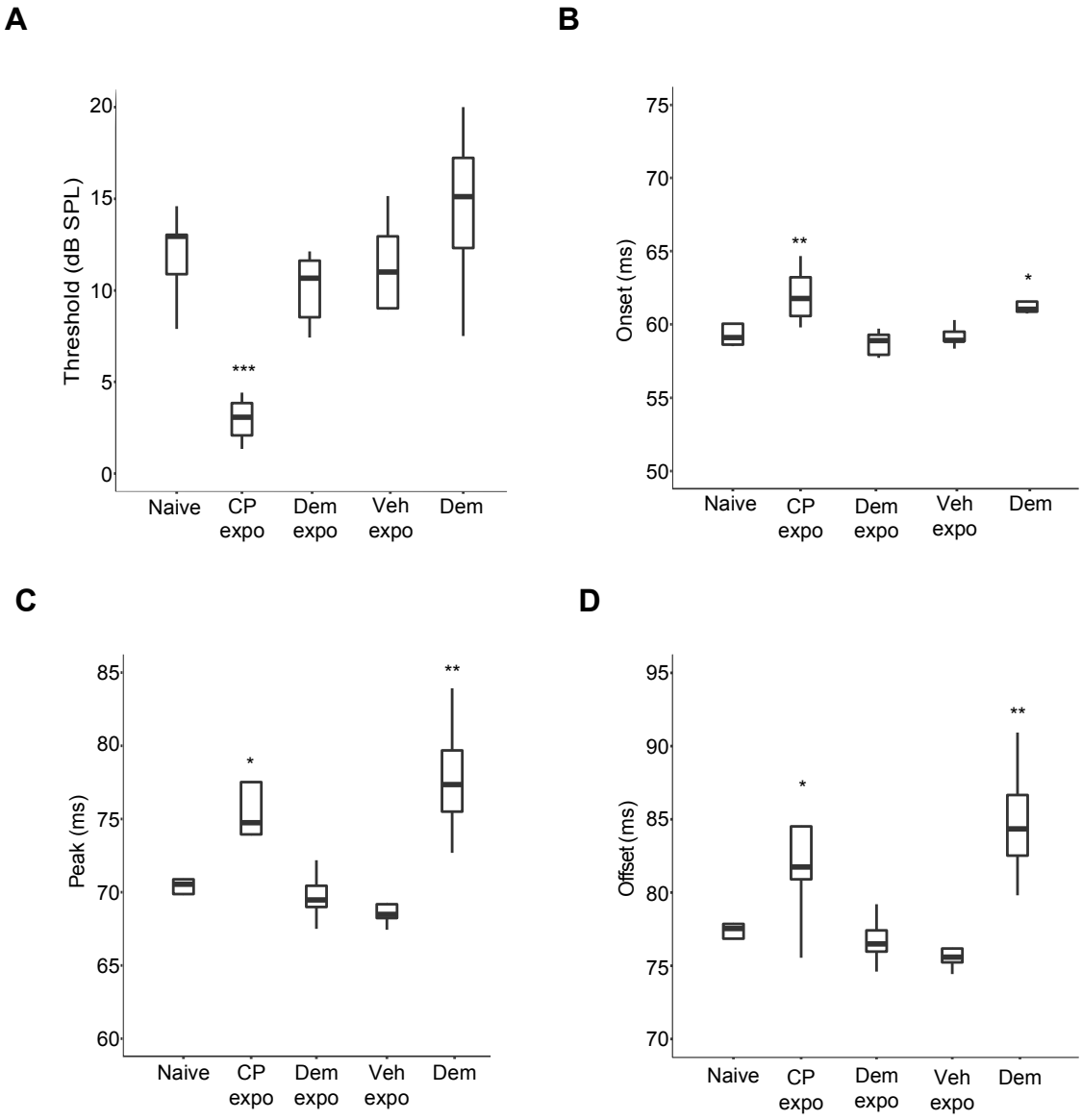

Figure 2.3: Pharmacological DNA demethylation in adults reverts some receptive field traits towards CP levels. A) A box and whisker plot showing the distribution of average thresholds for the five groups of mice (n= 5 for Naïve, CP-expo, Dem-expo and Veh-expo. n=4 for Dem). CP mice had a significantly lower threshold relative to the other groups. **B), C) and D),** show response onset, peak, and offset for the five groups. The CP and Dem groups had a prolonged response latency for each feature relative to the Naïve group. *p <0.05, **p<0.005, ***p<0.0005.

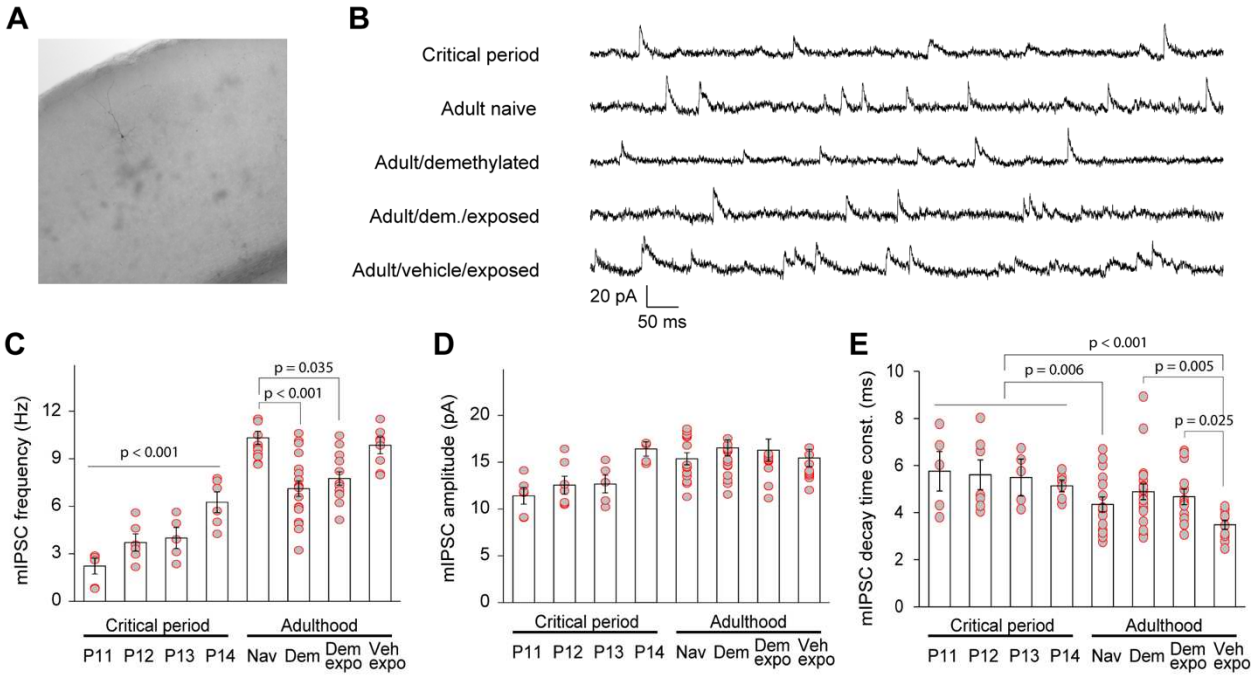

Figure 2.4: Pharmacological DNA demethylation reverts inhibitory synaptic function to an immature state. **A)** Image of biocytin stained pyramidal neuron within auditory cortex, used for patch clamp analysis. **B)** Representative current traces recorded from pyramidal neurons for the 5 groups tested: CP (n = 4 mice), adult Naïve (n = 4 mice), adult 5-aza treated with no exposure (Dem; n = 4 mice), adult 5-aza treated with exposure (Dem-expo; n = 4 mice) and adult vehicle treated with exposure (Veh-expo; n = 4 mice). **C)** Graph displaying the average mIPSC frequency for the 5 experimental groups. Both the Dem and Dem-expo groups had a significantly lower mIPSC frequency than Naïve adult animals, which is in line with the difference between CP animals and Naïve adult animals. **D)** Graph displaying the average mIPSC amplitude for the 5 experimental groups. No significant difference was found between any of the groups. **E)** Graph displaying the average mIPSC decay time constant. The Naïve and Veh-expo had a significantly lower average decay time constant compared to the CP group, which recapitulates previous reports. Both the Dem and Dem-expo groups had a significantly higher mIPSC decay time constant compared to the Veh-expo group but did not have a significantly different mIPSC decay time constant compared to the CP group.

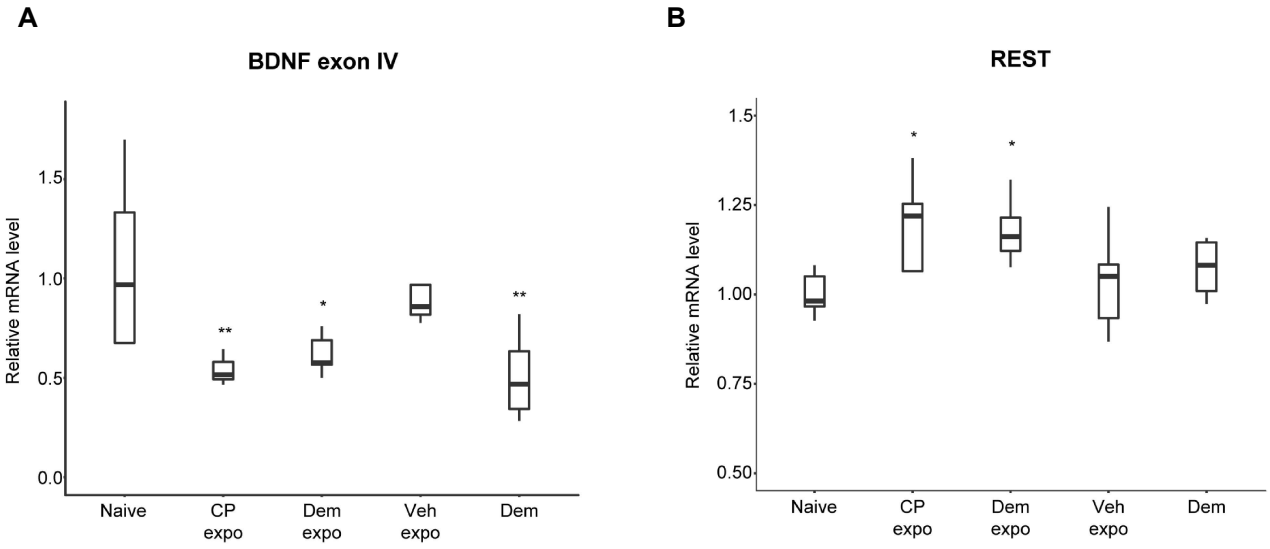

Figure 2.5: Pharmacological DNA demethylation reverses expression of developmentally regulated genes back to critical period levels. **A)** Relative BDNF mRNA expression level for the five experimental groups: CP (n = 5 mice), adult Naïve (n = 5 mice), Dem (n = 4 mice), Dem-expo (n = 5 mice) and Veh-expo (n = 4 mice). CP, Dem, and Dem-expo mice had significantly lower levels of BDNF expression relative to Naïve adult mice. **B)** Relative REST mRNA expression level for the five experimental groups: CP (n = 5 mice), adult Naïve (n = 5 mice), Dem (n = 4 mice), Dem-expo (n = 5 mice) and Veh-expo (n = 5 mice). Both CP mice and Dem-expo mice had significantly higher levels of REST compared to Naïve adult mice, while Dem mice were not significantly different from Naïve adult. *p <0.05, **p<0.005.

3

TNF-α Deficiency Disrupts Cortical Parvalbumin Neuron Maturation, Homeostatic Plasticity and Critical Period Closure

Schwartz BA, Wang W, Bao S (**2021**) TNF-α Deficiency Disrupts Cortical Parvalbumin Neuron Maturation, Homeostatic Plasticity and Critical Period Closure. *To be submitted*.

3.1: Abstract

Plasticity levels in the brain are highest during an early developmental epoch known as the critical period. Tumor necrosis factor-alpha (TNF-α), a proinflammatory cytokine, is required for a homeostatic component of visual critical period plasticity. It also modulates synaptic excitatory/inhibitory (E/I) balance and indirectly interacts with parvalbumin neurons, both of which are hypothesized as modulators of the critical period. Here, we examined the effect of TNF-α deficiency on auditory cortical circuitry and plasticity. Compared to wildtype (WT) control mice, TNF-α KO mice had reduced PV neuron density and PV expression levels. Pyramidal neurons in the auditory cortex of TNF-α KO mice had larger mEPSC amplitude. Furthermore cortical multiunit showed increased spontaneous and evoked activity and broadened tunning bandwidth indicating a shifted E/I balance. Importantly, unlike WT mice, TNF-α KO mice retained critical period-type plasticity into adulthood. Following exposure to a single-frequency tone, the representation of the tone was enlarged in adult TNF-α KO, but not WT mice. These results suggest that TNF-α, and its actions on regulating the excitatory-inhibitory balance, are necessary for the closure of the critical period for cortical frequency map plasticity.

3.2: Introduction

Brain plasticity is the ability of the nervous system to adapt to the environment by reorganizing its structure, function and connections. Plasticity is heightened during an early developmental epoch known as the critical period (CP) (Hensch, 2005a). During the CP experience shapes the cortical maps that facilitate basic sensory and motor function. In the auditory system, the critical period is marked by development of the tonotopic frequency map within the primary auditory cortex (AI), as well as fine-tuning of other auditory processing features such as receptive field bandwidth, latency, threshold, evoked amplitude, and frequency modulation selectivity (Zhang et al., 2001; Chang et al., 2005; Villers-Sidani, 2007; Insanally et al., 2009). During the auditory CP, passive exposure to sound is sufficient to induce significant changes to the representation of sound within AI (Zhang et al., 2001; Chang and Merzenich, 2003; Villers-Sidani, 2007; de Villers-Sidani et al., 2008; Schwartz et al., 2020). Once the CP closes, plasticity weakens and often involves additional neuromodulatory mechanisms for induction (Keuroghlian and Knudsen, 2007; Kral, 2013).

CP plasticity involves both Hebbian and homeostatic mechanisms. In the visual CP, for example, monocular deprivation first leads to Hebbian long-term depression of the synapses from the deprived eye, followed by homeostatic upregulation of synapses from both eyes, resulting in a ocular dominance shift from the deprived eye to the nondeprived eye. Mice with deficient homeostatic plasticity exhibit impaired ocular dominance plasticity during the critical period (Kaneko et al., 2008; Ranson et al., 2012). Furthermore, mice deficient in TNF-α do not show the homeostatic component of the ocular dominance plasticity (Kaneko et al., 2008). Thus, it

appears that certain aspects of critical period plasticity in the visual system require the actions of TNF-α in regulating homeostatic plasticity.

The synaptic excitation-to-inhibition (E/I) ratio within the cortex has been proposed as a determinant of the critical period time window (Hensch and Fagiolini, 2005). Enhancing cortical inhibition can precociously initiate and terminate the critical period, while reducing inhibition can reopen the critical period in the adulthood (Huang, 1999; Iwai et al., 2003; Takesian and Hensch, 2013; Cisneros-Franco and de Villers-Sidani, 2019). TNF-α expression increases during the critical period, and it has been shown to shift the E/I balance by synaptic AMPA receptor insertion and GABA receptor internalization (Beattie et al., 2002; Ogoshi et al., 2005; Stellwagen et al., 2005; Stellwagen and Malenka, 2006; Pribiag and Stellwagen, 2013). Thus TNF-α may regulate the critical period window through its control of the E/I balance.

Cortical PV neurons form inhibitory synapses on the perisomatic compartments and axon initial segments of pyramidal cells, exerting a powerful influence on E/I balance of the cortical circuits. PV neuron maturation parallels the opening and closing of the critical period (Huang, 1999; de Villers-Sidani et al., 2008). Manipulation of PV neuron activity can shift the timing of the critical period (Takesian et al., 2018; Cisneros-Franco and de Villers-Sidani, 2019). Recent results show that TNF-α can activate microglia, which in turn can interact with PV neurons to reopen the critical period in adulthood (Venturino et al., 2021).

In the present study, we examined the effects of TNF-α gene deficiency on PV neuron development, synaptic E/I balance and critical period plasticity in the auditory cortex. We found

that adult TNF-α KO mice had a significantly lower PV neuron density and PV expression in the auditory cortex relative to WT animals. They also had a higher synaptic E/I ratio compared to the WT mice. Consistent with the shifted synaptic balance, neurons in primary auditory cortex of the TNF-α KO mice had a wider tuning bandwidth, as well as elevated spontaneous and evoked activity. Importantly, adult TNF-α KO mice retain the capacity for CP-type frequency map plasticity, while WT mice do not. Overall, our results suggest that TNF-α signaling is necessary for the maturation of cortical PV neurons and a proper excitatory-inhibitory balance. In its absence, the auditory cortex retains critical period plasticity into adulthood.

3.3: Methods

Animals: All procedures in this study were approved by the Animal Care and Use committee at the University of Arizona. C57BL/6J control and TNF-α knockout mice (B6.129S/SvEv-Gpi1-Tnf^{tm1Gkl}) were used in these experiments (Jackson Laboratory, Bar Harbor, ME). A total of 40 mice, both males and females, were used for these experiments.

Sound Exposure: Sound exposure was performed as previously described (Zhang et al., 2001). Litters of 1-3 mice were placed in a ventilated, sound-shielded, calibrated test chamber for 10-12 days (a time period shown to induce frequency map plasticity in CP mice, but not adult mice (Schwartz et al., 2020)), and exposed to pure tones centered on 9.2 kHz. A 25-ms tone (5-ms ramps) at 60-70 dB SPL was applied from a speaker placed approximately 15 cm above the mice, at 6 pulses per second with 1-s intervals to minimize adaptation effects. No noticeable distortion of tonal stimuli was detected from sound spectrum recorded inside the test chamber.

There were no significant spectral peaks for the normal environmental noise background. The total sound pressure level in the animal room was 5-10 dB lower than that of exposed tonal stimulus intensity. Inside the sound attenuation chamber with the presence of mice but in the absence of the tone stimulus, the noise level was about 15-25 dB below that in the animal room at all frequencies within the mouse's hearing spectrum. No significant harmonic signal was found in the chamber when a tonal stimulus was being delivered.

Immunostaining of PV neurons: The procedure was modified from those of previous reports (Wang et al., 2018; Wang et al., 2019). Mice were transcardially perfused under deep anesthesia with ice-cold PBS followed by 4% paraformaldehyde. Brains were removed and fixed in the same fixative overnight at 4°C, equilibrated in 30% sucrose and embedded in Tissue-Tek (Sankura Finetek). Frozen coronal sections (16 μm) were collected on gelatinized glass slides. After air drying, sections were washed in PBS and penetrated with 0.1% Triton-X at room temperature for 10 min. The samples were blocked with Dako Serum-free blocking buffer (Dako) and incubated with primary antibodies for PV (PV rabbit polyclonal antibody, PA1-933, Invitrogen) overnight at 4°C. Samples were then washed in PBS and incubated with the secondary antibody conjugated with Alexa Fluor 488 (Invitrogen) for 1 hour at room temperature to enable fluorescent detection. After rinsing with PBS, the sections were mounted with fluorescence mounting medium (Dako) and viewed under the Olympus BX40 microscope with a digital microscope camera C11440; (Hamamatsu). Immunofluorescent images were systematically and randomly sampled from the AI with the experimenters "blind" to the sample groups. All the images for the same experiment were taken on the same day using the same parameters. The Paxino's Mouse Brain Atlas was used to determine the location of AI. For

image analysis the area of AI was calculated and the numbers of PV+ cells were quantified in ImageJ manually. PV neuron density (numbers of cells/mm^2), PV signal intensity, and PV puncta size were then compared between WT and TNF-α knockout mice.

Patch Clamp Electrophysiology: Mice were deeply anesthetized with isoflurane and then decapitated. The brain was extracted and immediately placed in an oxygenated (95% O_2/5% CO_2) external solution (87 mM NaCl, 2.5 mM KCl, 7 mM $MgCl_2$, 25 mM D-glucose, 25 mM $NaHCO_3$, 1.3 mM NaH_2PO_4, 0.5 mM $CaCl_2$, and 75 mM Sucrose at pH 7.3). The brain was sectioned along the transverse plane into 300-μm slices with a vibrating microtome (Leica; VT1000S), and brain slices were stabilized in oxygenated external solution in a tissue chamber for 30 min at 32.5℃ followed by acclimation to room temperature (22.5°C) for at least 30 min before recordings. All recordings were performed at room temperature. The chamber was continuously perfused with artificial cerebrospinal fluid (ACSF) (125 mM NaCl, 2.5 mM KCl, 1 mM $MgCl_2$, 25 mM D-glucose, 25 mM $NaHCO_3$, 1.3 mM NaH_2PO_4 and 2 mM $CaCl_2$ at pH 7.3) at a rate of 2 mL/min. A fixed stage microscope (Olympus; BX51WI) equipped with differential interference contrast optics and a 40× water-immersion objective was used to visualize individual neurons in the auditory cortex. Patch electrodes were fabricated from 1.5-mm-diameter borosilicate glass micropipettes and had an impedance of 3–5 MΩ when back-filled with the internal solutions for mIPSCs and mEPSCs measurement (135 mM Cs methanesulfonate, 10 mM CsCl, 10 mM Hepes, 0.2 mM EGTA, 4 mM ATP-Mg, 0.4 mM GTP-Na at pH 7.3 and 290 mOsm). In whole-cell configuration, the initial access resistance typically ranged from 15 to 23 MΩ and remained stable during the recording session.

Series resistance was also continuously monitored with a brief voltage pulse. Recordings were accepted when a cell had a resting membrane potential of at least –68 mV and a series resistance of 15–25 MΩ (< 20% change during the recording session). Miniature excitatory postsynaptic currents (mEPSCs) were recorded from in oxygenated ACSF solution containing 1 μM tetrodotoxin (TTX) with the cell held at -80 mV. Miniature inhibitory postsynaptic currents (mIPSCs) were recorded in oxygenated ACSF solution containing 1 μM TTX, 10 μM 6-cyano-7-nitroquinoxaline-2,3-dione (CNQX) and 100 μM d-2-amino-5-phosphonovalerate (d-AP5) with the cell held at 0 mV. Signals were low pass filtered at 2kHz. All recordings were performed with Multiclamp 700B amplifier (Molecular Devices) and with pCLAMP10 software (Molecular Devices), and data were analyzed using MiniAnalysis software (Synaptosoft) by experienced experimenters "blind" to the experimental groups.

In vivo Electrophysiology: AI of WT and TNF-α KO mice were mapped as previously described (Kim et al., 2013; Schwartz et al., 2020). Mice were anesthetized with ketamine (100 mg/kg, i.p.) and xylazine (10 mg/kg, i.p.), and kept anesthetized with, a steady flow of 1% isoflurane. The cortex was maintained under a layer of silicone oil, that was reapplied as necessary. Multiunit responses to 25 ms pure tone pips (2–74 or 4 –74 kHz, 0.1 octave increments at 0–70 dB, 10 dB increments) were recorded using tungsten micro-electrodes (FHC) in the thalamorecipient layer of AI (350–450 micrometers below the cortical surface). Tones were presented to the left ear through an electrostatic speaker (Tucker Davis Technologies) at 3 pips per second and each frequency- intensity combination was repeated three times. Cortical penetration locations were recorded on a high-resolution image, which was later used to construct the map.

AI Receptive Field Analysis: Receptive fields and response properties were isolated using custom made programs in MATLAB as previously described (Insanally et al., 2010; Masri et al., 2018), except as follows. The peak of the peristimulus time histogram (PSTH) within a window from 7 to 50 ms after the stimulus onset was defined as the response latency. The response window was defined as a period encompassing the PSTH peak, in which the firing rate was higher than the baseline firing rate. The spikes in the response window were counted to reconstruct the receptive field. The map of AI was generated using the Voronoi tessellation algorithm, in which the best frequency (BF), of the receptive field is converted to a polygon of a certain area. The best frequency was taken as the center of mass of the entire receptive field. The border of AI was determined by unresponsive sites or sites with BF's that did not match the AI tonotopic gradient. To determine the area dedicated to each of the frequency bands, the area of the polygons dedicated to a specific frequency band, +/- 0.2 octaves, was summed and divided by the total area of the map to determine percent area. The spontaneous firing rate of the multiunit response was taken as the mean firing rate in the 50-ms window before stimulus onset. The maximum receptive field response was the maximum number of spikes activated by a single frequency-intensity combination. The mean and median receptive field responses were the mean and median number of spikes for all frequency-intensity combinations within the receptive field. Tuning bandwidth (BW) was defined as the bandwidth (in octaves, logarithmically), at the specified intensity. For all receptive field properties, values were averaged to create means per individual mouse.

Statistics: All statistical analysis was performed in SPSS software. When individual animals were the unit of comparison (e.g., cortical frequency maps, receptive fields, response properties,

mEPSC frequencies and amplitudes), ANOVAs were used. When left and right hemispheres were examined in the same animals (PV neuron density), repeated measures ANOVAs were used. Normality and homogeneity of variances were checked using a Shapiro-Wilk test and Levene's test (based on median), respectively. When heterogenous variances were found, a Kruskal-Wallis test followed by a *post hoc* Dunn Test with Bonferroni correction for multiple comparisons was performed. When unit of comparison was neurons (e.g., PV signal intensities, PV puncta sizes) linear mixed model analyses were used with the animal ID as a random factor. The significance level was set at $\alpha = 5\%$. Data were presented as mean ± SEM unless otherwise stated.

3.4: Results

PV neuron density and PV expression are reduced in the auditory cortex of TNF-α KO mice

We first examined PV neuron density in adult WT and TNF-α KO mice (4 mice/group). The PV neuron density was significantly lower in AI of adult TNF-α KO mice compared to WT mice (genotype-by-side repeated measures ANOVA, effect of genotype, $F_{1,6} = 11.026$, $p = 0.016$; effects of side, $F_{1,6} = 0.002$, $p = 0.970$; genotype x side interaction $F_{1,6} = 0.459$, $p = 0.523$; Figure 3.1 A-B). Since no side difference was observed, we combined both sides in each animal in subsequent analysis of PV expression levels and puncta sizes. Parallel to the reduced PV neuron density, the PV expression level as measured with the PV fluorescence staining intensity was also lower in the adult TNF-α KO than in WT mice (linear mixed model analysis with animal ID as a random factor, effect of genotype on PV signal intensity, $F_{1,5.872} = 17.058$, $p = 0.006$; Figure 3.1 C). Further analysis of the size of PV fluorescent punctas suggests the size of the PV neurons

was not different between WT and TNF-α KO mice (linear mixed model analysis, effect of genotype on PV puncta size, $F_{1,5.935} = 0.803$, $p = 0.405$; Figure 3.1 D). Since PV expression has been correlated with PV neuron function, the observed reduction of PV neuron density and PV expression are suggestive of PV neuron dysfunction in TNF-α KO mice.

Excitatory synaptic transmission was enhanced, and homeostatic plasticity was impaired in the auditory cortex of TNF-α KO mice

We next examined the hearing loss-induced homeostatic plasticity in the auditory cortex of adult WT and TNF-α KO mice. Mice in the noise-exposed group (n = 5 mice for each genotype) were exposed to a continuous loud tone (8 kHz, 124 dB SPL) in the left ear for 2 hours. Mice in the control group (n = 5 for each genotype) underwent a similar procedure except no tone was played. This noise exposure procedure reliable increases of the threshold of auditory brainstem responses in the exposed ear in both WT and TNF-α KO mice (Miyakawa et al., 2019; Wang et al., 2019). Acute auditory cortical slices were prepared from the hemisphere contralateral to the exposed ear 10-15 days after the exposure procedure, and miniature EPSCs were recorded from Layer 2/3 pyramidal neurons. Analysis of the mEPSC amplitude revealed a significant difference between the WT and TNF-α KO mice (n = 5 mice/group, repeated measures ANOVA, effects of genotype, $F_{1,16} = 8.334$, $p = 0.011$; effect of noise exposure, $F_{1,16} = 0.056$, $p = 0.815$; genotype x noise exposure interaction, $F_{1,16} = 6.722$, $p = 0.020$; Figure 3.2). Post hoc comparison indicated a significant difference only between WT controls and TNF-α KO controls ($p = 0.008$). Although mEPSC amplitude was not altered by noise-induced hearing loss, mEPSC frequency was significantly increased in the WT, but not TNF-α KO mice, following noise exposure (repeated measures ANOVA, effects of genotype, $F_{1,16} = 23.129$, $p = 0.001$; effect of noise exposure, $F_{1,16}$

= 21.769, $p = 0.001$; genotype x noise exposure interaction, $F_{1,16} = 6.034$, $p = 0.026$; Post hoc analysis, WT control vs. WT NE, $p = 0.001$; KO control vs. KO NE, $p = 0.827$; Figure 3.2). These data indicate that not only do adult TNF-α KO mice lack the capacity for deprivation-induced homeostatic plasticity, but also that under normal conditions, adult TNF-α KO animals display signs of altered E/I balance, relative to adult WT mice.

TNF-α KO mice retain auditory critical period plasticity into adulthood

Both reduced PV neuron function and increased E/I ratio have been shown to enable critical period plasticity in adult mice. We examined whether the reduced PV neuron density and increased E/I ratio in the auditory cortex of TNF-α KO mice might facilitate extension of the auditory critical period window. In the auditory system, the primary way to assess whether the critical period is open, is to expose animals to pure tone frequencies, and then electrophysiologically map AI to check if significant exposure-based frequency map reorganization has occurred (Zhang et al., 2001; Chang and Merzenich, 2003; Villers-Sidani, 2007). Therefore, we passively exposed groups of adult (postnatal day 60) WT and TNF-α KO mice to pure tone pips centered around 9.2 kHz for 10-12 days, and recorded receptive fields in AI to compare tonotopy between the exposed and naïve WT and TNF-α KO mice (Figure 3.3). Qualitatively, AI tonotopic maps from all the groups looked similar, in that the complete spectrum of frequencies, from high to low, were represented (Figure 3.3 A). This differs from results recorded in TNF-α KO animals during the CP, which showed incomplete frequency representations (Yang et al., 2014b). Exposure to 9.2 kHz pure tones led to a significant expansion in the frequency band dedicated to 9.2 kHz in adult TNF-α KO mice, but not in adult WT mice (Figure 3.3 B). A two-way ANOVA (genotype X exposure) on the 9.2 frequency bin

revealed significant main effects, and a significant interaction between genotype and exposure condition (main effect: $F_{3,20}$=6.23, P =0.004; genotype: $F_{1,20}$=3.99, P = 0.059; exposure: $F_{1,20}$=9.36, P = 0.006; interaction: $F_{1,20}$=5.35, P =0.032). Significant main effects were also found in the 21.1 kHz frequency bin, however there was no significant interaction found (Figure 3.3 C) (main effect: $F_{3,20}$=3.87, P =0.025; genotype: $F_{1,20}$=2.27, P = 0.148; exposure: $F_{1,20}$=9.32, P = 0.006; interaction: $F_{1,20}$=0.007, P =0.932). Together, these results indicate that TNF-α KO animals retain CP plasticity into adulthood, and thus TNF-α signaling is necessary for CP closure.

TNF-α KO animals show alterations in receptive field properties indicative of increased E/I ratio

As the CP progresses into adulthood, auditory processing features such as bandwidth, latency, evoked and spontaneous activity, develop alongside tonotopy (Chang et al., 2005; Villers-Sidani, 2007). The maturation of these receptive field properties coincides with the shift in E/I balance, and thus the progressive loss of CP plasticity. To better understand why TNF-α KO animals retain CP plasticity into adulthood, we analyzed auditory receptive field properties from adult TNF-α KO mice and compared them to adult WT mice. A total of 633 receptive fields were included in this analysis (Figure 3.4). Measures of both spontaneous and evoked activity were significantly higher in TNF-α KO mice compared to WT mice regardless of exposure condition (Figure 3.4A-C). A two-way ANOVA (genotype X exposure) for spontaneous activity revealed a significant effect of genotype, but none for exposure nor any interaction between the two (spontaneous activity, main effect: $F_{3,20}$=8.52, P = 0.001, genotype: $F_{1,20}$=24.80, P < 0.001, exposure: $F_{1,20}$=0.55, P=0.469, interaction: $F_{1,20}$=0.210, P =0.652). Just as with spontaneous activity, mean and max spike amplitude were significantly higher in exposed and naïve TNF-α

KO mice relative to WT mice. A Kruskal-Wallis H test was found to be significant for both mean and max spike amplitude (mean, H = 12.69, P = 0.005; max, H = 14.35, P = 0.002). *Post hoc* pairwise comparisons revealed a significant difference in max and mean spike amplitude for both naïve and exposed TNF-α KO mice relative to WT naïve mice (mean, TNF-α naïve vs. WT naïve: P = 0.029, TNF-α exposed vs. WT naïve: P = 0.015; max, TNF-α naïve vs. WT naïve: P = 0.020, TNF-α exposed vs. WT naïve: P = 0.012).

Tuning bandwidth was found to be significantly higher at multiple thresholds, in both the naïve and exposed TNF-α KO mice relative to WT (Figure 4D). A two-way ANOVA (genotype X exposure) analyzing bandwidth at 60, 50 and 40 dB revealed a significant effect of genotype, but no significant interaction (60 dB, main effect: $F_{3,20}$=3.90, P = 0.024, genotype: $F_{1,20}$=10.81, P = 0.004, exposure: $F_{1,20}$=0.55, P=0.467, interaction: $F_{1,20}$=0.345, P =0.563; 50 dB, main effect: $F_{3,20}$=408, P = 0.021, genotype: $F_{1,20}$=10.80, P = 0.004, exposure: $F_{1,20}$=0.1.01, P=0.327, interaction: $F_{1,20}$=0.428, P =0.520; 40 dB, main effect: $F_{3,20}$=5.06, P = 0.009, genotype: $F_{1,20}$=14.80, P = 0.001, exposure: $F_{1,20}$=0.002, P=0.966, interaction: $F_{1,20}$=0.376, P =0.547) Bandwidth was also found to be significantly higher in TNF-α KO mice relative to WT mice at 30 and 40 dB above threshold (Data not shown) (30 dB above threshold, main effect: $F_{3,20}$=6.57, P = 0.003, genotype: $F_{1,20}$=16.10, P = 0.001, exposure: $F_{1,20}$=0.24, P=0.627, interaction: $F_{1,20}$=3.37, P =0.081; 40 dB above threshold, main effect: $F_{3,20}$=6.33, P = 0.003, genotype: $F_{1,20}$=15.17, P = 0.001, exposure: $F_{1,20}$=1.93, P=0.180, interaction: $F_{1,20}$=1.89, P =0.184). Taken together, the increases in activity measures, alongside the increases in tuning bandwidth, indicates a disruption in the excitatory-inhibitory balance in TNF-α KO mice in favor of more excitation.

3.5: Discussion

In the present study, we showed that TNF-α deficiency leads to reduced PV neuron density and PV expression, increased synaptic E/I ratio, enhanced cortical activity, and a prolonged critical period into adulthood. It is interesting to note that similar changes were also observed when TNF-α levels were elevated. For example, exogenous TNF-α application leads to upscaling of glutamate synapses and weakening of GABAergic synapses, leading to increase synaptic E/I ratio (Beattie et al., 2002; Stellwagen et al., 2005). Increased TNF-α expression in the auditory cortex after noise exposure was correlated with reduced PV neuron density (Deng et al., 2020a; Zinsmaier et al., 2020) TNF-α can activate microglia, and activation of microglia has been shown to enable critical period-type ocular dominance plasticity in adult mice (Venturino et al., 2021). Thus, it seems that the effects of TNF-α on sensory cortical circuits and plasticity have a U-shaped curve. A high level and a lack of TNF-α expression both results in reduced PV neuron function, increased E/I ratio, and heightened cortical plasticity.

Elevated TNF-α expression has been associated with reduced PV neuron density and PV expression in pathological conditions. For example, noise-induced hearing loss leads to elevated TNF-α expression and reduced PV neuron density in the auditory cortex. Furthermore, intracerebroventricular infusion of TNF-α lowers the threshold of noise-induced reduction of PV neuron density in the auditory cortex (Deng et al., 2020b; Deng et al., 2020a; Zinsmaier et al., 2020). These findings are consistent with noise and TNF-α-induced reduction of GABAergic synaptic transmission. In the present study, reduced PV neuron density and PV expression were

observed in TNF-α KO mice suggesting that a basal level of TNF-α is required for maturation of PV neurons and/or maintaining PV neuron function.

TNF-α modulates excitatory synapses in a complex fashion. In dissociated cultured neurons, it triggers insertion of AMPA receptors into the synapse (Beattie et al., 2002; Stellwagen et al., 2005). Blocking TNF-α or knocking out TNFR1 reduced AMPA receptor density in the synapses, and lowered mEPSC amplitude and frequency, suggesting that a basal TNF-α signaling is required for maintaining excitatory synaptic function. Exogenous TNF-α enhanced glutamate synapses. However, the effect of TNF-α appears to depend on the state of the neuron, as blockade of the neuronal activity with TTX prevented TNF-α-induced upregulation of glutamatergic synapses. The effect of TNF-α on glutamatergic synapses also depends on the duration of treatment and the type of neurons investigated. Short treatments result in enhanced excitatory synaptic transmission in hippocampal and cortical pyramidal neurons, whereas long-term (24-48 hours) treatments lead to reduced AMPA receptor-mediated currents (Stellwagen et al., 2005; Steinmetz and Turrigiano, 2010). Treatment with TNF-α also weakens excitatory synapses in striatal medium spiny neurons (Lewitus et al., 2014). In the present study, we observed increased basal mEPSC amplitude in pyramidal neurons of acute auditory cortical slices from TNF-α knockout mice, as compared to wildtype mice. Interestingly, basal mEPSC amplitude was not altered in pyramidal neurons of cultured visual cortical slices from TNF-α knockout mice (Kaneko et al., 2008). These differences may be due to differences innate differences between the auditory cortex and visual cortex, or differences in slice preparation.

In addition to modulating basal excitatory synaptic transmission, TNF-α is also involved in homeostatic plasticity following activity blockade or input denervation. TNF-α sequestration with soluble TNFR prevented TTX-induced upscaling of excitatory synapses (Stellwagen and Malenka, 2006; Steinmetz and Turrigiano, 2010). In addition to activity blockade, homeostatic plasticity can also be induced by input denervation and sensory deprivation (Becker et al., 2015; Teichert et al., 2017). For example, input denervation induced upscaling of excitatory synapses on dentate granule cells (Vlachos et al., 2012) This mechanism seems to have two distinct phases—an early TNF-α-independent phase 1-2 days after denervation followed by a late TNF-α dependent phase (Becker et al., 2015). This denervation induced synaptic scaling plateaued 2-7 days after denervation, and decayed back to baseline by 14 days after denervation (Vlachos et al., 2012). Consistent with their findings, we observed no difference in mEPSC amplitude between control and noise-exposed groups of wild type mice. In the present study, we found an increased mEPSC frequency in auditory cortical pyramidal neurons 10-15 days after noise-induced hearing loss. This form of homeostatic plasticity was absent in TNF-α knockout mice.

The observed reduction in cortical PV neuron density and enhancement in basal excitatory synaptic transmission in the present study are suggestive of an E-I imbalance in the auditory cortical circuit of TNF-α knockout mice. This was corroborated by our observation of a significant increase in spontaneous and evoked activity, as well as an increase in tuning bandwidth, in the AI of TNF-α KO mice relative to WT mice. Studies have shown that both bandwidth selectivity and network activity levels are directly influenced by the balance between excitation and inhibition (Chang et al., 2005; Kirmse et al., 2015; Li et al., 2019). Interestingly, the elevated activity level and broadened tuning bandwidth was observed in TNF-α KO mice in

the present study at postnatal Day 60, but not at Day 20 as in a previous report (Yang et al., 2014b). While the CP for frequency map plasticity ends around the second postnatal week in the auditory system, other auditory processing features such as latency, bandwidth and threshold continue to be fine-tuned through postnatal Day 60 (Chang and Merzenich, 2003; Villers-Sidani, 2007; Insanally et al., 2009). Thus, it is possible that the phenotypic increase in tuning bandwidth and network activity in TNF-α KO animals develop after postnatal Day 20. The increased activity and responsiveness may be driven by sensory inputs since cortical activity is upregulated by sensory stimulation in TNF-α KO but downregulated in wildtype mice (Yang et al., 2014b).

TNF-α KO mice were impaired in a homeostatic component of ocular dominance plasticity, but exhibited normal auditory cortical frequency map plasticity in the critical period, suggesting that the two forms of plasticity are mediated by partially different mechanisms (Kaneko et al., 2008; Yang et al., 2014b). Monocular deprivation-induced ocular dominance shift may involve long-term depression of the synapses from the deprived eye, and subsequent homeostatic upregulation of the excitatory synapses from both eyes (Kaneko et al., 2008; Ranson et al., 2012). Sound stimulation-induced frequency map reorganization likely involves potentiation of stimulated synapses, and possibly homeostatic downregulation of excitatory synapses to stabilize the level of activity in cortical neurons (Yang et al., 2014a; Yang et al., 2014b).

Critical period-type plasticity can be extended into, or restored in the adulthood by sensory, genetic and pharmacological manipulations (Sale et al., 2007; de Villers-Sidani et al., 2008; Zhou et al., 2011; Cisneros-Franco and de Villers-Sidani, 2019; Schwartz et al., 2020). These manipulations often lead to reduced inhibition and a shift in E-I balance. Our observations of

extended critical period in mice with reduced PV neuron density and enhanced basal excitatory synaptic transmission are consistent with previously report roles of PV neurons and E/I balance in modulation of the critical period (Hensch and Fagiolini, 2005; van Versendaal and Levelt, 2016; Reh et al., 2020).

TNF-α plays key role in cell proliferation and neurogenesis (Borsini et al., 2015). Although TNF-α KO mice do not exhibit gross brain abnormality or behavioral deficits, more detailed examination revealed important difference between TNF-α KO and WT mice (Golan et al., 2004; Yli-Karjanmaa et al., 2019). For example, compared to WT mice, TNF-α KO mice had fewer proliferating cells and microglia, and more neurons in the cortex (Yli-Karjanmaa et al., 2019). TNF-α KO mice also had accelerated maturation of the hippocampal dentate gyrus and smaller dendritic trees in CA1 and CA3 regions (Golan et al., 2004). TNF-α deficiency also reduced the expression of WNT signal-related proteins (Yli-Karjanmaa et al., 2019). Behaviorally, compared to WT mice, TNF-α KO mice performed better in spatial learning tasks (Golan et al., 2004; Yli-Karjanmaa et al., 2019). These findings indicate that TNF-α plays an important role in neuronal development and maturation. In the present study, we found that the maturation of PV neurons was also impaired in the TNF-α KO mice. The mechanisms by which TNF-α deficiency leads to reduced PV neuron density is unknown, but might be related to reduced expression of BDNF (Golan et al., 2004; Liu et al., 2017), a neurotrophic factor that is involved in PV neuron maturation and critical period modulation (Hanover et al., 1999; Huang, 1999). TNF-α may also modulate PV neuron function through its receptors on PV neurons (Richter et al., 2014). Future studies should elucidate mechanisms underly the complex modulations of PV neuron density by TNF-α signaling

3.6: Figures

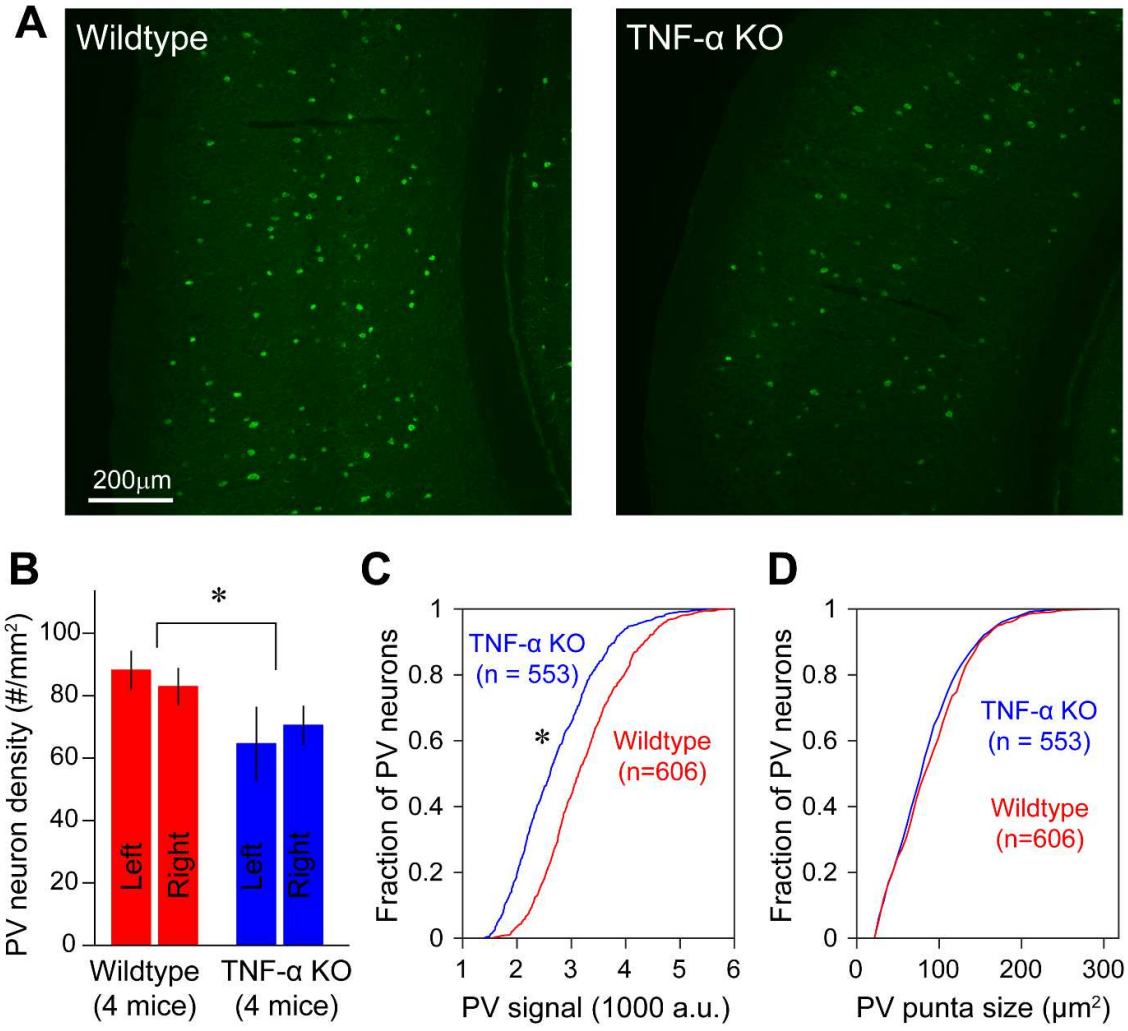

Figure 3.1: PV neuron density and PV expression are reduced in the auditory cortex of TNF-α KO mice. A) Example images of PV staining in the auditory cortex of WT and TNF-α KO mice. AI is in the center of the images. **B)** PV neuron density in AI of both hemispheres and in WT and TNF-α KO mice. PV neuron density was lower in the TNF-α KO mice than in WT mice. **C)** Cumulative distributions of PV signal intensity of cortical PV neurons. PV expression level was significantly reduced in the TNF-α KO mice compared to the WT mice. **D)** Cumulative distribution of the size of PV staining puncta. The puncta size was not different between the TNF-α KO and WT mice. * indicates $p < 0.05$.

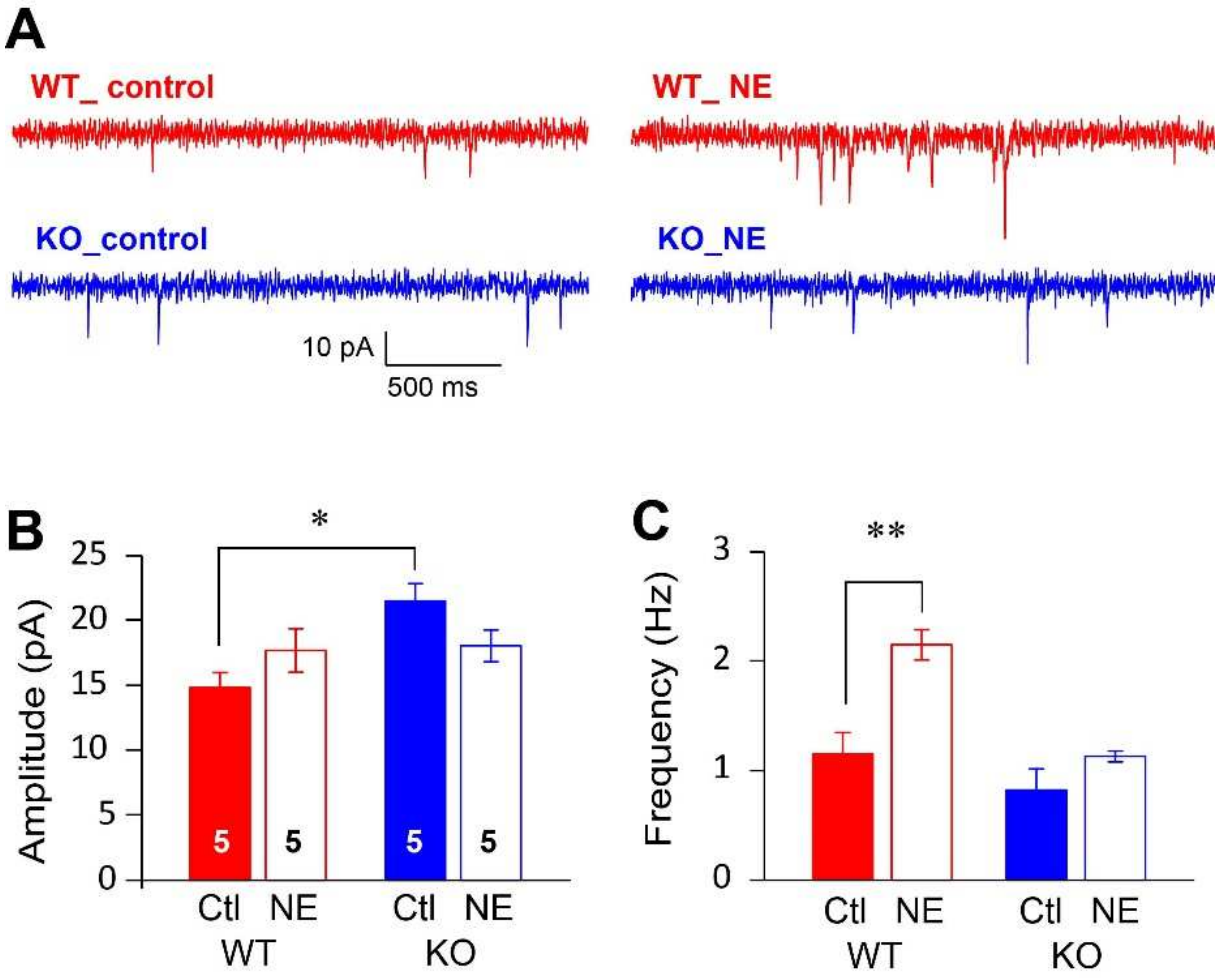

Figure 3.2: Hearing loss-induced homeostatic plasticity is impaired in cortical pyramidal neurons of TNF-α KO mice. A) Representative traces of mEPSCs recorded from pyramidal neurons in the auditory cortex of control and noise-exposed TNF-α KO and WT mice. **B**) Amplitude of mEPSCs. mEPSC amplitude was higher in control TNF-α KO mice than in control WT mice, but was not altered by noise-induced hearing loss. **C**) Frequency of mEPSCs. No difference was observed in control mEPSC frequency between WT and TNF-α KO mice. noise-induced hearing loss increase mEPSC frequency in WT but not in TNF-α KO mice. * and ** indicate $p < 0.05$ and $p < 0.005$, respectively.

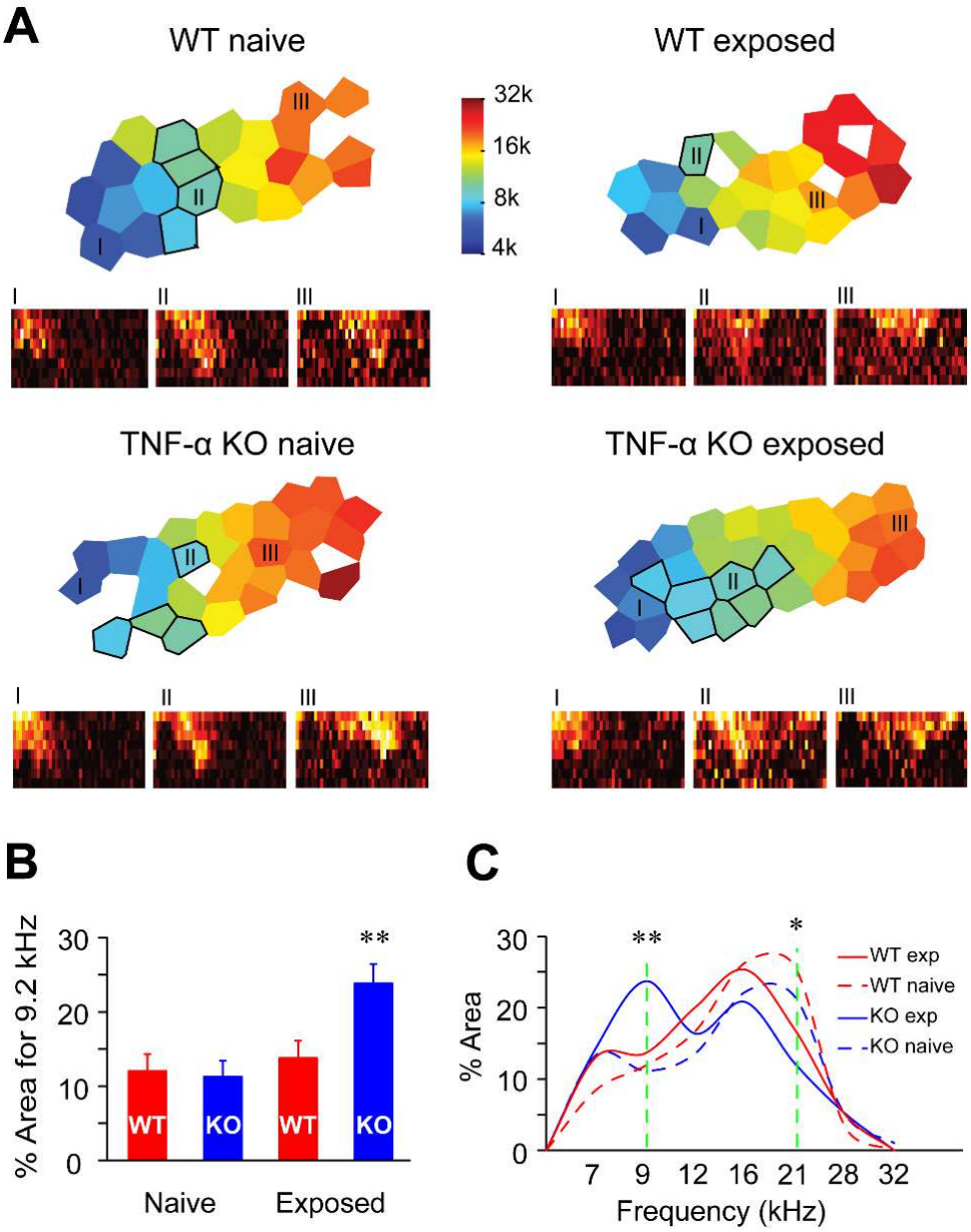

Figure 3.3: TNF-α KO mice retain capacity for critical period plasticity into adulthood. A) Example frequency maps recorded from AI of each experimental group (n = 6 mice for all groups). Areas outlined in black indicate sites with BF within the exposure frequency of 9.2 kHz (+/- 0.2 octaves). Underneath each map are representative images of recorded receptive fields in I) low frequency, II) middle frequency, and III) high frequency band. Adult TNF-α KO mice showed an expansion in the exposure frequency band, relative to WT animals and unexposed TNF-α KO animals. Significance represents 2 x 2 ANOVA (genotype x exposure) main effect. * and ** indicate $p < 0.05$ and $p < 0.005$, respectively.

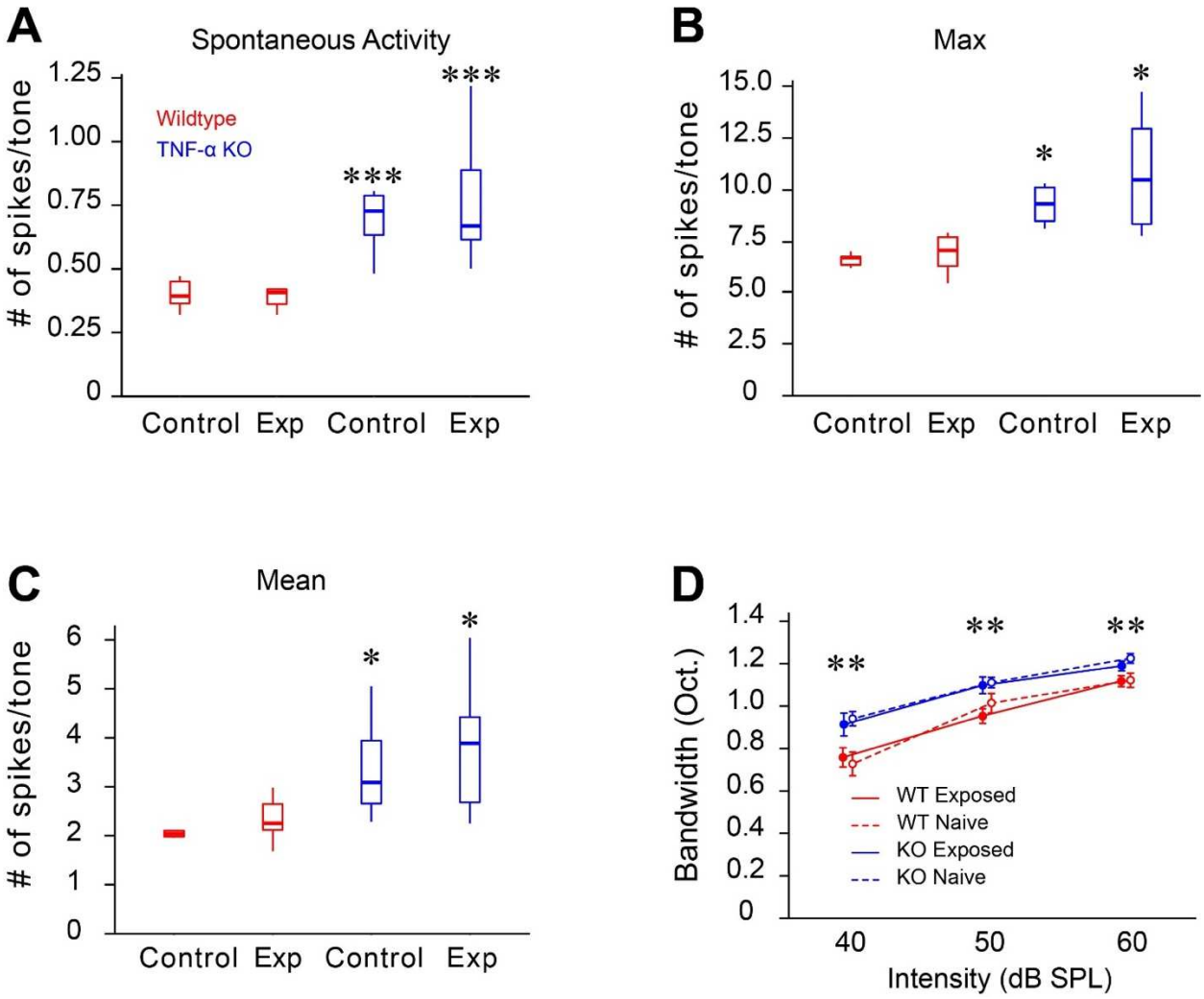

Figure 3.4: TNF-α KO mice show disruptions in receptive field properties indicative of altered excitatory-inhibitory balance. Graphs displaying average **A)** spontaneous activity, **B)** max response, **C)** mean response, **D)** and bandwidth for each group. TNF-α KO mice had significantly increased measures for all properties shown above. Bandwidth is measured at intensities of 40, 50, and 60 dB SPL. Significance for **A** and **D** represents 2X2 ANOVA (genotype x exposure) effect of genotype. Significance for **B** and **C** represents pairwise comparison with Bonferroni correction to WT Naïve. *, ** and *** indicate $p < 0.05$, 0.005 and 0.0003, respectively.

4

Unilateral Hearing Lesion Re-establishes Critical Period Plasticity and Induces a Binaural Shift

Schwartz BA, Bao S (**2021**) Unilateral Hearing Lesion Re-establishes Critical Period Plasticity and Induces a Binaural Shift. *To be submitted*.

4.1: Abstract

Plasticity is the brain's capability to adapt to intrinsic and extrinsic stimuli. Following an early developmental epoch known as the critical period, plasticity drops precipitously in the cortex to stabilize the sensory and motor circuits that facilitate basic functions. However, certain environmental stimuli can destabilize these circuits and yield a plastic state as seen during the critical period. In these experiments we probe the question whether noise-induced hearing lesions are sufficient to re-establish critical period plasticity along the auditory pathway. Compared to naïve control mice and lesioned mice that did not receive pure tone exposure, hearing lesioned mice that were exposed to 16 kHz pure tones had a significantly enlarged cortical area dedicated to the 16 kHz frequency band. Furthermore, noise-induced hearing lesions induced a binaural shift, in that ipsilaterally recorded receptive field properties shifted towards values recorded from the contralateral auditory pathway. These results indicate that following noise-induced hearing lesions, the central nervous system engages a complex plasticity response to facilitate re-wiring of damaged auditory pathways.

4.2: Introduction

Plasticity is the brains capability to adapt or respond to intrinsic and extrinsic stimuli. Throughout an organisms lifetime, plasticity is highest during an early developmental epoch known as the critical period (Hensch, 2005a). The high levels of plasticity during development facilitates experience-dependent wiring of sensory pathways. Once the critical period ends, the requirements for plasticity induction change in that passive exposure to sensory stimuli no longer induces plastic change (Keuroghlian and Knudsen, 2007). There are many factors of critical period closure that have been investigated such as shifting the excitatory/inhibitory balance (Hensch and Fagiolini, 2005), condensation of perineuronal nets around parvalbumin positive interneurons (PV+) (Pizzorusso et al., 2002), and epigenetic mechanisms (Baroncelli et al., 2016; Schwartz et al., 2020). The closure of the critical period is important for crystalizing sensory circuits and accordingly establishing the capability for stable sensory perception.

Studies have been conducted to explore mechanisms of re-opening the critical period in adulthood. Genetic and molecular manipulations such as degradation of perineuronal nets (Pizzorusso et al., 2002; Carulli et al., 2010), and reducing intracortical inhibition (Harauzov et al., 2010) have been shown to be effective mechanisms for re-opening the critical period in adulthood. This work has been extended by exploring whether specific environmental experiences can also induce critical period plasticity. Specifically, studies show that environmental enrichment (Sale et al., 2007) and dark exposure (He et al., 2006; Murase et al., 2017) are sufficient to re-open visual system critical period plasticity. In the auditory system, masking temporal acoustic input was also sufficient to re-open critical period plasticity in the

adult rat (Thomas et al., 2019). More studies are required to investigate whether other experiences in adulthood can re-open critical period plasticity.

One environmental experience that may engage plasticity mechanisms is traumatic brain injury. In the auditory system, traumatic brain injury can be induced through loud noise-exposure, or blast exposure (Masri et al., 2018; Wang et al., 2019). (Masri et al., 2018; Wang et al., 2019). Both blast-exposure and noise-exposure have been shown to dramatically alter frequency map organization in the auditory cortex (Norena and Eggermont, 2005; Masri et al., 2018). Noise-exposure and cochlear ablations have also been shown to shift the excitatory/inhibitory balance along the auditory pathway towards higher levels of excitation (Norena et al., 2003; Kotak et al., 2005; Zhao et al., 2016; Wang et al., 2019). Furthermore, blast and noise-exposure have been shown to significantly decrease the density of PV interneurons in the auditory cortex, as well as decrease the intensity of perineuronal nets fluorescence in the auditory cortex (Nguyen et al., 2017; Wang et al., 2018; Deng et al., 2020a). Frequency map changes, excitatory/inhibitory balance shifts, PV+ neuron density, and the fidelity of perineuronal nets are indicators of critical period plasticity. However, the question remains: is the significant re-organization of primary auditory cortex that occurs due to noise-induced lesions caused by re-establishing critical period plasticity, or is it just a function of the damage along the auditory pathway?

In this study, we induced hearing lesions in adult mice, and subsequently exposed them to pure-tones in order to access whether critical period-like plasticity is present in the auditory cortex of lesioned mice. Our results show that noise-induced hearing lesions followed by pure tone exposure led to a significant increase in the area dedicated to the exposure frequency relative to

hearing lesioned mice without exposure and naïve mice. Furthermore, noise-induced hearing lesions engaged binaural plasticity mechanisms, leading to a shift in auditory pathway bias. Before hearing lesion, ipsilateral auditory receptive fields had a longer latency, a smaller bandwidth, and a significantly lower average amplitude of response. Following hearing lesion, ipsilateral receptive field latency, bandwidth and amplitude of response shifted towards values seen along the contralateral auditory pathway. These results indicate that noise-induced hearing lesions engage plasticity mechanisms to both re-organize the primary auditory cortex, and shift hearing bias from the contralateral to the ipsilateral auditory pathway.

4.3: Methods

Animals: All procedures in this study were approved by the Animal Care and Use committee at the University of Arizona. A total of 20 C57BL/6J (B6.129S/SvEv-Gpi1-Tnftm1Gkl) (8-week-old male, Jack- son Laboratory, Bar Harbor, ME) were used in this experiment (both males and females).

Noise-induced hearing lesions: Animals were anesthetized with ketamine (100 mg/kg, IP) and xylazine (10 mg/kg, IP) and maintained at 36.5℃ with a homeothermic heating pad (Harvard Apparatus, Holliston, MA). Unilateral NIHL was induced by playing a continuous 112–114 dB SPL noise centered at 8 kHz through a custom-made piezoelectric earphone speaker to the left ear for 2 hours. The right ear was protected with sound attenuating clay. The sound level was measured with a Bruel and Kjaer 4135 condenser microphone (Nærum, Denmark).

Sound exposure: Sound exposure was performed as previously described in (Zhang et al., 2001). Litters of 2-3 mice were placed in a ventilated, sound-shielded, calibrated test chamber for 10 days (directly following noise-induced hearing lesion) and exposed to 16 kHz pure tone pips. A 25-ms tone (5-ms ramps) at 60–70 dB SPL was applied from a speaker placed about 15 cm above the mice, at 6 pulses per second with 1-s intervals to minimize adaptation effects. No noticeable distortion of tonal stimuli was detected from sound spectrum recorded inside the test chamber. There were no significant spectral peaks for the normal environmental noise background. The total sound pressure level in the animal room was 5–10 dB lower than that of exposed tonal stim- ulus intensity. Inside the sound attenuation chamber with the presence of mice, but in the absence of the tone stim- ulus, the noise level was about 15–25 dB below that in the animal room at all frequencies within the mouse's hearing spectrum. No significant harmonic signal was found in the chamber when a tonal stimulus was being delivered.

Electrophysiological recording procedure: The primary auditory cortex of mice was mapped as previously described (Schwartz et al., 2020), except as follows. Mice were anesthetized with ketamine (100 mg/kg, i.p.) and xylazine (10 mg/kg, i.p.), and kept anesthetized with, a steady flow of 1% isoflurane. The cortex was maintained under a layer of silicone oil, that was reapplied as necessary. Multiunit responses to 25 ms pure tone pips (2–74 or 4 –74 kHz, 0.1 octave increments at 0–70 dB, 10 dB increments) were recorded using tungsten micro-electrodes (FHC) in the thalamorecipient layer of AI (350–450 micrometers below the cortical surface). References to neurons in this text refer to multiunit responses recorded extracellularly. Tones were presented to the left ear through an electrostatic speaker (Tucker Davis Technologies) at 3 pips per second and each frequency-intensity combination was repeated three times. Cortical

penetration locations were recorded on a high-resolution image, which was later used to construct the map. For hearing lesioned animals, the recording procedure was the same, except the speaker was inserted into the right ear (non-lesioned ear), for auditory stimulation. Naïve animals had a speaker in both the left and right ear, due to the fact ipsilateral auditory signal is weak in non-lesioned animals.

Primary auditory cortex mapping analysis: Receptive fields and response properties were isolated using custom-made programs in MATLAB as previously described (Insanally et al., 2010), except as follows. The peak of the peristimulus time histogram (PSTH) within a window from 7 to 50 ms after the stimulus onset was defined as the response latency. The response window was defined as a period encompassing the PSTH peak, in which the firing rate was higher than the baseline firing rate. The spikes in the response window were counted to reconstruct the receptive field. The map of the primary auditory cortex was generated using the voroni tessellation algorithm, in which the best frequency (BF) of the receptive field is converted to a polygon of a certain area. The area of the polygons dedicated to a CF of 16 kHz (+/-0.2 octaves) were summed and then divided by the total area to determine the percent of AI dedicated to 16 kHz. For comparing the ratio of area dedicated to 16 kHz, to low frequency, the area of the polygons dedicated to 9.2kHz and 12.1kHz (+/-0.2 octaves) were summed. We then divided the area dedicated to 16 kHz by the summation of the area dedicated to the two low frequency bins. Tuning bandwidth (BW) was defined as the bandwidth (in octaves, logarithmically), at the specified intensity. The onset latency was defined at the onset of the response window, while the peak and offset latency were defined at the peak amplitude and end of the response window, respectively. The median receptive field responses were the median

number of spikes for all frequency-intensity combinations within the receptive field. For all receptive field properties, values were averaged to create means per individual mouse.

Statistics: All statistical analysis was performed in SPSS software. Dataset normality and homogeneity of variances were tested using the Shapiro-Wilk and Levine test, respectively. All analysis of receptive field area were tested using a one-way ANOVA. When comparing contralateral receptive field properties to ipsilateral properties, a paired samples t-test was used. When comparing ipsilateral receptive field properties from mice in different experimental groups, a one-way ANOVA was used. The *post hoc* test used following one-way ANOVA was a least significant difference test (LSD). The significance level was set at $\alpha = 5\%$. Data were presented as mean ± SEM unless otherwise stated.

4.4: Results

Noise-induced hearing lesions restore capacity for frequency map plasticity

As mentioned previously, damage along the auditory pathway can induce significant changes within the central nervous system. Specifically, noise-induced hearing lesions have been shown to alter tonotopy within primary auditory cortex, shift excitatory/inhibitory balance in the brain, alter PV neuron density, and disrupt the fidelity of perineuronal nets. These results highlight the possibility that noise-induced hearing lesions re-establish critical period-like plasticity.

To test this hypothesis, we subjected adult mice to noise induced hearing lesions, and subsequently exposed those animals to pure tone pips centered on 16 kHz, for 10 days (HL+E).

Following the 10 day exposure period, the animals' primary auditory cortex was electrophysiologically mapped. The maps of HL+E animals (n =8) were compared to those of naïve control animals (control, n =6), and hearing lesioned animals that were not exposed to tone pips (HL+NE, n =6). Due to the fact the left ear was the ear used for hearing lesions, animals that were lesioned had their right ears stimulated with sound (ipsilateral auditory pathway), for the mapping procedure. Representative maps of primary auditory cortex can be seen in figure 4.1A. HL+E animals saw a significant increase in the area dedicated to 16 kHz relative to controls and HL+NE animals (Figure 4.1B, ANOVA: $F_{2,19} = 15.49$, $p < 0.001$). *Post hoc* analysis revealed that the HL+E mice were significantly different from both control and HL+NE (*post hoc* LSD: HL+E to control $p < 0.001$, HL+E to HL+NE $p = 0.016$). To better understand how the nature of the shift in tonotopy, we compared the ratio of the area dedicated to 16 kHz to the area dedicated to low frequency bins (from 9.2 kHz to 12.1 kHz). Similar to the overall area, the ratio of the area dedicated to 16 kHz to the area dedicated to low frequency bins was significantly higher in HL+E group relative to the two other experimental groups (Figure 4.1C: ANOVA: $F_{2,19} = 5.78$, $p = 0.012$; *post hoc* LSD: HL+E to control $p = 0.007$, HL+E to HL+NE $p = 0.019$). Together, these results indicate that following noise-induced hearing lesions, the brain shifts to a more plastic state that facilitates auditory cortical map re-organization.

Contralateral receptive fields have different characteristics compared to ipsilateral receptive fields

In the visual system, depriving one eye of light during the critical period causes a binocular shift in bias from the contralateral visual pathway to the ipsilateral visual pathway (Wiesel and Hubel, 1963). Noise-induced hearing lesions are a form of auditory deprivation in that the damaged

pathway can no longer transmit auditory information. Therefore we tested the hypothesis that since hearing lesions seem to re-establish critical period plasticity, they may also facilitate binaural plasticity. However, before we accessed binaural plasticity following noise-induced hearing lesion, we established a baseline for contralateral and ipsilateral receptive field properties.

Contralateral and ipsilateral receptive fields were recorded in naïve controls and compared within subject. Qualitatively, ipsilateral tonotopic maps from healthy mice were variable, and thus difficult to access. This follows previous studies which show that mice with intact hearing respond meagerly to ipsilateral auditory stimuli (Polley et al., 2013). There were multiple properties that significantly differed depending on whether they were contralaterally or ipsilaterally recorded. Tuning bandwidth at multiple threshold intensities was found to be significantly higher when recorded from the contralateral auditory pathway compared to the ipsilateral auditory pathway (Figure 4.2, paired t-test- dB70: $t_5 = 2.766$, $p = 0.04$; dB60: $t_5 = 3.49$, $p = 0.017$; dB50: $t_5 = 3.13$, $p = 0.026$). Furthermore, all ipsilaterally recorded latencies were found to be significantly slower than receptive fields recorded from the contralateral auditory pathway (Figure 4.3, paired t-test- onset: $t_5 = 3.58$, $p = 0.016$; peak: $t_5 = 3.88$, $p = 0.012$; offset: $t_5 = 3.97$, $p = 0.011$). In terms of average amplitude of response, the median amplitude for ipsilaterally recorded receptive fields was significantly lower than the median amplitude for contralaterally recorded receptive fields (Figure 4.4, paired t-test- median amplitude: $t_5 = 2.82$, $p = 0.37$). These results confirm that in healthy mice, auditory processing differs immensely between the contralateral auditory pathway and the ipsilateral auditory pathway.

Noise-induced hearing lesions lead to binaural shift in hearing bias

After establishing a baseline of receptive field properties between the contralateral and ipsilateral auditory pathway, we were able to interrogate how noise-induced hearing lesions impact auditory processing. Many properties of ipsilateral auditory processing changed as a function of hearing lesions. For example, ipsilateral receptive field bandwidth at multiple intensities was found to be significantly different between hearing lesioned animals and animals with intact hearing (Figure 4.5, one-way ANOVA- dB70: $F_{2,19} = 7.802$, $p = 0.004$; dB60: $F_{2,19} = 5.2$, $p = 0.017$; dB50: $F_{2,19} = 6.281$, $p = 0.009$). *Post hoc* analysis revealed that at all of the analyzed intensities, the HL+NE group was found to have a significantly higher bandwidth than naïve control animals (LSD, HL+NE to control- dB70: $p = 0.001$; dB60: $p = 0.005$; dB50: $p = 0.003$). The HL+E group had bandwidths that fell between the values of the control group and the HL+NE group. *Post hoc* analysis further revealed that HL+E was different from HL+NE at dB60, and dB50 (LSD, HL+NE to HL+E- dB70: $p = 0.052$; dB60: $p = 0.048$; dB50: $p = 0.041$). Together, these results indicate that noise-induced hearing lesions lead to increased bandwidth in the ipsilateral auditory pathway, and that exposure following hearing-lesion led to an intermediate increase in bandwidth following hearing lesion.

Another property that changed as a function of hearing damage were receptive field latencies. As mentioned previously, latencies in animals with intact hearing were found to be significantly longer along the ipsilateral auditory pathway compared to the contralateral auditory pathway. Following noise-induced hearing lesions, ipsilateral pathway latency decreased significantly. One-way ANOVA revealed that both peak and offset latencies were significantly different between the three ipsilateral groups (Figure 4.6, one-way ANOVA- peak: $F_{2,19} = 7.17$, $p = 0.006$;

offset: $F_{2,19} = 7.39$, $p = 0.005$). The onset latency data group had unequal variances, so a Kruskal-Wallis non-parametric test was used and found not to be significant (Kruskal-Wallis; onset: $H_2 = 3.31$, $p = 0.192$). *Post hoc* analysis revealed that both the HL+E and HL+NE had significantly shorter peak and offset latencies relative to naïve controls (LSD, HL+E to control- peak: $p = 0.002$; offset: $p = 0.002$; HL+NE to control- peak: $p = 0.015$; offset: $p = 0.014$). Together these results indicate that in the presence of damage along the contralateral auditory pathway, ipsilateral latencies decrease.

The final property we investigated was median amplitude. In animals with intact hearing, median amplitude of auditory evoked response was found to be significantly higher along the contralateral auditory pathway compared to the ipsilateral auditory pathway. Noise-induced hearing lesion led to a non-significant increase in median amplitude relative to naïve controls (Figure 4.7, one-way ANOVA- Rmedian: $F_{2,19} = 1.02$, $p = 0.381$). As similarly seen with bandwidth and latency, the HL+E experimental group had intermediate median amplitude values relative to HL+NE and naïve control values. Therefore, even though there was no significant difference in median amplitude, the pattern of properties shifting as a function of noise-induced hearing loss remains the same. Noise-induced hearing lesions shift auditory processing properties towards values seen in the contralateral pathway, while including pure-tone exposure following noise-induced hearing lesions, reduces the binaural shift in auditory processing.

4.5: Discussion

The main finding of this study was that noise-induced hearing lesions were found to re-establish exposure-based frequency map plasticity in the primary auditory cortex. Furthermore, noise-induced hearing lesions engaged binaural plasticity mechanisms as well, leading to a shift in auditory response properties. Properties such as latency, and bandwidth along the ipsilateral pathway shifted to values seen along the contralateral auditory pathway. Together, these results indicate that inducing damage along the auditory pathway leads to a considerable increase in the plasticity within the auditory pathway, which leads to wholescale changes in the frequency map structure, and auditory pathway bias.

Following noise-induced hearing damage, exposure to 16 kHz pure tones led to a significant increase in the area dedicated to 16 kHz in exposed mice relative to unexposed lesioned mice and naïve mice. Furthermore, the ratio of the area dedicated 16 kHz versus the area dedicated to low frequency bins also revealed a significant increase for the lesioned exposed animals relative to lesioned unexposed and naïve mice. To our knowledge, this is the first demonstration that following damage to the auditory pathway, the central nervous system re-establishes critical period plasticity to re-wire the damaged frequency map. A previous study showed that exposure of auditory environmental enrichment (pure tones spanning the audible frequency range for cats), following noise trauma, reduced hearing loss and blocked the shift in frequency map organization that occurs normally after noise trauma (Norena and Eggermont, 2005). The authors interpretation of their results was that the environmental enrichment provided a protective buffer to the damage that had occurred following noise trauma. However, our results which show that

noise trauma leads to increased plasticity, indicate that rather than a protective buffer, the enrichment following trauma is providing beneficial auditory input to facility proper re-wiring. This information could have significant impact on how we treat neural damage following exposure to traumatic noise. Following injury, the brain enters a plastic state where the effect of experience on structure and function is especially strong. Thus, the best course of action following exposure to a traumatic sound, may be immediate exposure-based therapy, to leverage the increased plasticity in the brain.

Interestingly, our results also show that the central nervous system engages binaural plasticity as well as frequency map plasticity, following the induction of hearing lesions. Comparing receptive field properties from the ipsilateral and contralateral auditory pathways within naïve subjects, we saw that ipsilateral receptive fields had a longer latency, a smaller bandwidth, and lower median response amplitude, which follows with previous reports (Polley et al., 2013). Following noise-induced hearing damage, ipsilateral receptive fields saw a decrease in latency, an increase in bandwidth and a non-significant increase in median response amplitude. Thus, noise-induced hearing damage shifted ipsilateral receptive field properties towards values recorded from the contralateral auditory pathway. This form of binaural plasticity is similar to ocular dominance plasticity, in which closing one eye shifts ocular bias towards the non-disrupted eye (Wiesel and Hubel, 1963). In the presence of auditory damage along the contralateral auditory pathway, the central nervous system induces a binaural bias shift such that the ipsilateral auditory pathway can more efficiently transmit auditory information. Exposing animals to pure tones following induction of hearing lesions attenuated the binaural shift. The increase in bandwidth and median response amplitude was lower in animals that received 16 kHz

tone exposure following noise-induced hearing lesion relative to animals that did not receive pure-tone exposure. Therefore, band-limited auditory enrichment facilitated a recovery of ipsilateral receptive field properties towards values recorded in naïve animals. The exposure was limited to the 16kHz frequency band, which makes up only a portion of the primary auditory cortex. An interesting follow-up experiment would be to expose animals to pure tones that span the entire audible frequency range following noise-induced hearing lesions, and probe whether the magnitude of the binaural shift was attenuated to a larger degree.

One question that remains is how do noise-induced hearing lesion re-establish critical period plasticity? There are many parallel mechanisms that may contribute to the increase in plasticity following noise-induced hearing lesions. For example, the expression of neuroinflammatory cytokines like tumor-necrosis factor alpha (TNF-α). Previous results from our lab show that noise-induced hearing lesions significantly increases the activation of microglia, as well as the expression of cytokines such as TNF-α and interleukin 1β, in the auditory cortex (Wang et al., 2019). TNF-α expression has been shown to induce significant functional changes to neuronal circuits, specifically increasing excitatory input as well as decreasing inhibitory input via AMPA receptor insertion and GABA receptor internalization, respectively (Beattie et al., 2002; Ogoshi et al., 2005; Stellwagen et al., 2005; Stellwagen and Malenka, 2006; Pribiag and Stellwagen, 2013). Furthermore, administration of diffusible TNF-α concurrently with noise-induced hearing lesions yielded a significant loss in the density of PV interneurons, a subset of interneurons that has a significant effect on the regulation of cortical excitatory/inhibitory balance (Ferguson and Gao, 2018; Deng et al., 2020a). Thus, the actions of increased TNF-α expression following noise-induced hearing lesions may shift the excitatory/inhibitory balance towards excitation,

which is a hypothesized mechanism for regulation of critical period plasticity (Hensch and Fagiolini, 2005). This follows from previous results which show that noise-induced hearing lesions yield a significant shift in the excitatory-inhibitory balance towards excitation, that is dependent on TNF-α expression (Norena et al., 2003; Kotak et al., 2005; Zhao et al., 2016; Wang et al., 2019).

Another possible explanation for the increased plasticity following noise-induced hearing lesion, is that the damage to the neural pathway led to auditory input deprivation, which in turn upregulated cortical plasticity. Deprivation has been shown to yield significant effects on plasticity during the critical period and in adulthood. During the critical period, exposure to broadband white noise holds the auditory cortex in a plastic state until the animal is removed from the white noise (Chang and Merzenich, 2003; de Villers-Sidani et al., 2008). The lack of temporally modulated auditory input acts as a form of deprivation that accordingly delays the progression of the critical period. In multiple sensory systems, sensory deprivation in adulthood has been shown to upregulate plasticity levels. In the visual system, light deprivation followed by re-exposure and subsequent monocular deprivation was sufficient to induce an ocular dominance shift in adult rats (He et al., 2006; Murase et al., 2017). In the somatosensory system, sensory deprivation via whisker trimming following induction of ischemic stroke, accelerated the functional remapping of damaged cortical regions (Kraft, 2018). In the auditory system, masking of temporal auditory input via white noise exposure re-established frequency map plasticity in the adult rat (Thomas et al., 2019). Therefore, the damage done to the auditory pathway via noise-induced hearing lesion may reduce auditory input into the cortex, which engages mechanisms that drive deprivation-based plasticity.

The reduced fidelity of perineuronal nets following noise-induced hearing lesions provide another possible explanation for the increased plasticity. Perineuronal nets are extracellular scaffolds, made primarily of chondroitin sulfate proteoglycans, that condense around neurons following the closure of the critical period (Sorg et al., 2016). Perineuronal nets are believed to stabilize neuronal circuits by repressing synaptic plasticity. Perineuronal nets repress synaptic plasticity in many ways, for example, by restricting AMPA receptor trafficking (Frischknecht et al., 2009), inhibiting neurite outgrowth (Corvetti and Rossi, 2005), and acting as a physical barrier to incoming axons trying to form new synaptic contacts (Moon et al., 2001). Many studies have shown that enzymatic degradation as well as genetic disruption of perineuronal nets yields a hyper-plastic state in which neuronal circuits are destabilized (Pizzorusso et al., 2002; Gogolla et al., 2009; Carulli et al., 2010; Happel et al., 2014). Recently, evidence has emerged indicating that noise-induced hearing lesions yield significant changes to the fidelity of perineuronal nets in the auditory cortex. While the density of perineuronal nets was unchanged by noise-induced hearing lesions, the fluorescence intensity of individual nets was significantly reduced across all layers of the auditory cortex (Nguyen et al., 2017). Thus, the repressive properties of perineuronal nets may be attenuated following noise-induced hearing lesion, which may explain the damage dependent increase in plasticity.

Each of the discussed mechanisms have important interactions to consider. Perineuronal nets have been shown to increase the excitability of PV interneurons (the subset of neurons they preferentially engulf) (Balmer, 2016). Accordingly, reduction in perineuronal net function following noise-induced hearing lesion, may lead to a reduction in PV interneuron excitability,

which in turn, would shift the excitatory/inhibitory balance towards higher levels of excitation. Deprivation studies in the visual system show that the increased plasticity following dark exposure is facilitated by molecular degradation of perineuronal nets (Murase et al., 2017). *In vitro* studies show that input deprivation, via pharmacological activity blockade of excitatory synapses, leads to increased release of glial TNF-α (Stellwagen and Malenka, 2006; Heir and Stellwagen, 2020). Further *in vitro* studies show that inducing activation of microglia leads to a significant upregulation in the expression of cytokines such as TNF-α. The increased expression of cytokines correlated with a significant reduction in staining intensity and overall reduction in fluorescence area for perineuronal nets (Wegrzyn et al., 2021). Therefore, while each of the mechanisms discussed above provide a possible explanation for increased plasticity following noise-induced hearing lesion, the possibility remains that each of these mechanisms feed into each other to yield a plastic milieu that facilitates cortical remapping. Future studies are required to further probe the complex molecular and cellular interactions that regulate plasticity following damage to the central nervous system.

4.6: Figures

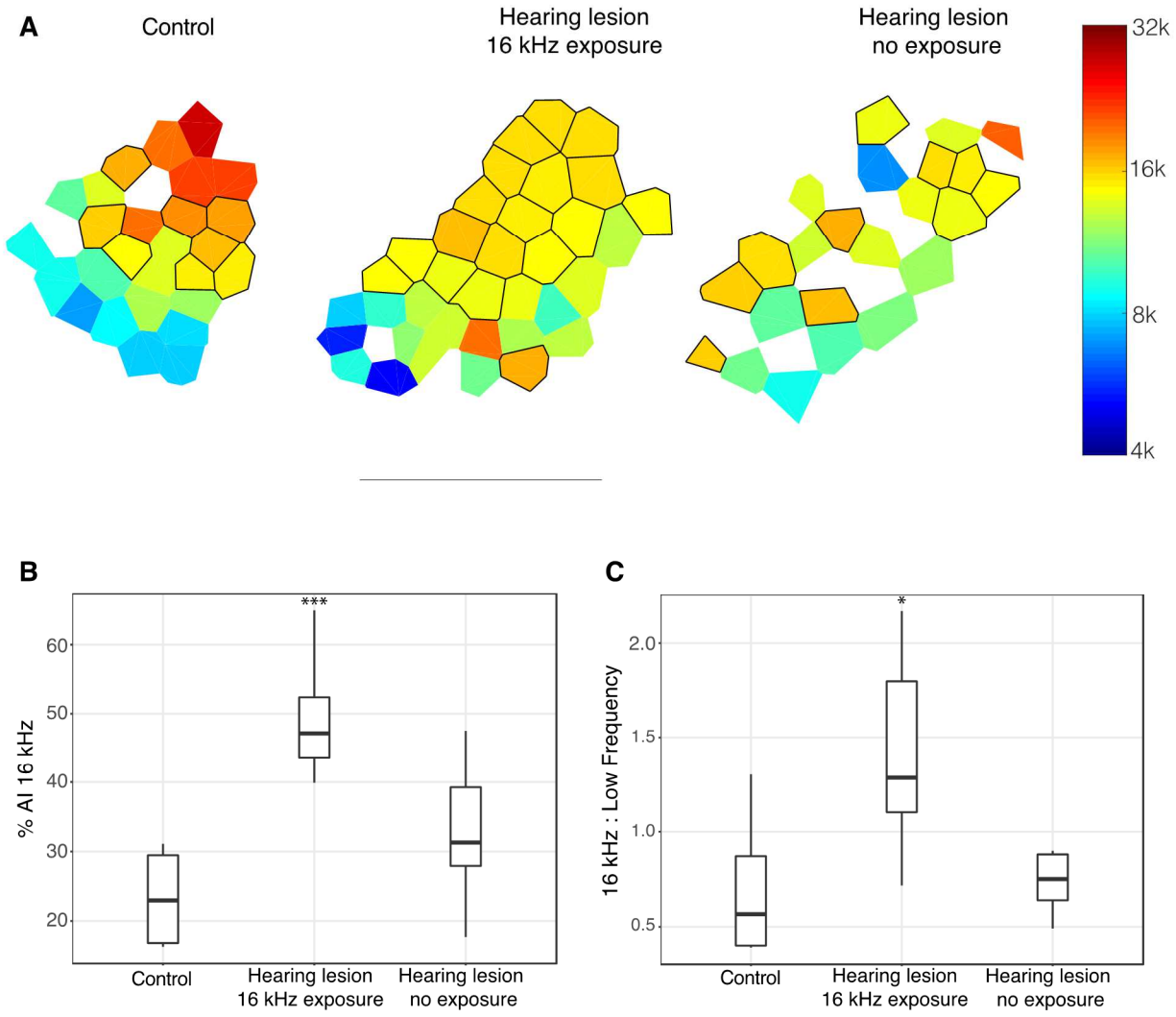

Figure 4.1: Noise-induced hearing lesions re-establish critical period plasticity. **A)** Representative frequency maps recorded from the primary auditory cortex of naïve control mice, hearing lesioned exposed mice, and hearing lesioned mice that did not receive pure tone exposure. Areas outlined in black indicate sites with a BF within the exposure frequency of 16 kHz (+/- 0.2 octaves). **B) and C)** Quantifications of area dedicated to 16 kHz band, and the ratio of area dedicated to 16 kHz versus the area dedicated to low frequency bands. Hearing lesion animals had a significantly higher area dedicated to 16 kHz and area ratio. Significance represents a one-way ANOVA with *post hoc* LSD test. * indicate $p < 0.05$.

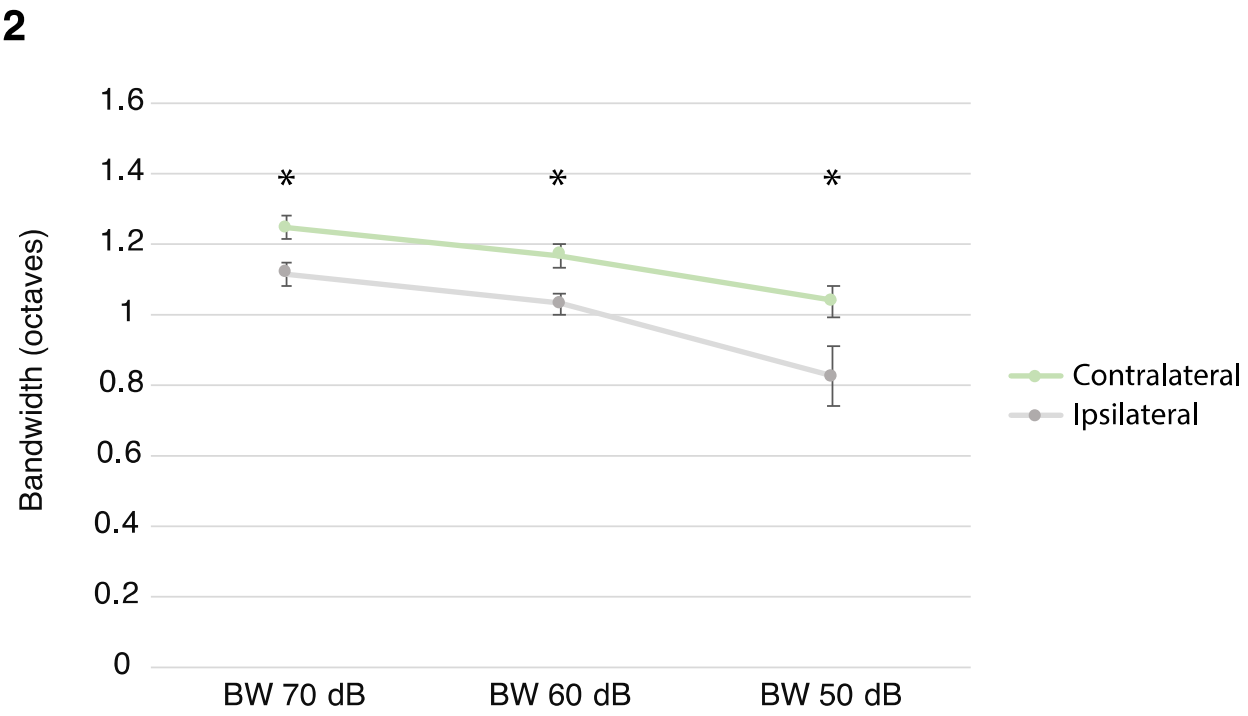

Figure 4.2: Contralateral receptive fields have a larger bandwidth than ipsilateral receptive fields. Representative graph displaying the average bandwidth for contralateral and ipsilateral receptive fields at threshold intensities of 70, 60 and 50 dB. Contralateral receptive fields had a significantly higher bandwidth than ipsilateral receptive fields at the measured intensities. Significance represents paired t-test. * indicate $p < 0.05$.

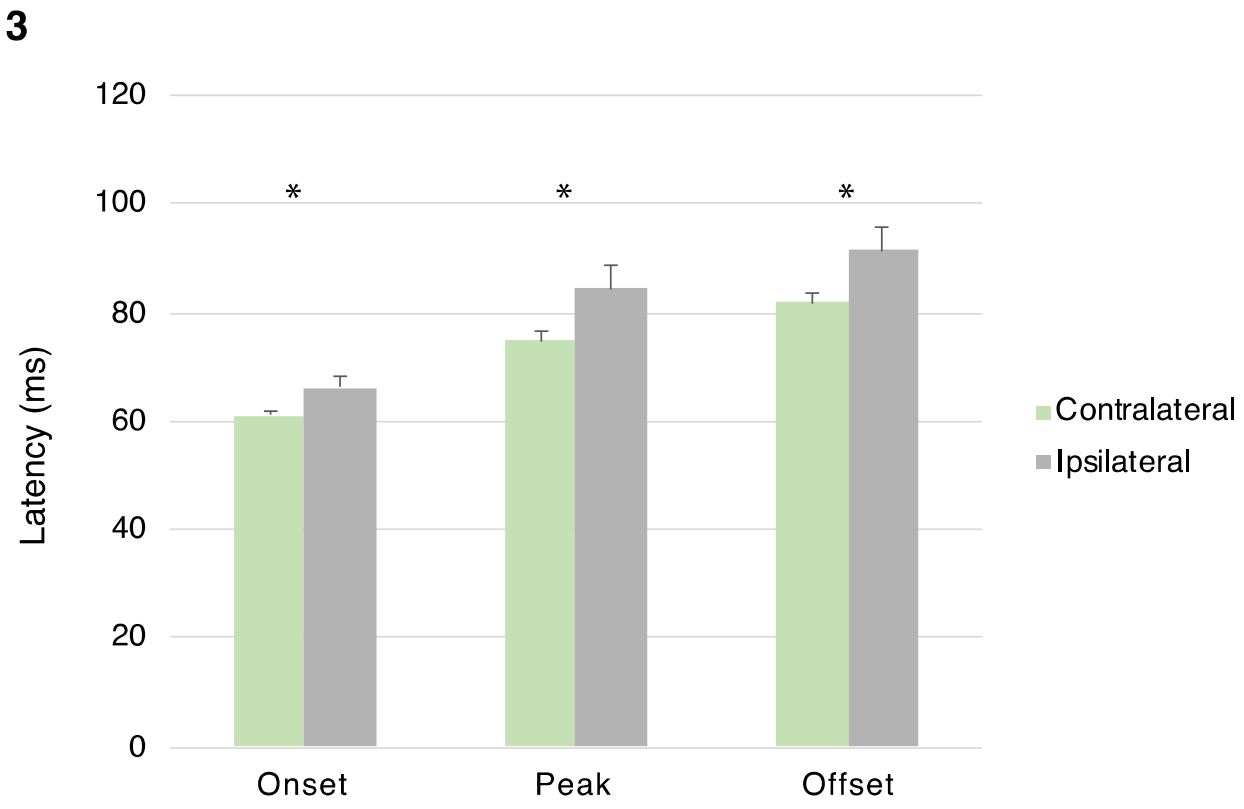

Figure 4.3: Contralateral receptive field latencies are faster than ipsilateral latencies. Representative graph displaying the average onset, peak and offset latencies for contralaterally and ipsilaterally recorded receptive fields. Contralateral receptive fields were significantly faster for all measures of latency. Significance represents paired t-test. * indicate $p < 0.05$.

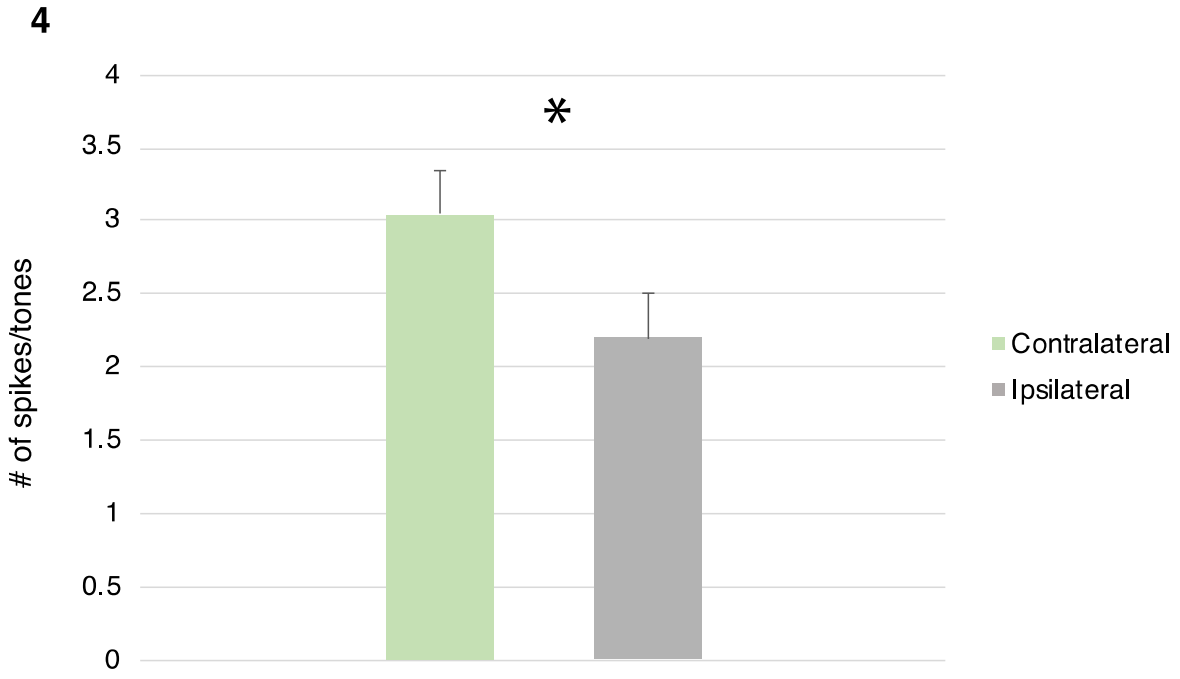

Figure 4.4: Median response amplitude is higher in contralateral receptive fields relative to ipsilateral receptive fields. Representative graph displaying the median response amplitude for contralateral and ipsilateral receptive fields. Contralateral receptive fields had a higher median response amplitude than ipsilateral receptive fields. Significance represents paired t-test. * indicate $p < 0.05$.

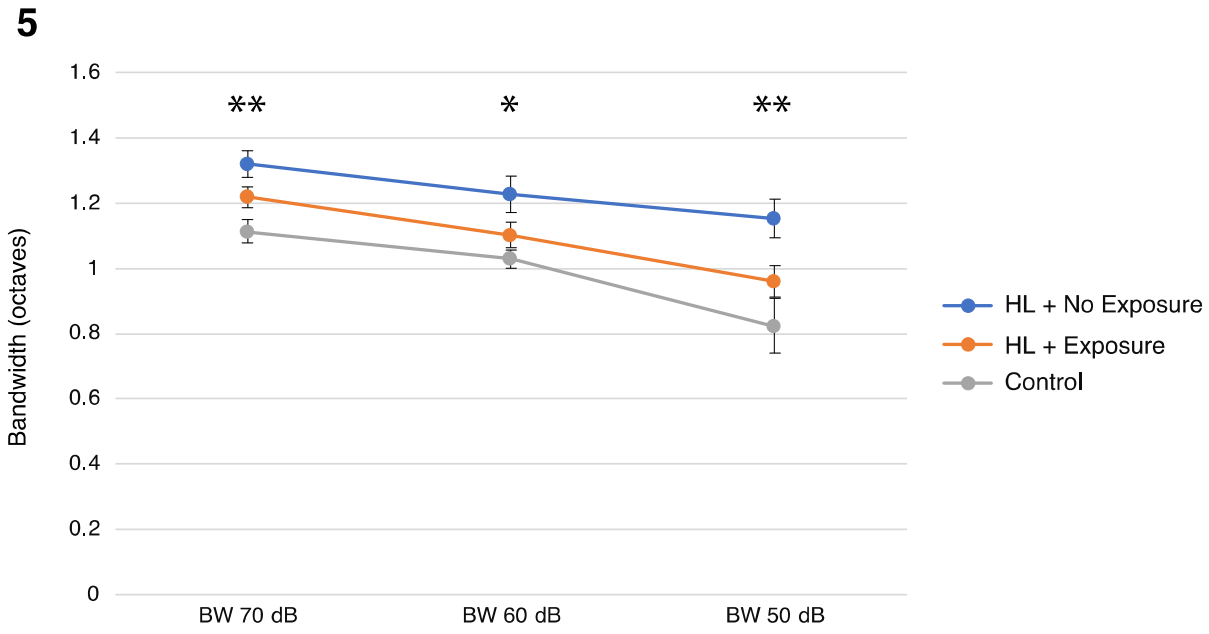

Figure 4.5: Noise-induce hearing lesions increased ipsilateral receptive field bandwidth. Representative graph displaying average ipsilateral receptive field bandwidth for naïve control, hearing lesion exposed mice, and hearing lesioned mice that did not receive pure tone exposure. Noise-induced hearing lesioned increased receptive field bandwidth at the measured intensities for lesioned animals that were exposed and unexposed. Significance represents one-way ANOVA. * and ** indicate $p < 0.05$, and $p < 0.005$, respectively.

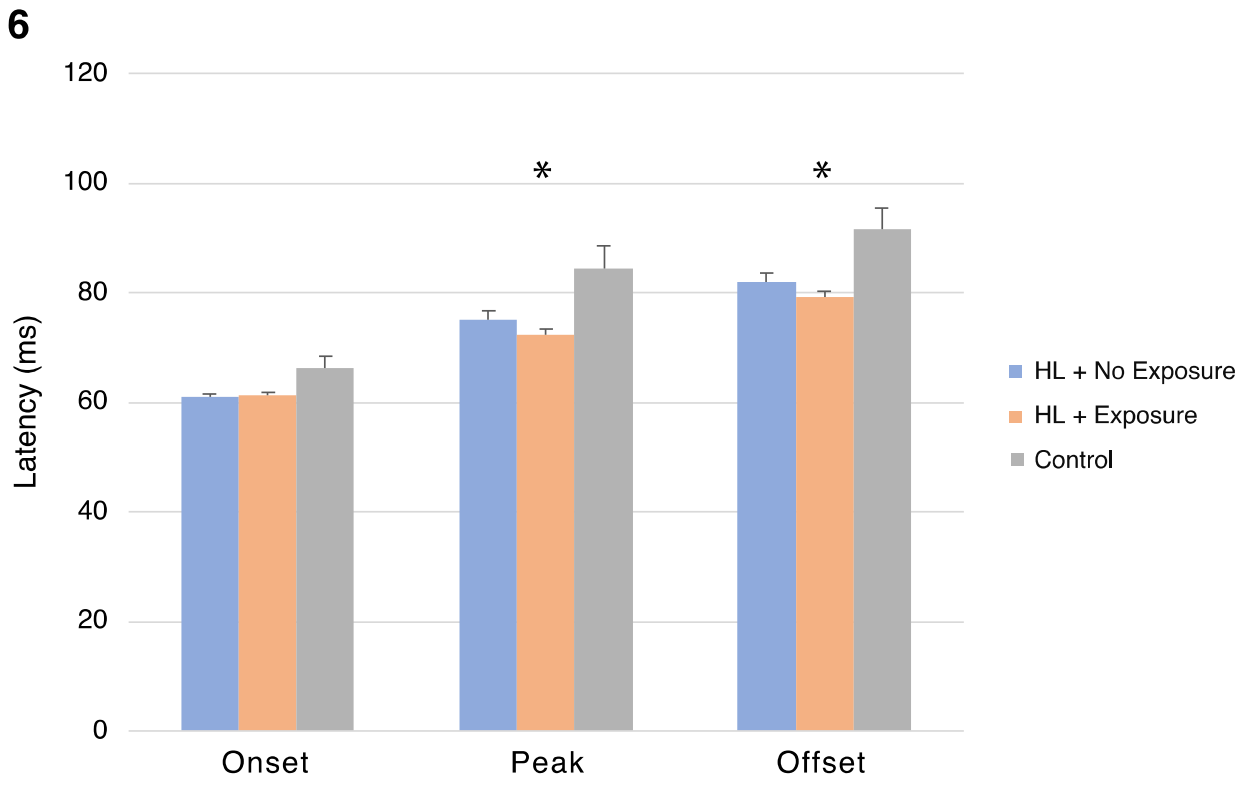

Figure 4.6: Noise-induce hearing lesions decreased ipsilateral receptive field latencies. Representative graph displaying the average onset, peak and offset latencies for ipsilaterally recorded receptive fields in naïve control, hearing lesion exposed mice, and hearing lesioned mice that did not receive pure tone exposure. Noise-induced hearing lesions led to decreased peak and offset latencies in both hearing-lesioned exposed mice and hearing-lesioned unexposed mice relative to naïve controls. Significance represents one-way ANOVA. * indicates $p < 0.05$.

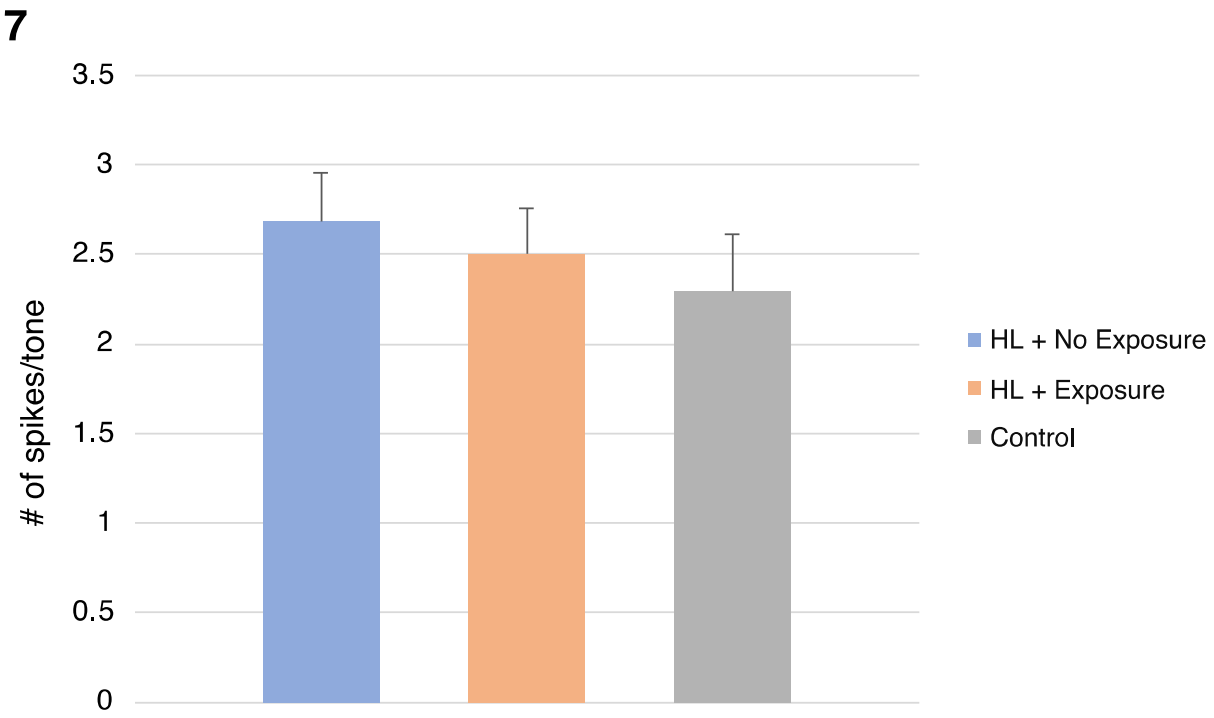

Figure 4.7: Noise-induce hearing lesions yield a non-significant increase in median response amplitude. Representative graph displaying median ipsilateral receptive field response amplitude for naïve control, hearing lesion exposed mice, and hearing lesioned mice that did not receive pure tone exposure. Animals that received hearing lesions had a non-significant increase in response amplitude relative to naïve controls.

5

Conclusions and Future Directions

The research presented in this dissertation attempts to further elucidate molecular, cellular and physiological mechanisms of plasticity regulation within the primary auditory cortex. In Chapter 2, I show that the primary auditory cortex accumulates DNA-ME as it progresses through the critical period. The DNA-ME acts to shift gene transcription, and accordingly excitatory-inhibitory balance in the cortex, which progressively restricts plasticity. Pharmacological removal of DNA-ME in adulthood re-established critical period plasticity, indicating that the accumulation of DNA-ME as the brain progresses through the critical period acts to push the brain into a less plastic state. In Chapter 3 I show that TNF-α is necessary for proper developmental maturation of PV interneurons. Disruption of PV neuron development in TNF-α KO animals correlated with higher cortical excitation levels. TNF-α KO animals had higher basal mEPSC levels, as well as increased measures of bandwidth, spontaneous and evoked activity. Interestingly, TNF-α animals also retained the capacity for critical period plasticity into adulthood, indicating the effects of TNF-α on regulating PV neuron development, and excitatory-inhibitory balance are necessary for the closure of the critical period. In Chapter 4, I show that noise-induced hearing lesions, a form of traumatic brain injury along the auditory pathway, are sufficient to re-establish critical period plasticity in adulthood. Noise-induced hearing lesions also yielded a binaural shift in hearing bias in that the features of ipsilateral auditory processing (such as bandwidth and latency) shifted to similar values recorded from the contralateral auditory pathway. These results suggest that traumatic brain injury engages

plasticity mechanisms to re-write damaged auditory pathways, and to assure a baseline of auditory input is received by the cortex.

Each study provides some answers to questions within the plasticity field, however, many questions and possible lines of research remain. The results in chapter 2 heavily implicate proper regulation of epigenetic mechanisms for regulation of the critical period window. This aligns with previous reports which showed that global knockout of DNA-ME binding protein, MeCP2, accelerates functional maturation and progression through the critical period while conditional knockout of MeCP2 from PV neurons abolishes critical period plasticity (He et al., 2014; Krishnan et al., 2015). MeCP2 deletion is a common genetic model for Rett syndrome, an autism spectrum disorder characterized by relatively normal development followed by the onset of symptoms such as deceleration of head growth, gait abnormalities, loss of speech and breathing abnormalities (Lyst and Bird, 2015). Interestingly, the pathogenesis of Rett syndrome appears after normal development. This indicates that the complications that arise from Rett Syndrome may occur due to a disrupted critical period window, which in turn closes before cortical circuits are allowed to be shaped by their environment. This would explain why disruptions to speech and motor functions, which are usually acquired during the critical period, do not appear until after development. This illuminates the possibility that patients with Rett syndrome could recover function with targeted therapies to increase plasticity, which would allow the cortical circuits to be properly shaped by experience. To that end, one study showed that transgenic expression of MeCP2 in adult MeCP2 knockout mice led to a robust recovery of both behavioral and physiological phenotypes (Guy et al., 2007). Many follow up studies have been published reporting a similar capability for phenotype recovery within MeCP2-null mice

(Gadalla et al., 2011). Our research strengthens the connection between DNA-ME dynamics and the regulation of the critical period window. More research is required to better understand the progressive changes in DNA-ME that occur during the critical period, and the possibility of epigenetic manipulations as a targeted therapy for recovery of defects in patients with Rett syndrome, and possibly other autism spectrum disorders.

Another question that remains from Chapter 2, is the nature of the methylation that's accumulated during the critical period. As previously mentioned, there are varying reports on how methylation patterns change over the course of the critical period. One report showed that MeCP2 foci fluorescence changed in area rather than overall intensity, indicative of a DNA-ME pattern shift rather than an accumulation of DNA-ME (Apulei et al., 2018). Sequencing experiments within the frontal cortex and dentate gyrus revealed that neurons within this region rapidly accumulate DNA-ME during early development that persists into adulthood (Lister et al., 2013; Guo et al., 2014). Our results indicate that between PN day 11 and PN day 60, neurons in the primary auditory cortex accumulate a significant amount of DNA-ME. However, our method of measuring DNA-ME levels was a non-specific antibody for 5-methylcytosine. This antibody does not distinguish between DNA-ME within distinct contexts, such as non-CG methylation versus CG methylation. Canonically, DNA-ME is associated with stretches of cytosine/guanine repeats, commonly referred to as CpG islands (Jones, 2012). Much of the research on DNA-ME has focused on CG methylation, however, recently, it was discovered that mammals contain methylation within multiple contexts (referred to as CH methylation, with H referring to any nucleotide that's not G) (He and Ecker, 2015). Interestingly, genome wide single-base resolution analysis revealed that while CH methylation is absent in the fetal cortex, it rapidly accumulates

during early postnatal development (predominantly in the CA context), to the point that CH methylation becomes the predominant form of methylation in both the human and mouse brain (Lister et al., 2013).

Therefore, it is possible that DNA-ME's role in regulating the critical period window may be more connected to the function of CH methylation, rather than CG methylation. Recently, evidence has emerged linking the pathogenesis of Rett syndrome, to disruptions in CA methylation dynamics within the bodies of long genes that are selectively expressed within neurons (Gabel et al., 2015; Zylka et al., 2015), highlighting the relevance of non-CG methylation within developmental research. CH methylation is particularly enriched in neurons, while glia have a considerably diminished level of CH methylation, indicating that CH methylation is more central to neuronal function (Lister et al., 2013; Kozlenkov et al., 2016; Kozlenkov et al., 2018). Reports on the effects of CH methylation on gene expression are varied. Some studies report a direct repression of genes enriched in CH methylation (Lister et al., 2013; Guo et al., 2014; Mo et al., 2015), while another report suggests a nonlinear relationship between CH methylation and gene expression (Kozlenkov et al., 2018). Therefore, while CH methylation provides an interesting subject for probing regulation of critical period plasticity, more research is required to better understand its role in regulating neuronal function. A possible future experiment would be to selectively decrease CH methylation in adult mice, and subsequently probe the effect on plasticity levels within the cortex. Of the multiple forms of DMNT's, DMNT 3a has been shown to preferentially maintain CH methylation in postmitotic neurons. Conditional knockdown of DMNT 3a was shown to significantly decrease CH methylation, without effecting CG methylation levels, while conditional knockdown of DMNT 1 did not have

this effect (Guo et al., 2014). Therefore, one could perform a conditional knockdown of each of the DMNT's in the adult brain, and then subsequently access each knockdowns effect on cortical plasticity. This experiment could eventually be extended to knockdowns of DMNT within specific cell-types such as PV neurons or glutamatergic neurons, to further isolate the role of CH methylation in regulating plasticity.

The results from chapter 3 and chapter 4 depict an interesting mechanism for TNF-α 's role in regulating cortical plasticity. In chapter 3, I showed that mice deficient in TNF-α expression retain the capacity for critical period plasticity into adulthood. In chapter 4, I showed that noise-induced hearing lesions, which are a potent inducer of TNF-α expression (Fuentes-Santamaria et al., 2017; Wang et al., 2019), are sufficient to re-establish critical period-like plasticity. Together, these confluence of results suggest a U-shaped relationship between TNF-α expression and cortical plasticity. Increased and decreased expression of TNF-α promote cortical plasticity, while baseline levels promote cortical stability.

Since TNF-α has been shown to be an important regulator of homeostatic plasticity (Heir and Stellwagen, 2020), this line of thought leads to a fundamental question about the relationship between homeostatic plasticity and Hebbian plasticity. In general, theories pertaining to homeostatic plasticity's role in regulating Hebbian plasticity focus on the faciliatory relationship between the two (Yee et al., 2017). Studies have shown that visual deprivation, which induces homeostatic plasticity, facilitates LTP, and is sufficient to re-establish ocular dominance plasticity in adulthood (Kirkwood et al., 1996; He et al., 2006). Similar sensory deprivation experiments have led to increased Hebbian plasticity in the auditory system (Thomas et al.,

2019), and somatosensory system (Kraft, 2018), as well. However, the results from chapter 3 suggest that homeostatic plasticity may also have a repressive effect on Hebbian plasticity. TNF-α KO mice retained auditory frequency map plasticity, which is primarily driven by Hebbian plasticity mechanisms, into adulthood. Furthermore, we confirmed that adult TNF-α KO mice have disrupted homeostatic plasticity, in that glutamatergic synapses in TNF-α KO mice did not upscale mEPSC frequency following noise-induced hearing lesions. Intuitively, homeostatic plasticity repressing Hebbian plasticity makes sense. Homeostatic plasticity was initially proposed theoretically as a counter-balance to the destabilizing force Hebbian plasticity brings to neuronal circuits (Miller, 1996). Thus, the induction of Hebbian plasticity eventually requires homeostatic plasticity's repressive actions in order to stabilize cortical circuits. Without homeostatic plasticity, cortical circuits persist in an unstable state, rendered liable to constant change, which would explain why animals deficient in TNF-α retain the capacity for frequency map plasticity into adulthood. To that end, a study investigating the learning and memory capabilities of TNF-α KO mice found that these mice had increased spatial memory capabilities relative to control mice (Golan et al., 2004). As mentioned previously, results from our lab indicate that noise-induced hearing lesions yield a significant increase in TNF-α expression within the auditory cortex. Interestingly, results from a different study show that acoustic trauma leads to a significant reduction in BDNF expression (a key regulator of Hebbian plasticity) within the auditory cortex (Tan et al., 2007). Furthermore a study from the pain field investigating spared nerve injury showed that spared nerve injury led to a significant increase in TNF-α expression and a concomitant decrease in BDNF expression within the hippocampus. The increased TNF-α and decreased BDNF expression that followed spared nerve injury correlated with a disruption of LTP induction within the hippocampus (Liu et al., 2017). However, the

mechanism is not as simple as TNF-α directly repressing BDNF expression, and thus Hebbian plasticity. The same study showed that spared nerve injury also boosted TNF-α expression in the dorsal horn of the spinal cord, which correlated with an increased expression of BDNF, and enhanced LTP capabilities. These results highlight the complex nature of the relationship between homeostatic and Hebbian plasticity. More studies are required to better understand the interactions between the molecular mediators of both homeostatic and Hebbian plasticity.

Another interesting result from Chapter 3 was that TNF-α deficient mice had a decreased density of PV neurons relative to control mice. This result is of note because previous reports from our lab indicate that increased TNF-α expression also leads to decreased PV neuron density in the auditory cortex (Wang et al., 2019; Deng et al., 2020a). Therefore once again, a U-shaped relationship for TNF-α exists, this time as it pertains to regulation of PV neuron density. However, the question remains, how does TNF-α expression modulate PV neuron density, and thus function? PV neuron density increases over the course of the critical period, and has been shown to be regulated by multiple molecular factors such as OTX2 (Sugiyama et al., 2008), and BDNF (Huang, 1999). As mentioned previously, TNF-α has been shown to exert bidirectional control on BDNF expression depending on the context (Liu et al., 2017). Just as BDNF, TNF-α expression has been shown to progressively increase in sensory cortex, as the brain progresses through the critical period (Man WH, 2015; Schwartz et al., 2020). Therefore, the lack of developmental increase in TNF-α expression as the critical period progresses may disrupt the normal expression pattern of BDNF, which would explain the decreased PV neuron density in TNF-α KO mice. A possible follow up experiment could be to track BDNF expression in TNF-α KO mice as the critical period progresses, to see if TNF-α deficiency disrupts BDNF signaling.

Our results from Chapter 4 show that following the induction of acoustic trauma, the brain re-establishes critical period plasticity, and induces a binaural bias shift. These results indicate that in response to acoustic trauma the brain upregulates cortical plasticity to re-wire damaged auditory pathways, and to assure a baseline of auditory input reaches the cortex. Acoustic trauma is a significant issue within many sectors of society. According to a CDC study, upwards of 40 million adults in the U.S. have features of hearing loss due to exposure to loud noise (https://www.nidcd.nih.gov/health/noise-induced-hearing-loss). Our results could impact the way acoustic trauma is treated. Based on our results, following exposure to acoustic trauma, the best course of action may be immediate sound based exposure therapy, to maximize the potentiated cortical plasticity levels and facilitate beneficial re-mapping.

One interesting question that remains is whether the plasticity induced following noise-induced hearing lesions is a general increase in plasticity, or if noise-induced hearing lesions engage multiple plasticity mechanisms within the brain? In other words, is the re-established frequency map plasticity a separate mechanism from the binaural plasticity that is also induced following acoustic trauma? In the visual system, induction of ocular dominance plasticity engages two separate plasticity mechanisms, a Hebbian decrease in the closed eye, and a homeostatic increase in input from the spared eye (Kaneko et al., 2008). Inducing auditory system plasticity has been shown not to be reliant on homeostatic mechanisms (Yang et al., 2014b), however, our results from Chapter 3 show that in the absence of TNF-α mediated homeostatic plasticity, mice retain critical period plasticity into adulthood, indicating a clear role for homeostatic plasticity within auditory system plasticity. A possible experiment to test this hypothesis would be to repeat the

experiments in Chapter 4 with TNF-α KO mice. Theoretically, these mice should show frequency map plasticity following noise-induced hearing lesions because in Chapter 3 we showed that adult TNF-α KO mice retain critical period plasticity. However, if following noise-induced hearing lesions, the TNF-α KO mice do not show a binaural shift in hearing bias, then we can assume there are two separate plasticity mechanisms in play following acoustic trauma. Answering this question can provide further insights to the complex plasticity mechanisms engaged following acoustic trauma and can lead to more targeted therapies for those affected by acoustic trauma.

Another question that remains from this study is whether the plasticity induced following acoustic trauma is beneficial or more deleterious to proper brain function? Acoustic trauma not only leads to hearing loss in the affected individual, but can also induce other central auditory processing disorders such as tinnitus (perpetual ringing in the ears), and hyperacusis (hypersensitivity to normal sound intensities) (Axelsson and Sandh, 1985; Sun et al., 2012; Hickox and Liberman, 2014). These central auditory processing deficits can significantly hamper communication abilities in those affected and have been found to be co-morbid with cognitive issues such as depression, and anxiety (Iliadou et al., 2017), indicating that central auditory processing deficits can have a severe influence on quality of life. Interestingly, previous studies from our lab suggest that the generation of tinnitus behavior in mice following noise-induced hearing lesions is dependent upon a homeostatic downregulation of inhibition (Yang et al., 2011). Furthermore, while noise-induced hearing lesions were sufficient to induce tinnitus behavior in control mice, noise-induced hearing lesions were not sufficient to induce tinnitus in

TNF-α KO mice, indicating that without the molecular regulator of homeostatic plasticity, tinnitus cannot be induced.

Therefore, while the increased plasticity following noise-induced hearing lesions may be an attempt by the brain to restore function, the result may be changes to network function that yield central auditory processing deficits such as tinnitus. To answer the question whether the plasticity following acoustic trauma is beneficial, one could selectively block plasticity following noise-induced hearing lesions and subsequently access auditory processing. To block cortical plasticity, one could use an inhibitor of microglia, such as PLX3397, to eliminate microglia in the cortex. Previous studies show that eliminating microglia leads to a significant increase in perineuronal net signal (Crapser et al., 2020; Crapser et al., 2021), and also blocked critical period plasticity in the visual system (Ma et al., 2020). Furthermore, activation of microglia stimulates the destruction of perineuronal nets and the re-establishment of visual critical period plasticity in adulthood (Venturino et al., 2021). Therefore, one could eliminate microglia populations following noise-induced hearing lesions, and subsequently access plasticity to assure elimination of microglia blocks plasticity. If elimination of microglia blocks noise-induced frequency map plasticity, one could follow-up with hearing assays and behavioral assessments for tinnitus and hyperacusis, to access whether blocking the plastic change is sufficient to block the induction of central auditory processing deficits. I would predict that while this manipulation may prevent tinnitus or hyperacusis, it may also prevent the progressive increase in hearing function that occurs during recovery from damage. Preliminary results from our lab indicate that eliminating microglia populations is sufficient to block induction of tinnitus following noise-induced hearing lesions (Wang et al., 2019). More research is needed to isolate whether blocking

tinnitus induction is mediated through blocking microglia's effect on cortical plasticity, or through other regulatory mechanisms.

References

Apulei J, Kim N, Testa D, Ribot J, Morizet D, Bernard C, Jourdren L, Blugeon C, Di Nardo AA, Prochiantz A (2018) Non-cell Autonomous OTX2 Homeoprotein Regulates Visual Cortex Plasticity Through Gadd45b/g. Cereb Cortex.

Axelsson A, Sandh A (1985) Tinnitus in noise-induced hearing loss. Br J Audiol 19:271-276.

Babola TA, Li S, Gribizis A, Lee BJ, Issa JB, Wang HC, Crair MC, Bergles DE (2018) Homeostatic Control of Spontaneous Activity in the Developing Auditory System. Neuron 99:511-524 e515.

Bahar Halpern K, Vana T, Walker MD (2014) Paradoxical role of DNA methylation in activation of FoxA2 gene expression during endoderm development. J Biol Chem 289:23882-23892.

Ballas N, Grunseich C, Lu DD, Speh JC, Mandel G (2005) REST and its corepressors mediate plasticity of neuronal gene chromatin throughout neurogenesis. Cell 121:645-657.

Balmer TS (2016) Perineuronal Nets Enhance the Excitability of Fast-Spiking Neurons. eNeuro 3.

Baroncelli L, Scali M, Sansevero G, Olimpico F, Manno I, Costa M, Sale A (2016) Experience Affects Critical Period Plasticity in the Visual Cortex through an Epigenetic Regulation of Histone Post-Translational Modifications. J Neurosci 36:3430-3440.

Beattie EC, Stellwagen D, Morishita W, Bresnahan JC, Ha BK, Von Zastrow M, Beattie MS, Malenka RC (2002) Control of synaptic strength by glial TNFalpha. Science 295:2282-2285.

Becker D, Deller T, Vlachos A (2015) Tumor necrosis factor (TNF)-receptor 1 and 2 mediate homeostatic synaptic plasticity of denervated mouse dentate granule cells. Sci Rep 5:12726.

Bernard C, Prochiantz A (2016) Otx2-PNN Interaction to Regulate Cortical Plasticity. Neural Plast 2016:7931693.

Beurdeley M, Spatazza J, Lee HH, Sugiyama S, Bernard C, Di Nardo AA, Hensch TK, Prochiantz A (2012) Otx2 binding to perineuronal nets persistently regulates plasticity in the mature visual cortex. J Neurosci 32:9429-9437.

Blankenship AG, Feller MB (2010) Mechanisms underlying spontaneous patterned activity in developing neural circuits. Nat Rev Neurosci 11:18-29.

Bolton MM, Pittman AJ, Lo DC (2000) Brain-derived neurotrophic factor differentially regulates excitatory and inhibitory synaptic transmission in hippocampal cultures. J Neurosci 20:3221-3232.

Borsini A, Zunszain PA, Thuret S, Pariante CM (2015) The role of inflammatory cytokines as key modulators of neurogenesis. Trends Neurosci 38:145-157.

Buonomano DV, Merzenich MM (1998) Cortical plasticity: from synapses to maps. Annu Rev Neurosci 21:149-186.

Carulli D, Pizzorusso T, Kwok JC, Putignano E, Poli A, Forostyak S, Andrews MR, Deepa SS, Glant TT, Fawcett JW (2010) Animals lacking link protein have attenuated perineuronal nets and persistent plasticity. Brain 133:2331-2347.

Celikel T, Szostak VA, Feldman DE (2004) Modulation of spike timing by sensory deprivation during induction of cortical map plasticity. Nat Neurosci 7:534-541.

Chabot GG, Rivard GE, Momparler RL (1983) Plasma and cerebrospinal fluid pharmacokinetics of 5-Aza-2'-deoxycytidine in rabbits and dogs. Cancer Res 43:592-597.
Chahrour M, Jung SY, Shaw C, Zhou X, Wong ST, Qin J, Zoghbi HY (2008) MeCP2, a key contributor to neurological disease, activates and represses transcription. Science 320:1224-1229.
Chang EF, Merzenich MM (2003) Environmental noise retards auditory cortical development. Science 300:498-502.
Chang EF, Bao S, Imaizumi K, Schreiner CE, Merzenich MM (2005) Development of spectral and temporal response selectivity in the auditory cortex. Proc Natl Acad Sci U S A 102:16460-16465.
Chattopadhyaya B, Di Cristo G, Higashiyama H, Knott GW, Kuhlman SJ, Welker E, Huang ZJ (2004) Experience and activity-dependent maturation of perisomatic GABAergic innervation in primary visual cortex during a postnatal critical period. J Neurosci 24:9598-9611.
Cisneros-Franco JM, de Villers-Sidani E (2019) Reactivation of critical period plasticity in adult auditory cortex through chemogenetic silencing of parvalbumin-positive interneurons. Proc Natl Acad Sci U S A.
Corvetti L, Rossi F (2005) Degradation of chondroitin sulfate proteoglycans induces sprouting of intact purkinje axons in the cerebellum of the adult rat. J Neurosci 25:7150-7158.
Crapser JD, Arreola MA, Tsourmas KI, Green KN (2021) Microglia as hackers of the matrix: sculpting synapses and the extracellular space. Cell Mol Immunol.
Crapser JD, Spangenberg EE, Barahona RA, Arreola MA, Hohsfield LA, Green KN (2020) Microglia facilitate loss of perineuronal nets in the Alzheimer's disease brain. EBioMedicine 58:102919.
Dahmen JC, Hartley DE, King AJ (2008) Stimulus-timing-dependent plasticity of cortical frequency representation. J Neurosci 28:13629-13639.
de Villers-Sidani E, Simpson KL, Lu YF, Lin RC, Merzenich MM (2008) Manipulating critical period closure across different sectors of the primary auditory cortex. Nat Neurosci 11:957-965.
Deng D, Wang W, Bao S (2020a) Diffusible Tumor Necrosis Factor-Alpha (TNF-alpha) Promotes Noise-Induced Parvalbumin-Positive (PV+) Neuron Loss and Auditory Processing Impairments. Front Neurosci 14:573047.
Deng D, Masri S, Yao L, Ma X, Cao X, Yang S, Bao S, Zhou Q (2020b) Increasing endogenous activity of NMDARs on GABAergic neurons increases inhibition, alters sensory processing and prevents noise-induced tinnitus. Sci Rep 10:11969.
Desai NS, Cudmore RH, Nelson SB, Turrigiano GG (2002) Critical periods for experience-dependent synaptic scaling in visual cortex. Nat Neurosci 5:783-789.
Dunning DD, Hoover CL, Soltesz I, Smith MA, O'Dowd DK (1999) GABA(A) receptor-mediated miniature postsynaptic currents and alpha-subunit expression in developing cortical neurons. J Neurophysiol 82:3286-3297.
Fagiolini M, Jensen CL, Champagne FA (2009) Epigenetic influences on brain development and plasticity. Curr Opin Neurobiol 19:207-212.
Fagiolini M, Hensch, T.K. (2000) Inhibitory threshold for critical-period activation in primary visual cortex. Nature 404:183-186.
Ferguson BR, Gao WJ (2018) PV Interneurons: Critical Regulators of E/I Balance for Prefrontal Cortex-Dependent Behavior and Psychiatric Disorders. Front Neural Circuits 12:37.

Frischknecht R, Heine M, Perrais D, Seidenbecher CI, Choquet D, Gundelfinger ED (2009) Brain extracellular matrix affects AMPA receptor lateral mobility and short-term synaptic plasticity. Nat Neurosci 12:897-904.

Fuentes-Santamaria V, Alvarado JC, Melgar-Rojas P, Gabaldon-Ull MC, Miller JM, Juiz JM (2017) The Role of Glia in the Peripheral and Central Auditory System Following Noise Overexposure: Contribution of TNF-alpha and IL-1beta to the Pathogenesis of Hearing Loss. Front Neuroanat 11:9.

Gabel HW, Kinde B, Stroud H, Gilbert CS, Harmin DA, Kastan NR, Hemberg M, Ebert DH, Greenberg ME (2015) Disruption of DNA-methylation-dependent long gene repression in Rett syndrome. Nature 522:89-93.

Gadalla KK, Bailey ME, Cobb SR (2011) MeCP2 and Rett syndrome: reversibility and potential avenues for therapy. Biochem J 439:1-14.

Gallegos DA, Chan U, Chen LF, West AE (2018) Chromatin Regulation of Neuronal Maturation and Plasticity. Trends Neurosci 41:311-324.

Galuske RA, Kim DS, Castren E, Singer W (2000) Differential effects of neurotrophins on ocular dominance plasticity in developing and adult cat visual cortex. Eur J Neurosci 12:3315-3330.

Gervain J, Vines BW, Chen LM, Seo RJ, Hensch TK, Werker JF, Young AH (2013) Valproate reopens critical-period learning of absolute pitch. Front Syst Neurosci 7:102.

Gogolla N, Caroni P, Luthi A, Herry C (2009) Perineuronal nets protect fear memories from erasure. Science 325:1258-1261.

Golan H, Levav T, Mendelsohn A, Huleihel M (2004) Involvement of tumor necrosis factor alpha in hippocampal development and function. Cereb Cortex 14:97-105.

Guo JU, Su Y, Shin JH, Shin J, Li H, Xie B, Zhong C, Hu S, Le T, Fan G, Zhu H, Chang Q, Gao Y, Ming GL, Song H (2014) Distribution, recognition and regulation of non-CpG methylation in the adult mammalian brain. Nat Neurosci 17:215-222.

Guy J, Gan J, Selfridge J, Cobb S, Bird A (2007) Reversal of neurological defects in a mouse model of Rett syndrome. Science 315:1143-1147.

Hanover JL, Huang ZJ, Tonegawa S, Stryker MP (1999) Brain-derived neurotrophic factor overexpression induces precocious critical period in mouse visual cortex. J Neurosci 19:RC40.

Happel MF, Niekisch H, Castiblanco Rivera LL, Ohl FW, Deliano M, Frischknecht R (2014) Enhanced cognitive flexibility in reversal learning induced by removal of the extracellular matrix in auditory cortex. Proc Natl Acad Sci U S A 111:2800-2805.

Harauzov A, Spolidoro M, DiCristo G, De Pasquale R, Cancedda L, Pizzorusso T, Viegi A, Berardi N, Maffei L (2010) Reducing intracortical inhibition in the adult visual cortex promotes ocular dominance plasticity. J Neurosci 30:361-371.

Hata K, Mizukami H, Sadakane O, Watakabe A, Ohtsuka M, Takaji M, Kinoshita M, Isa T, Ozawa K, Yamamori T (2013) DNA methylation and methyl-binding proteins control differential gene expression in distinct cortical areas of macaque monkey. J Neurosci 33:19704-19714.

He HY, Hodos W, Quinlan EM (2006) Visual deprivation reactivates rapid ocular dominance plasticity in adult visual cortex. J Neurosci 26:2951-2955.

He LJ, Liu N, Cheng TL, Chen XJ, Li YD, Shu YS, Qiu ZL, Zhang XH (2014) Conditional deletion of Mecp2 in parvalbumin-expressing GABAergic cells results in the absence of critical period plasticity. Nat Commun 5:5036.

He Y, Ecker JR (2015) Non-CG Methylation in the Human Genome. Annu Rev Genomics Hum Genet 16:55-77.
Heir R, Stellwagen D (2020) TNF-Mediated Homeostatic Synaptic Plasticity: From in vitro to in vivo Models. Front Cell Neurosci 14:565841.
Hensch TK (2005a) Critical period plasticity in local cortical circuits. Nat Rev Neurosci 6:877-888.
Hensch TK (2005b) Critical period mechanisms in developing visual cortex. Curr Top Dev Biol 69:215-237.
Hensch TK, Fagiolini M (2005) Excitatory-inhibitory balance and critical period plasticity in developing visual cortex. Prog Brain Res 147:115-124.
Hensch TK, Fagiolini, M., Mataga, N., Stryker, M. P., Baekkeskov, S., Kash, S. F. (1998) Local GABA Circuit Control of Experience-Dependent Plasticity in Developing Visual Cortex. Science 282:1504-1508.
Hickox AE, Liberman MC (2014) Is noise-induced cochlear neuropathy key to the generation of hyperacusis or tinnitus? J Neurophysiol 111:552-564.
Huang JZ, Kirkwood, A., Pizzorusso, T., Porciatti, V., Morales, B., Bear, M. F., Maffei, L., Tonegawa, S. (1999) BDNF regulates the maturation of inhibition and the critical period of plasticity in mouse visual cortex. Cell 98:739-755.
Iliadou VV et al. (2017) A European Perspective on Auditory Processing Disorder-Current Knowledge and Future Research Focus. Front Neurol 8:622.
Insanally MN, Albanna BF, Bao S (2010) Pulsed noise experience disrupts complex sound representations. J Neurophysiol 103:2611-2617.
Insanally MN, Kover H, Kim H, Bao S (2009) Feature-dependent sensitive periods in the development of complex sound representation. J Neurosci 29:5456-5462.
Isaacson JS, Scanziani M (2011) How inhibition shapes cortical activity. Neuron 72:231-243.
Itami C, Kimura F, Nakamura S (2007) Brain-derived neurotrophic factor regulates the maturation of layer 4 fast-spiking cells after the second postnatal week in the developing barrel cortex. Journal of Neuroscience 27:2241-2252.
Iwai Y, Fagiolini M, Obata K, Hensch TK (2003) Rapid critical period induction by tonic inhibition in visual cortex. J Neurosci 23:6695-6702.
Jones PA (2012) Functions of DNA methylation: islands, start sites, gene bodies and beyond. Nat Rev Genet 13:484-492.
Jones PL, Veenstra GJ, Wade PA, Vermaak D, Kass SU, Landsberger N, Strouboulis J, Wolffe AP (1998) Methylated DNA and MeCP2 recruit histone deacetylase to repress transcription. Nat Genet 19:187-191.
Kaneko M, Stellwagen D, Malenka RC, Stryker MP (2008) Tumor necrosis factor-alpha mediates one component of competitive, experience-dependent plasticity in developing visual cortex. Neuron 58:673-680.
Katz LC, Crowley JC (2002) Development of cortical circuits: lessons from ocular dominance columns. Nature Review Neuroscience 3:34-42.
Kelsom C, Lu W (2013) Development and specification of GABAergic cortical interneurons. Cell Biosci 3:19.
Keuroghlian AS, Knudsen EI (2007) Adaptive auditory plasticity in developing and adult animals. Progress in Neurobiology 82:109-121.
Kim H, Gibboni R, Kirkhart C, Bao S (2013) Impaired critical period plasticity in primary auditory cortex of fragile X model mice. J Neurosci 33:15686-15692.

Kirkwood A, Rioult MC, Bear MF (1996) Experience-dependent modification of synaptic plasticity in visual cortex. Nature 381:526-528.
Kirmse K, Kummer M, Kovalchuk Y, Witte OW, Garaschuk O, Holthoff K (2015) GABA depolarizes immature neurons and inhibits network activity in the neonatal neocortex in vivo. Nat Commun 6:7750.
Kotak VC, Fujisawa S, Lee FA, Karthikeyan O, Aoki C, Sanes DH (2005) Hearing loss raises excitability in the auditory cortex. J Neurosci 25:3908-3918.
Kozlenkov A, Li J, Apontes P, Hurd YL, Byne WM, Koonin EV, Wegner M, Mukamel EA, Dracheva S (2018) A unique role for DNA (hydroxy)methylation in epigenetic regulation of human inhibitory neurons. Sci Adv 4:eaau6190.
Kozlenkov A, Wang M, Roussos P, Rudchenko S, Barbu M, Bibikova M, Klotzle B, Dwork AJ, Zhang B, Hurd YL, Koonin EV, Wegner M, Dracheva S (2016) Substantial DNA methylation differences between two major neuronal subtypes in human brain. Nucleic Acids Res 44:2593-2612.
Kraft AW, Bauer, A. Q., Culver, J. P., Lee, J. (2018) Sensory deprivation after focal ischemia in mice accelerates brain remapping and improves functional recovery through Arc-dependent synaptic plasticity. Science Translational Medicine 10:1-10.
Kral A (2013) Auditory critical periods: a review from system's perspective. Neuroscience 247:117-133.
Krishnan K, Wang BS, Lu J, Wang L, Maffei A, Cang J, Huang ZJ (2015) MeCP2 regulates the timing of critical period plasticity that shapes functional connectivity in primary visual cortex. Proc Natl Acad Sci U S A 112:E4782-4791.
Lee HHC, Bernard C, Ye Z, Acampora D, Simeone A, Prochiantz A, Di Nardo AA, Hensch TK (2017) Genetic Otx2 mis-localization delays critical period plasticity across brain regions. Mol Psychiatry 22:785.
Lewitus GM, Pribiag H, Duseja R, St-Hilaire M, Stellwagen D (2014) An adaptive role of TNFalpha in the regulation of striatal synapses. J Neurosci 34:6146-6155.
Li H, Liang F, Zhong W, Yan L, Mesik L, Xiao Z, Tao HW, Zhang LI (2019) Synaptic Mechanisms for Bandwidth Tuning in Awake Mouse Primary Auditory Cortex. Cereb Cortex 29:2998-3009.
Lister R et al. (2013) Global epigenomic reconfiguration during mammalian brain development. Science 341:1237905.
Liu Y, Zhou LJ, Wang J, Li D, Ren WJ, Peng J, Wei X, Xu T, Xin WJ, Pang RP, Li YY, Qin ZH, Murugan M, Mattson MP, Wu LJ, Liu XG (2017) TNF-alpha Differentially Regulates Synaptic Plasticity in the Hippocampus and Spinal Cord by Microglia-Dependent Mechanisms after Peripheral Nerve Injury. J Neurosci 37:871-881.
Lu Y, Christian K, Lu B (2008) BDNF: a key regulator for protein synthesis-dependent LTP and long-term memory? Neurobiol Learn Mem 89:312-323.
Lyckman AW, Horng S, Leamey CA, Tropea D, Watakabe A, Van Wart A, McCurry C, Yamamori T, Sur M (2008) Gene expression patterns in visual cortex during the critical period: synaptic stabilization and reversal by visual deprivation. Proc Natl Acad Sci U S A 105:9409-9414.
Lyst MJ, Bird A (2015) Rett syndrome: a complex disorder with simple roots. Nat Rev Genet 16:261-275.
Ma X, Chen K, Cui Y, Huang G, Nehme A, Zhang L, Li H, Wei J, Liong K, Liu Q, Shi L, Wu J, Qiu S (2020) Depletion of microglia in developing cortical circuits reveals its critical role

in glutamatergic synapse development, functional connectivity, and critical period plasticity. J Neurosci Res 98:1968-1986.
Maffei L (2002) Plasticity in the visual system: role of neurotrophins and electrical activity. Arch Ital Biol 140:341-346.
Majdan M, Shatz CJ (2006) Effects of visual experience on activity-dependent gene regulation in cortex. Nature Neuroscience 9:650-659.
Man WH MC, Zhou X, Merzenich MM, Panizzutti R (2015) TNF-α Levels throughout the Critical Period for Experience-Dependent
Plasticity in the Rat Primary Auditory Cortex. Neurochemistry and Neuropharmacology 1.
Martinowich K, Hattori D, Wu H, Fouse S, He F, Hu Y, Fan G, Sun YE (2003) DNA methylation-related chromatin remodeling in activity-dependent BDNF gene regulation. Science 302:890-893.
Masri S, Zhang LS, Luo H, Pace E, Zhang J, Bao S (2018) Blast Exposure Disrupts the Tonotopic Frequency Map in the Primary Auditory Cortex. Neuroscience 379:428-434.
Meadows JP, Guzman-Karlsson MC, Phillips S, Brown JA, Strange SK, Sweatt JD, Hablitz JJ (2016) Dynamic DNA methylation regulates neuronal intrinsic membrane excitability. Sci Signal 9:ra83.
Meadows JP, Guzman-Karlsson MC, Phillips S, Holleman C, Posey JL, Day JJ, Hablitz JJ, Sweatt JD (2015) DNA methylation regulates neuronal glutamatergic synaptic scaling. Sci Signal 8:ra61.
Miller KD (1996) Synaptic economics: competition and cooperation in synaptic plasticity. Neuron 17:371-374.
Miyakawa A, Wang W, Cho SJ, Li D, Yang S, Bao S (2019) Tinnitus Correlates with Downregulation of Cortical Glutamate Decarboxylase 65 Expression But Not Auditory Cortical Map Reorganization. J Neurosci 39:9989-10001.
Mo A, Mukamel EA, Davis FP, Luo C, Henry GL, Picard S, Urich MA, Nery JR, Sejnowski TJ, Lister R, Eddy SR, Ecker JR, Nathans J (2015) Epigenomic Signatures of Neuronal Diversity in the Mammalian Brain. Neuron 86:1369-1384.
Moon LD, Asher RA, Rhodes KE, Fawcett JW (2001) Regeneration of CNS axons back to their target following treatment of adult rat brain with chondroitinase ABC. Nat Neurosci 4:465-466.
Morales B, Choi SY, Kirkwood A (2002) Dark rearing alters the development of GABAergic transmission in visual cortex. J Neurosci 22:8084-8090.
Murase S, Lantz CL, Quinlan EM (2017) Light reintroduction after dark exposure reactivates plasticity in adults via perisynaptic activation of MMP-9. Elife 6.
Nguyen A, Khaleel HM, Razak KA (2017) Effects of noise-induced hearing loss on parvalbumin and perineuronal net expression in the mouse primary auditory cortex. Hear Res 350:82-90.
Nord AS, Pattabiraman K, Visel A, Rubenstein JLR (2015) Genomic perspectives of transcriptional regulation in forebrain development. Neuron 85:27-47.
Norena AJ, Eggermont JJ (2005) Enriched acoustic environment after noise trauma reduces hearing loss and prevents cortical map reorganization. J Neurosci 25:699-705.
Norena AJ, Tomita M, Eggermont JJ (2003) Neural changes in cat auditory cortex after a transient pure-tone trauma. J Neurophysiol 90:2387-2401.
Nothias F, Fishell G, Ruiz i Altaba A (1998) Cooperation of intrinsic and extrinsic signals in the elaboration of regional identity in the posterior cerebral cortex. Curr Biol 8:459-462.

O'Leary DM, Ruff, N. L., .Dyck, R. H. (1994) Development, critical period plasticity, and adult reorganizations of mammalian somatosensory systems. Current Opinion in Neurobiology 4:535-544.

Ogoshi F, Yin HZ, Kuppumbatti Y, Song B, Amindari S, Weiss JH (2005) Tumor necrosis-factor-alpha (TNF-alpha) induces rapid insertion of Ca2+-permeable alpha-amino-3-hydroxyl-5-methyl-4-isoxazole-propionate (AMPA)/kainate (Ca-A/K) channels in a subset of hippocampal pyramidal neurons. Exp Neurol 193:384-393.

Oh YM, Mahar M, Ewan EE, Leahy KM, Zhao G, Cavalli V (2018) Epigenetic regulator UHRF1 inactivates REST and growth suppressor gene expression via DNA methylation to promote axon regeneration. Proc Natl Acad Sci U S A 115:E12417-E12426.

Ohba S, Ikeda T, Ikegaya Y, Nishiyama N, Matsuki N, Yamada MK (2005) BDNF locally potentiates GABAergic presynaptic machineries: target-selective circuit inhibition. Cereb Cortex 15:291-298.

Okaty BW, Miller MN, Sugino K, Hempel CM, Nelson SB (2009) Transcriptional and Electrophysiological Maturation of Neocortical Fast-Spiking GABAergic Interneurons. Journal of Neuroscience 29:7040-7052.

Pizzorusso T, Medini P, Berardi N, Chierzi S, Fawcett JW, Maffei L (2002) Reactivation of ocular dominance plasticity in the adult visual cortex. Science 298:1248-1251.

Polley DB, Thompson JH, Guo W (2013) Brief hearing loss disrupts binaural integration during two early critical periods of auditory cortex development. Nat Commun 4:2547.

Pribiag H, Stellwagen D (2013) TNF-alpha downregulates inhibitory neurotransmission through protein phosphatase 1-dependent trafficking of GABA(A) receptors. J Neurosci 33:15879-15893.

Putignano E, Lonetti G, Cancedda L, Ratto G, Costa M, Maffei L, Pizzorusso T (2007) Developmental downregulation of histone posttranslational modifications regulates visual cortical plasticity. Neuron 53:747-759.

Ranson A, Cheetham CE, Fox K, Sengpiel F (2012) Homeostatic plasticity mechanisms are required for juvenile, but not adult, ocular dominance plasticity. Proc Natl Acad Sci U S A 109:1311-1316.

Reh RK, Dias BG, Nelson CA, 3rd, Kaufer D, Werker JF, Kolb B, Levine JD, Hensch TK (2020) Critical period regulation across multiple timescales. Proc Natl Acad Sci U S A 117:23242-23251.

Ribic A, Biederer T (2019) Emerging Roles of Synapse Organizers in the Regulation of Critical Periods. Neural Plast 2019:1538137.

Richter F, Lutz W, Eitner A, Leuchtweis J, Lehmenkuhler A, Schaible HG (2014) Tumor necrosis factor reduces the amplitude of rat cortical spreading depression in vivo. Ann Neurol 76:43-53.

Rodenas-Ruano A, Chavez AE, Cossio MJ, Castillo PE, Zukin RS (2012) REST-dependent epigenetic remodeling promotes the developmental switch in synaptic NMDA receptors. Nat Neurosci 15:1382-1390.

Sakai A, Sugiyama S (2018) Experience-dependent transcriptional regulation in juvenile brain development. Dev Growth Differ 60:473-482.

Sale A, Maya Vetencourt JF, Medini P, Cenni MC, Baroncelli L, De Pasquale R, Maffei L (2007) Environmental enrichment in adulthood promotes amblyopia recovery through a reduction of intracortical inhibition. Nat Neurosci 10:679-681.

Sales AJ, Biojone C, Terceti MS, Guimaraes FS, Gomes MV, Joca SR (2011) Antidepressant-like effect induced by systemic and intra-hippocampal administration of DNA methylation inhibitors. Br J Pharmacol 164:1711-1721.

Schwartz BA, Wang W, Bao S (2020) Pharmacological DNA Demethylation Weakens Inhibitory Synapses in the Auditory Cortex and Re-opens the Critical Period for Frequency Map Plasticity. Neuroscience 440:239-248.

Sonntag M, Englitz B, Kopp-Scheinpflug C, Rubsamen R (2009) Early postnatal development of spontaneous and acoustically evoked discharge activity of principal cells of the medial nucleus of the trapezoid body: an in vivo study in mice. J Neurosci 29:9510-9520.

Sorg BA, Berretta S, Blacktop JM, Fawcett JW, Kitagawa H, Kwok JC, Miquel M (2016) Casting a Wide Net: Role of Perineuronal Nets in Neural Plasticity. J Neurosci 36:11459-11468.

Southwell DG, Froemke RC, Alvarez-Buylla A, Stryker MP, Gandhi SP (2010) Cortical plasticity induced by inhibitory neuron transplantation. Science 327:1145-1148.

Spatazza J, Di Lullo E, Joliot A, Dupont E, Moya KL, Prochiantz A (2013a) Homeoprotein signaling in development, health, and disease: a shaking of dogmas offers challenges and promises from bench to bed. Pharmacol Rev 65:90-104.

Spatazza J, Lee HH, Di Nardo AA, Tibaldi L, Joliot A, Hensch TK, Prochiantz A (2013b) Choroid-plexus-derived Otx2 homeoprotein constrains adult cortical plasticity. Cell Rep 3:1815-1823.

Steinmetz CC, Turrigiano GG (2010) Tumor necrosis factor-alpha signaling maintains the ability of cortical synapses to express synaptic scaling. J Neurosci 30:14685-14690.

Stellwagen D, Malenka RC (2006) Synaptic scaling mediated by glial TNF-alpha. Nature 440:1054-1059.

Stellwagen D, Beattie EC, Seo JY, Malenka RC (2005) Differential regulation of AMPA receptor and GABA receptor trafficking by tumor necrosis factor-alpha. J Neurosci 25:3219-3228.

Sugiyama S, Di Nardo AA, Aizawa S, Matsuo I, Volovitch M, Prochiantz A, Hensch TK (2008) Experience-dependent transfer of Otx2 homeoprotein into the visual cortex activates postnatal plasticity. Cell 134:508-520.

Sun W, Deng A, Jayaram A, Gibson B (2012) Noise exposure enhances auditory cortex responses related to hyperacusis behavior. Brain Res 1485:108-116.

Sweatt JD (2016) Dynamic DNA methylation controls glutamate receptor trafficking and synaptic scaling. J Neurochem 137:312-330.

Takesian AE, Hensch TK (2013) Balancing plasticity/stability across brain development. Prog Brain Res 207:3-34.

Takesian AE, Bogart LJ, Lichtman JW, Hensch TK (2018) Inhibitory circuit gating of auditory critical-period plasticity. Nat Neurosci 21:218-227.

Tan J, Ruttiger L, Panford-Walsh R, Singer W, Schulze H, Kilian SB, Hadjab S, Zimmermann U, Kopschall I, Rohbock K, Knipper M (2007) Tinnitus behavior and hearing function correlate with the reciprocal expression patterns of BDNF and Arg3.1/arc in auditory neurons following acoustic trauma. Neuroscience 145:715-726.

Tang Y, Stryker MP, Alvarez-Buylla A, Espinosa JS (2014) Cortical plasticity induced by transplantation of embryonic somatostatin or parvalbumin interneurons. Proc Natl Acad Sci U S A 111:18339-18344.

Teichert M, Liebmann L, Hubner CA, Bolz J (2017) Homeostatic plasticity and synaptic scaling in the adult mouse auditory cortex. Sci Rep 7:17423.
Thomas ME, Friedman NHM, Cisneros-Franco JM, Ouellet L, de Villers-Sidani E (2019) The Prolonged Masking of Temporal Acoustic Inputs with Noise Drives Plasticity in the Adult Rat Auditory Cortex. Cereb Cortex 29:1032-1046.
Tognini P, Napoli D, Tola J, Silingardi D, Della Ragione F, D'Esposito M, Pizzorusso T (2015) Experience-dependent DNA methylation regulates plasticity in the developing visual cortex. Nat Neurosci 18:956-958.
Torres RF, Hidalgo C, Kerr B (2017) Mecp2 Mediates Experience-Dependent Transcriptional Upregulation of Ryanodine Receptor Type-3. Front Mol Neurosci 10:188.
Tritsch NX, Bergles DE (2010) Developmental regulation of spontaneous activity in the Mammalian cochlea. J Neurosci 30:1539-1550.
Tropea D, Kreiman G, Lyckman A, Mukherjee S, Yu H, Horng S, Sur M (2006) Gene expression changes and molecular pathways mediating activity-dependent plasticity in visual cortex. Nat Neurosci 9:660-668.
Turrigiano G (2012) Homeostatic synaptic plasticity: local and global mechanisms for stabilizing neuronal function. Cold Spring Harb Perspect Biol 4:a005736.
Turrigiano GG, Nelson SB (2004) Homeostatic plasticity in the developing nervous system. Nat Rev Neurosci 5:97-107.
Turrigiano GG, Leslie KR, Desai NS, Rutherford LC, Nelson SB (1998) Activity-dependent scaling of quantal amplitude in neocortical neurons. Nature 391:892-896.
van Versendaal D, Levelt CN (2016) Inhibitory interneurons in visual cortical plasticity. Cell Mol Life Sci 73:3677-3691.
Venturino A, Schulz R, De Jesus-Cortes H, Maes ME, Nagy B, Reilly-Andujar F, Colombo G, Cubero RJA, Schoot Uiterkamp FE, Bear MF, Siegert S (2021) Microglia enable mature perineuronal nets disassembly upon anesthetic ketamine exposure or 60-Hz light entrainment in the healthy brain. Cell Rep 36:109313.
Vierci G, Pannunzio B, Bornia N, Rossi FM (2016) H3 and H4 Lysine Acetylation Correlates with Developmental and Experimentally Induced Adult Experience-Dependent Plasticity in the Mouse Visual Cortex. J Exp Neurosci 10:49-64.
Villers-Sidani E, Chang, E.F., Bao, S., Merzenich, M.M. (2007) Critical Period Window for Spectral Tuning Defined in the Primary Auditory Cortex (A1) in the Rat. The Journal of Neuroscience 27:180-189.
Vlachos A, Becker D, Jedlicka P, Winkels R, Roeper J, Deller T (2012) Entorhinal denervation induces homeostatic synaptic scaling of excitatory postsynapses of dentate granule cells in mouse organotypic slice cultures. PLoS One 7:e32883.
Wang W, Zinsmaier AK, Firestone E, Lin R, Yatskievych TA, Yang S, Zhang J, Bao S (2018) Blocking Tumor Necrosis Factor-Alpha Expression Prevents Blast-Induced Excitatory/Inhibitory Synaptic Imbalance and Parvalbumin-Positive Interneuron Loss in the Hippocampus. J Neurotrauma 35:2306-2316.
Wang W, Zhang LS, Zinsmaier AK, Patterson G, Leptich EJ, Shoemaker SL, Yatskievych TA, Gibboni R, Pace E, Luo H, Zhang J, Yang S, Bao S (2019) Neuroinflammation mediates noise-induced synaptic imbalance and tinnitus in rodent models. PLoS Biol 17:e3000307.
Wegrzyn D, Freund N, Faissner A, Juckel G (2021) Poly I:C Activated Microglia Disrupt Perineuronal Nets and Modulate Synaptic Balance in Primary Hippocampal Neurons in vitro. Front Synaptic Neurosci 13:637549.

West AE, Chen WG, Dalva MB, Dolmetsch RE, Kornhauser JM, Shaywitz AJ, Takasu MA, Tao X, Greenberg ME (2001) Calcium regulation of neuronal gene expression. Proc Natl Acad Sci U S A 98:11024-11031.

Wiesel TN, Hubel DH (1963) Single-Cell Responses in Striate Cortex of Kittens Deprived of Vision in One Eye. J Neurophysiol 26:1003-1017.

Yang S, Weiner BD, Zhang LS, Cho SJ, Bao S (2011) Homeostatic plasticity drives tinnitus perception in an animal model. Proc Natl Acad Sci U S A 108:14974-14979.

Yang S, Yang S, Park JS, Kirkwood A, Bao S (2014a) Failed stabilization for long-term potentiation in the auditory cortex of FMR1 knockout mice. PLoS One 9:e104691.

Yang S, Zhang LS, Gibboni R, Weiner B, Bao S (2014b) Impaired development and competitive refinement of the cortical frequency map in tumor necrosis factor-alpha-deficient mice. Cereb Cortex 24:1956-1965.

Yee AX, Hsu YT, Chen L (2017) A metaplasticity view of the interaction between homeostatic and Hebbian plasticity. Philos Trans R Soc Lond B Biol Sci 372.

Yli-Karjanmaa M, Larsen KS, Fenger CD, Kristensen LK, Martin NA, Jensen PT, Breton A, Nathanson L, Nielsen PV, Lund MC, Carlsen SL, Gramsbergen JB, Finsen B, Stubbe J, Frich LH, Stolp H, Brambilla R, Anthony DC, Meyer M, Lambertsen KL (2019) TNF deficiency causes alterations in the spatial organization of neurogenic zones and alters the number of microglia and neurons in the cerebral cortex. Brain Behav Immun 82:279-297.

Yu H, Su Y, Shin J, Zhong C, Guo JU, Weng YL, Gao F, Geschwind DH, Coppola G, Ming GL, Song H (2015) Tet3 regulates synaptic transmission and homeostatic plasticity via DNA oxidation and repair. Nat Neurosci 18:836-843.

Zhang LI, Bao S, Merzenich MM (2001) Persistent and specific influences of early acoustic environments on primary auditory cortex. Nat Neurosci 4:1123-1130.

Zhang LI, Bao S, Merzenich MM (2002) Disruption of primary auditory cortex by synchronous auditory inputs during a critical period. Proc Natl Acad Sci U S A 99:2309-2314.

Zhang Z, Jiao YY, Sun QQ (2011) Developmental maturation of excitation and inhibition balance in principal neurons across four layers of somatosensory cortex. Neuroscience 174:10-25.

Zhao Y, Song Q, Li X, Li C (2016) Neural Hyperactivity of the Central Auditory System in Response to Peripheral Damage. Neural Plast 2016:2162105.

Zhou C, Yan S, Qian S, Wang Z, Shi Z, Xiong Y, Zhou Y (2019) Atypical Response Properties of the Auditory Cortex of Awake MECP2-Overexpressing Mice. Front Neurosci 13:439.

Zhou X, Nagarajan N, Mossop BJ, Merzenich MM (2008) Influences of un-modulated acoustic inputs on functional maturation and critical-period plasticity of the primary auditory cortex. Neuroscience 154:390-396.

Zhou X, Panizzutti R, de Villers-Sidani E, Madeira C, Merzenich MM (2011) Natural restoration of critical period plasticity in the juvenile and adult primary auditory cortex. J Neurosci 31:5625-5634.

Zinsmaier AK, Wang W, Zhang L, Hossainy NN, Bao S (2020) Resistance to noise-induced gap detection impairment in FVB mice is correlated with reduced neuroinflammatory response and parvalbumin-positive neuron loss. Sci Rep 10:20445.

Zylka MJ, Simon JM, Philpot BD (2015) Gene length matters in neurons. Neuron 86:353-355.